

國立臺灣大學獸醫專業學院獸醫學研究所

博士論文

**Graduate Institute of Veterinary Medicine  
School of Veterinary Medicine  
National Taiwan University  
Doctoral Dissertation**



台灣野生食肉目動物疾病監控調查：鼬獾狂犬病毒鑑定  
與特性分析首例

**Disease Surveillance and Monitoring in Wild-Ranging Carnivores  
in Taiwan: The First Identification and Characterization of Rabies Virus in  
Ferret Badgers**

邱慧英

**Hue-Ying Chiou**

指導教授：龐 飛 博士

鄭謙仁 博士

**Advisors: Dr. Victor Fei Pang**

**Dr. Chian-Ren Jeng**

中華民國 104 年 6 月

**June 2015**



謹以此論文

獻給

我的師長、家人、朋友

以及直接或間接參與台灣野生動物救傷、疾病監測和

狂犬病研究的夥伴們

## 目錄 Contents



摘要		I
Abstract		III
Chapter I	General introduction	1
Chapter II	Disease Surveillance in Rescued and Road-killed Wild-Ranging Carnivores in Taiwan	17
	<i>Taiwan Veterinary Journal 2015, 41:1-12</i>	
Chapter III	Pathological Characterization and Molecular Detection of Rabies Virus in the Rabid Ferret Badgers of a Recent Outbreak in Taiwan	30
	<i>Journal of Wildlife Diseases, 2015, accepted</i>	
Chapter IV	Molecular Characterization of Cryptically Circulating Rabies Virus from Ferret Badgers, Taiwan	64
	<i>Emerging Infectious Diseases, 2014, 20:790-798</i>	
Chapter V	Conclusions	80

## 摘要



本研究的目的是調查台灣野生食肉目動物死亡與潛在病因，並針對發現的重要或有趣的疾病進行深入研究。在 2011 年 8 月至 2015 年 1 月期間共收集 51 例救傷死亡或路死的食肉目動物屍體，經由詳細解剖與組織病理學檢查、分子與免疫學分析、微生物學及寄生蟲學檢測等進行病因分析。這些案例包括 31 例台灣鼬獾(TWFBs) (*Melogale moschata subaurantiaca*)、12 例白鼻心(MPCs) (*Paguma larvate taiwana*)、5 例麝香貓(SCCs) (*Viverricula indica pallida*)及 3 例食蟹獾(CEMs) (*Herpestes urva*)。人畜共通狂犬病與致死性犬瘟熱分別於 4 例台灣鼬獾與 3 例白鼻心被確診。

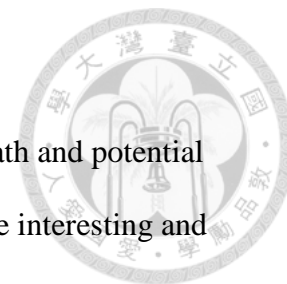
台灣鼬獾狂犬病的特徵性病理變化為非化膿性腦膜腦脊髓炎、神經節炎及形成典型的細胞質內包涵體- Negri bodies，受影響的中樞神經系統以腦幹病變最為嚴重。此外，大腦皮質部、丘腦與腦幹的神經元與神經氈具有不同程度的海綿狀變性。在非神經組織的代表性病變包括腎上腺壞死與間質淋巴球性唾液腺炎。經由免疫組織化學染色法(IHC)與螢光抗體試驗(FAT)，病毒抗原可在神經組織的神經元細胞與軸突/樹突等區域，以及全身不同組織間的巨噬細胞中被偵測到。結果顯示，腦幹、大腦皮質部、海馬角、丘腦與下視丘是台灣鼬獾狂犬病分子診斷的理想的採樣區。我們利用不同單位提供的 2004-2012 年間福馬林固定、石蠟包埋的舊有台灣鼬獾腦組織，進行免疫組織化學染色回溯性研究，發現狂犬病陽性案例最早可追溯至 2004 年。

為了分析台灣鼬獾狂犬病病毒的源起，我們完成三株狂犬病病毒全基因體定序分析，並由公告的幾株狂犬病毒(RABV)核蛋白(N)與糖蛋白(G)序列進行親緣地理學分析顯示，台灣鼬獾狂犬病病毒 (RABV-TWFB) 來自亞洲譜系並已獨立演化，其近緣病毒株 China I (包括中國鼬獾狂犬病病毒株; RABV-CNFB) 和菲律賓狂犬病病毒的分化年代在 158-210 年前，而台灣鼬獾狂犬病病毒株的

最近共祖起源年代約在 91-113 年前。我們的研究顯示，此次地方性台灣鼬獾狂  
犬病病毒基因分析的古老親緣結果說明了台灣鼬獾的狂犬病病毒株可能隱晦的  
潛藏在環境中長期的慢慢傳播，而致一直未被檢出，此病毒與宿主間的交互作  
用及其潛存的機制值得進一步研究。



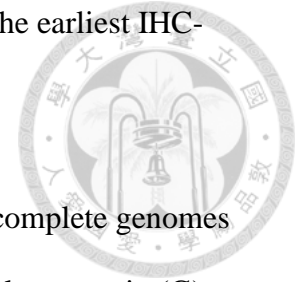
## Abstract



The objective of this study was to investigate the causes of death and potential diseases carried by the wild-ranging carnivores in Taiwan. For those interesting and essential diseases, further studies in depths were performed. A total of 51 carcasses from rescued but dead or road-killed carnivores, collected during the period of August 2011 to January 2015, were necropsied for histopathology, molecular and immunological assays, microbiology, and parasitology. The cases included 31 Taiwan ferret badgers (TWFBs) (*Melogale moschata subaurantiaca*), 12 masked palm civets (MPCs) (*Paguma larvate taivana*), 5 small Chinese civets (SCCs) (*Viverricula indica pallida*), and 3 crab-eating mongooses (CEMs) (*Herpestes urva*). Zoonotic rabies and fatal canine distemper were diagnosed in 4 TWFBs and 3 MPCs, respectively.

The characteristic pathological changes of rabid TWFBs were nonsuppurative meningoencephalomyelitis, ganglionitis, and formation of typical intracytoplasmic Negri bodies with brain stem affected the most. Additionally, variable spongiform degeneration, primarily in the perikaryon of neurons and neuropil, was observed in the cerebral cortex, thalamus, and brain stem. In the non-nervous tissue, representative lesions included adrenal necrosis and lymphocytic interstitial sialoadenitis. By immunohistochemical (IHC) staining as well as fluorescent antibody test (FAT), positive viral antigens were detected in the perikaryon of the neurons and axonal and/or dendritic processes in the nervous tissue and in the macrophages scattered in various tissues throughout the body. The findings suggest that brain stem, cerebral cortex, hippocampus, thalamus and hypothalamus are ideal sampling regions for molecular diagnosis of RABV in TWFBs. Retrospective study using archived

formalin-fixed and paraffin-embedded tissues of TWFBs revealed the earliest IHC-positive rabid TWFB case in 2004.



To examine the origin of this viral strain, we sequenced three complete genomes and acquired multiple rabies virus (RABV) nucleoprotein (N) and glycoprotein (G) sequences. Phylogeographic analyses demonstrated that the RABV of TWFB (RABV-TWFB) is a distinct lineage within the Asian group, and has been differentiated from its closest lineages, China I (including Chinese ferret badger isolates; RABV-CNFB) and Philippines, 158-210 years before present. The most recent common ancestor of RABV-TWFB was originated 91-113 years ago. The ancient origin of the endemic RABV-TWFB illustrates that this RABV variant could be cryptically circulated in the environment without being recognized for a long period of time. The underlying mechanism is worthy of further study and may shed light on the complex interaction between RABV and its host.

# Chapter I



## General Introduction





## 1.1 Background

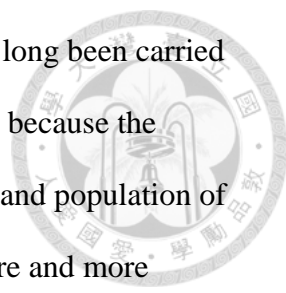
Zoonoses are a growing concern. The concept of “One World, One Health” has recently been repeatedly stressed, indicating a worldwide tight link between animal diseases and public health. It is known that approximately 60% of known human pathogens and over 75% of the emerging and re-emerging human diseases in the past two decades originate from domestic or wild animals; moreover, approximately 80% of the pathogens that could potentially be used in bioterrorism are of animal origin as well (Dehove, 2010). Additionally, wild animals often act as sentinels for animal diseases, which could serve as an effective management and control of these diseases in domestic animals. Therefore, surveillance of wildlife diseases must be considered as equally important as surveillance and control of diseases in domestic animals (Dehove, 2010). However, owing to the fact that symptoms and signs of disease in wildlife are not as readily observed as in domestic animals and specimens for laboratory analysis are more difficult to collect, the implementation of early detection of and response to disease outbreaks thus usually relatively slow.

The new and emerging wildlife diseases may pose a serious risk to animal welfare, human health, wildlife conservation, and economic productivity. Ebola virus infection is a good example, which has caused 26 outbreaks mainly in Central and West Africa since its first discovery in 1976, and the most recent outbreak in West Africa has resulted in 10,460 human deaths by the end of March 2015 (<http://apps.who.int/ebola/current-situation/ebola-situation-report-1-april-2015-0>). Current evidence has strongly implicated that bats, including fruit bats and insectivorous bats, are the reservoir hosts for Ebola viruses. It has been suggested that

uptake of partially eaten fruits and pulp dropped by Ebola virus-infected fruit bats by land mammals such as gorillas and duikers forms a possible indirect transmission chain from the natural host to animal populations; the outbreaks in human are acquired initially via close contact with these infected bats or land mammals followed by close contact among people (Leroy *et al.*, 2004).

Although dogs are considered the principal host of rabies, rabies virus (RABV) infection is also dispersed in many species of wild Carnivora and Chiroptera, which have become the major source of human infection in many countries in Europe and North America where dog vaccination programs are well established (Barbosa *et al.*, 2008). It was estimated that rabies caused over 60,000 human deaths in the world in 2010, primarily in Africa and Asia (World Health, 2013). Avian influenza (AI) is an infectious viral disease of birds, which often causes no apparent signs of illness in wild water fowl such as ducks and geese. AI viruses can sometimes spread to domestic poultry and cause large-scale outbreaks of serious disease leading to severe economic impact such as H5N1, H5N8, H7N1, H7N9 (Sartore *et al.*, 2010), some of which have also been reported to cross the species barrier and cause disease in humans and other mammals such as H5N1, H7N9 (Cowling *et al.*, 2013; Leong *et al.*, 2008; Li *et al.*, 2014).

Disease surveillance in animals is the key for early detection of the underlying, new or even emerging diseases (Cox-Witton *et al.*, 2014). Wildlife disease surveillance has become an integral component in the identification and control of emerging animal and zoonotic diseases potentially hazard to human and domestic animal welfare (Daszak *et al.*, 2000). Both passive and active surveillance strategies have been used in wildlife disease investigation (Stallknecht, 2007). Government-



supported active and passive wildlife disease survey programs have long been carried in Taiwan; however, zoo animals were often the major target simply because the majority of these exhibited animals were imported and the varieties and population of native wild-ranging wild animals are very limited. Owing to the more and more important role of wildlife on the emerging and re-emerging disease development in and between animals and humans, the target in the wildlife disease surveillance program has been readjusted and started to switch gradually from admixture of zoo and native wild-ranging wildlife to native wild-ranging wildlife only since 2011. Through this program, carcasses of native wild-ranging wildlife have been routinely submitted either to the National Taiwan University (NTU) or to the National Pingtung University of Science and Technology for disease surveillance and monitoring.

## 1.2 Rabies

Rabies is possibly one of the oldest zoonotic disease. It is caused by the rabies virus (RABV), a neurotropic virus belonging to the *Lyssavirus* of Rhabdoviridae (Warrell and Warrell, 2004). Rabies is a worldwide disease and only a small number of countries and regions are free from this disease. The RABV infects nearly all warm-blooded animals causing progressive, severe neurological signs and death invariably (Jackson and Fu, 2013). According to World Health Organization (WHO), there were over 60,000 rabies-associated human deaths worldwide in 2010, primarily in Africa and Asia (WHO, 2013). The virus cannot penetrate intact skin; thus, bitten by a rabid animal is the most important route of transmission in humans. Dogs are considered as the principal host of the disease in developing countries. In developed countries such as the United States, the important sources of transmission include bats and wild carnivores; animal exposures in other countries; and rare cases of infection

via inhalation or organs transplant. Interestingly, only 40% to 50% of victims of bites from rabid animals will develop rabies (Kauffman and Goldman, 1986).



### 1.3 Genome of rabies virus

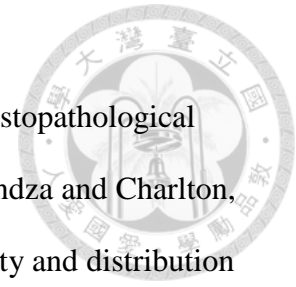
The RABV is enveloped and contains a single-stranded, negative-sense ribonucleic acid (RNA) genome of approximately 12 kb (Holmes *et al.*, 2002; Yousaf *et al.*, 2012). The genome of RABV encodes five genes whose order is highly conserved. These genes code for nucleoprotein (N), phosphoprotein (P), matrix protein (M), glycoprotein (G), and RNA-dependent RNA polymerase (L), are arranged in a strictly conserved order (3'-N-P-M-G-L-5') (Dietzschold *et al.*, 1983; Nagaraja *et al.*, 2008; Wunner and Conzelmann, 2013). All rhabdoviruses have two major structural components, a helical ribonucleoprotein (RNP) core and the surrounding envelop. The N protein forms the RNP core with the P and L proteins and plays a critical role in transcription and replication (Kuzmin *et al.*, 2012; Nagaraja *et al.*, 2008). The remaining two structural proteins of the rabies virion, the G and M, are associated with the lipid-bilayer envelope that surrounds the RNP core. N protein is involved in the encapsidation of the genome RNA and protection of the RNA from endogenous ribonucleases activity (Wunner and Conzelmann, 2013) as well as the modulation of viral RNA transcription and replication. The P protein is capable of oligomerization or binding to the nucleoprotein-RNA template (Gigant *et al.*, 2000); it interacts with the cytoplasmic dynein light chain protein, which helps the axoplasmic transport of viral nucleocapsid; it also acts as a chaperone of soluble nascent N protein (Raux *et al.*, 2000; Yang *et al.*, 1999). The M protein is involved in the down regulation of viral RNA transcription, condensation of helical nucleocapsid cores into tight coils, association with membrane bilayers, and cytopathogenesis of infected cells

(Wunner and Conzelmann, 2013). It confers the characteristic bullet shape to the virion. The G protein forms approximately 400 trimeric spikes which are tightly arranged on the surface of the virus; it plays important roles in the attachment of RABV to the host-cell surface as well as in the pathogenicity and neurovirulence of RABV (Morimoto *et al.*, 1999; Tuffereau *et al.*, 1989). The L protein is the polymerase of the RNP core and is involved in the majority of enzymatic activities of the polymerase complex in viral RNA transcription and replication (Morimoto *et al.*, 1999; Nagaraja *et al.*, 2008).

#### **1.4 Rabies in wildlife**

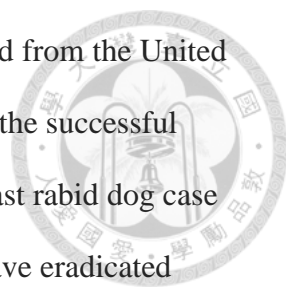
Wildlife has become an important source of RABV infection in many developed countries. Prior to 1951, domestic dogs and cats were the major source of rabies in the United States. More than 8,000 cases were reported among dogs in 1946. However, with the institution of vaccination programs for domestic animals carried on throughout the United States in the 1940s, the prevalence shifted from dogs and cats to wildlife. Rabies in wild animals, particularly bats, raccoons, foxes, and skunks, has accounted for almost 85% of all reported cases in the United States since 1976 (Kauffman and Goldmann, 1986; Krebs *et al.*, 2003a). The disease is generally regarded as having a single-species reservoir with spillover to other dead-end hosts (Krebs *et al.*, 2003a; Krebs *et al.*, 2003b). It is known that mustelids, including the genera *Melogale*, *Meles*, and *Mellivora* of the weasel family Mustelidae, are also susceptible to rabies (Barnard, 1979; Wandeler *et al.*, 1974a; Wandeler *et al.*, 1974b; Wandeler *et al.*, 1974c). The Chinese ferret badger (CNFB) (*Melogale moschata moschata*) has been considered as a primary rabies host and source of human rabies in southeast China (Liu *et al.*, 2010; Zhang *et al.*, 2009; Zhenyu *et al.*, 2007).

In natural or experimental RABV infection, non-suppurative meningoencephalomyelitis and ganglionitis are the characteristic histopathological findings (Abreu *et al.*, 2014; Balachandran and Charlton, 1994; Bundza and Charlton, 1988; Charlton *et al.*, 1983; Stein *et al.*, 2010). However, the severity and distribution of the lesion and the amount and distribution of viral antigens are variable, depending on the host, viral strain, and clinical course (Balachandran and Charlton, 1994; Charlton, 1984; Charlton *et al.*, 1987a; Charlton *et al.*, 1987b; Hamir *et al.*, 1992; Hamir *et al.*, 2011).



### **1.5 History of rabies in Taiwan**

The earliest written record regarding human rabies case in Taiwan could be traced back to the early nineteenth century when Taiwan was still under the colonial rule of Japanese. Starting from 1930, the Japanese began to control rabies in Taiwan by producing inactivated vaccine for prevention and treatment of human rabies and for canine use along with instituting strict dog registration and poisoning stray dogs. Prior to 1948 when rabies re-emerged in Taiwan, there had been no record of rabies for more than ten years. Following the ending of the World War II, traffics between Taiwan and Shanghai, Hongkong or Hainan, where rabies existed, became heavy. On June 17, 1948, a human rabies case originated from Shanghai was diagnosed at the Taiwan University Hospital. Owing to the lack of infectious disease specialist during the period of 1948 to 1958, dog-bite human cases were treated simply by surgeons without prevention and/or post-exposure vaccination and immunoglobulin treatment. A total of 782 deaths occurred during the outbreak with the highest number of 238 deaths in 1951 followed by 102 deaths in 1952. In 1956, the Joint Commission on Rural Reconstruction and the Taiwan Provincial Health Department instituted rabies



control measures, including vaccinating dogs with vaccines imported from the United States and culling stray dogs to control animal reservoir. Following the successful control measures, human death from rabies ended in 1958 and the last rabid dog case was reported in 1961 (Liu, 2013). Since then, Taiwan declared to have eradicated rabies and listed as rabies-free by the World Organisation for Animal Health (OIE) (Wu *et al.*, 2014) until 2013. Prior to the re-emerging of rabies in 2013, there were 3 imported dog-bite human rabies cases, in which 2 cases were from China occurring in 2002 and 2012 and 1 case was from the Philippines in 2013; all these three patients died. The Bureau of Animal and Plant Inspection and Quarantine (BAPIQ) of the Council of Agriculture has contracted National Taiwan University to conduct disease surveillance of wild animals since 2011. In 2013, rabies was added to the disease list under surveillance and in the same year rabies was diagnosed in Taiwan ferret-badgers (TWFBs) (*M. moschata subaurantiaca*) (Chiou *et al.*, 2014). The rabid TWFBs showed severe encephalopathy, but repeated testing for etiologies causing encephalopathy, including canine distemper and measles, failed to identify the cause of death; however, the results of RT-PCR for RABV turned out to be positive in June 2013. Following reporting the findings to BAPIQ on June 24, the specimens were then submitted to the Animal Health Research Institute, Council of Agriculture, on June 26 for confirmation, After the Council of Agriculture convened a rabies expert meeting on July 16, the diagnosis of rabies was confirmed and the incident was reported to OIE on July 17. May 23 of 2012, the date of the first rabid TWFB submitted for examination, became the onset date of the current endemic.

## **1.6 Objectives of study**

### **Disease surveillance in rescued and road-killed wild-ranging carnivores in**

## Taiwan (Chapter II)



Recent highly pathogenic avian influenza and rabies events have shown just how important disease surveillance of free-ranged wildlife can be in dealing with zoonotic diseases. Controlling the pathogen at its source in animals could help to avoid subsequent public health problems. This study was part of a continual disease surveillance and monitoring program in captive and free-range wildlife. Routine clinical observation and pathological examination for wildlife in Taiwan were performed. The gross and histopathological examination for each animal was recorded. In addition, bacteriological, parasitic and PCR examination were included. Potential zoonotic and important infectious diseases were monitored in order to prevent their spreading to humans and domestic animals. Results obtained from the study can provide information regarding the current status of wildlife diseases in Taiwan to the government, which will be beneficial to animal welfare, human health, wildlife conservation, and economic productivity.

## Pathological characterization and viral detection in rabid Taiwan ferret badgers (Chapter III)

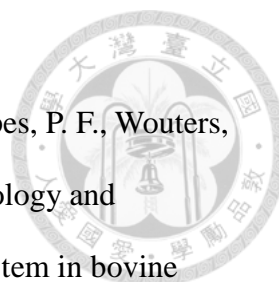
Wildlife has become an important source of RABV infection in many developed countries due to well established canine vaccination programs. The Chinese ferret badger (CNFB) (*Melogale moschata moschata*) is known to be a primary rabies host and source of human rabies in southeast China. It is known that the severity and distribution of rabies-associated pathological changes and the amount and distribution of viral antigens vary among different hosts, viral strains, and durations of the clinical disease. Although rabies-associated lesions have been reported in various animal species and in human beings, the associated pathological



changes and the distribution of viral antigens have not yet been fully described in ferret badgers (FBs). However, the information is essential for establishing more accurate sampling and diagnosis modalities for FB-associated rabies, especially when composite sampling is not feasible. The present study was to characterize the pathological changes and the pattern of viral antigen distribution regarding the recent outbreak of rabies in TWFBs.

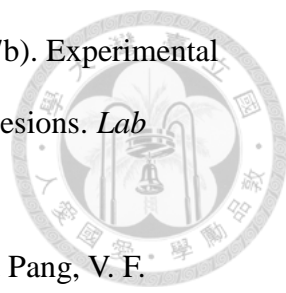
### **Genomic organization and characterization of the rabies virus of Taiwan ferret badger-associated rabies (Chapter IV)**

The recent outbreak of rabies in TWFBs has caused widespread panic among public. As there has been no reported rabid case in dogs or humans for more than 50 years in Taiwan, it is important to understand whether the current outbreak is an emerging, a re-emerging or actually a cryptically circulated disease, its relations with the other RABV lineages. The present study tried to clarify whether the current outbreak of the Taiwanese ferret badger-associated rabies (TWFB-AR) is an emerging, a re-emerging or actually a cryptically circulated disease. The possible origin of this outbreak and its relations with the CNFB-associated rabies (CNFB-AR) in mainland China via the genomic organization and characterization as well as the analysis of genetic diversity and phylogeographic origin of RABV-TWFB were investigated. In addition, a possible mechanism contributing to the limited host range of RABV-TWFB is also discussed.



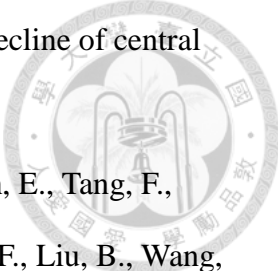
## References:

- Abreu, C. C., Nakayama, P. A., Nogueira, C. I., Mesquita, L. P., Lopes, P. F., Wouters, F., Varaschin, M. S. and Bezerra, P. S., Jr. (2014). Histopathology and immunohistochemistry of tissues outside central nervous system in bovine rabies. *J Neurovirol*, **20**, 388-397.
- Balachandran, A. and Charlton, K. (1994). Experimental rabies infection of non-nervous tissues in skunks (*Mephitis mephitis*) and foxes (*Vulpes vulpes*). *Vet Pathol*, **31**, 93-102.
- Barbosa, T. F., Medeiros, D. B., Travassos da Rosa, E. S., Casseb, L. M., Medeiros, R., Pereira Ade, S., Vallinoto, A. C., Vallinoto, M., Begot, A. L., Lima, R. J., Vasconcelos, P. F. and Nunes, M. R. (2008). Molecular epidemiology of rabies virus isolated from different sources during a bat-transmitted human outbreak occurring in Augusto Correa municipality, Brazilian Amazon. *Virology*, **370**, 228-236.
- Barnard, B. J. (1979). The role played by wildlife in the epizootiology of rabies in South Africa and South-West Africa. *Onderstepoort J Vet Res*, **46**, 155-163.
- Bundza, A. and Charlton, K. M. (1988). Comparison of spongiform lesions in experimental scrapie and rabies in skunks. *Acta Neuropathol*, **76**, 275-280.
- Charlton, K. M. (1984). Rabies: spongiform lesions in the brain. *Acta Neuropathol*, **63**, 198-202.
- Charlton, K. M., Casey, G. A. and Campbell, J. B. (1983). Experimental rabies in skunks: mechanisms of infection of the salivary glands. *Can J Comp Med*, **47**, 363-369.
- Charlton, K. M., Casey, G. A. and Campbell, J. B. (1987a). Experimental rabies in skunks: immune response and salivary gland infection. *Comp Immunol Microbiol Infect Dis*, **10**, 227-235.

- 
- Charlton, K. M., Casey, G. A., Webster, W. A. and Bundza, A. (1987b). Experimental rabies in skunks and foxes. Pathogenesis of the spongiform lesions. *Lab Invest*, **57**, 634-645.
- Chiou, H. Y., Hsieh, C. H., Jeng, C. R., Chan, F. T., Wang, H. Y. and Pang, V. F. (2014). Molecular characterization of cryptically circulating rabies virus from ferret badgers, Taiwan. *Emerg Infect Dis*, **20**, 790-798.
- Cowling, B. J., Jin, L., Lau, E. H., Liao, Q., Wu, P., Jiang, H., Tsang, T. K., Zheng, J., Fang, V. J., Chang, Z., Ni, M. Y., Zhang, Q., Ip, D. K., Yu, J., Li, Y., Wang, L., Tu, W., Meng, L., Wu, J. T., Luo, H., Li, Q., Shu, Y., Li, Z., Feng, Z., Yang, W., Wang, Y., Leung, G. M. and Yu, H. (2013). Comparative epidemiology of human infections with avian influenza A H7N9 and H5N1 viruses in China: a population-based study of laboratory-confirmed cases. *Lancet*, **382**, 129-137.
- Cox-Witton, K., Reiss, A., Woods, R., Grillo, V., Baker, R. T., Blyde, D. J., Boardman, W., Cutter, S., Lacasse, C., McCracken, H., Pyne, M., Smith, I., Vitali, S., Vogelnest, L., Wedd, D., Phillips, M., Bunn, C. and Post, L. (2014). Emerging infectious diseases in free-ranging wildlife-Australian zoo based wildlife hospitals contribute to national surveillance. *PLoS One*, **9**, e95127.
- Daszak, P., Cunningham, A. A. and Hyatt, A. D. (2000). Emerging infectious diseases of wildlife--threats to biodiversity and human health. *Science*, **287**, 443-449.
- Dehove, A. (2010). One world, one health. *Transbound Emerg Dis*, **57**, 3-6.
- Dietzschold, B., Wunner, W. H., Wiktor, T. J., Lopes, A. D., Lafon, M., Smith, C. L. and Koprowski, H. (1983). Characterization of an antigenic determinant of the glycoprotein that correlates with pathogenicity of rabies virus. *Proc Natl Acad Sci U S A*, **80**, 70-74.
- Gigant, B., Iseni, F., Gaudin, Y., Knossow, M. and Blondel, D. (2000). Neither phosphorylation nor the amino-terminal part of rabies virus phosphoprotein is



- required for its oligomerization. *J Gen Virol*, **81**, 1757-1761.
- Hamir, A. N., Moser, G. and Rupprecht, C. E. (1992). Morphologic and immunoperoxidase study of neurologic lesions in naturally acquired rabies of raccoons. *J Vet Diagn Invest*, **4**, 369-373.
- Hamir, A. N., Niezgoda, M. and Rupprecht, C. E. (2011). Recovery from and clearance of rabies virus in a domestic ferret. *J Am Assoc Lab Anim Sci*, **50**, 248-251.
- Holmes, E. C., Woelk, C. H., Kassis, R. and Bourhy, H. (2002). Genetic constraints and the adaptive evolution of rabies virus in nature. *Virology*, **292**, 247-257.
- Jackson, A. C. and Fu, Z. F. (2013). Pathogenesis. In: *Rabies*, A. C. Jackson and W. H. Wunner, Eds, Elsevier Academic Press, pp. 299-349.
- Kauffman, F. H. and Goldmann, B. J. (1986). Rabies. *Am J Emerg Med*, **4**, 525-531.
- Krebs, J. W., Wheeling, J. T. and Childs, J. E. (2003a). Rabies surveillance in the United States during 2002. *J Am Vet Med Assoc*, **223**, 1736-1748.
- Krebs, J. W., Williams, S. M., Smith, J. S., Rupprecht, C. E. and Childs, J. E. (2003b). Rabies among infrequently reported mammalian carnivores in the United States, 1960-2000. *J Wildl Dis*, **39**, 253-261.
- Kuzmin, I. V., Shi, M., Orciari, L. A., Yager, P. A., Velasco-Villa, A., Kuzmina, N. A., Streicker, D. G., Bergman, D. L. and Rupprecht, C. E. (2012). Molecular inferences suggest multiple host shifts of rabies viruses from bats to mesocarnivores in Arizona during 2001-2009. *PLoS Pathog*, **8**, e1002786.
- Leong, H. K., Goh, C. S., Chew, S. T., Lim, C. W., Lin, Y. N., Chang, S. F., Yap, H. H. and Chua, S. B. (2008). Prevention and control of avian influenza in Singapore. *Ann Acad Med Singapore*, **37**, 504-509.
- Leroy, E. M., Rouquet, P., Formenty, P., Souquiere, S., Kilbourne, A., Froment, J. M., Bermejo, M., Smit, S., Karesh, W., Swanepoel, R., Zaki, S. R. and Rollin, P. E.

- 
- (2004). Multiple Ebola virus transmission events and rapid decline of central African wildlife. *Science*, **303**, 387-390.
- Li, Q., Zhou, L., Zhou, M., Chen, Z., Li, F., Wu, H., Xiang, N., Chen, E., Tang, F., Wang, D., Meng, L., Hong, Z., Tu, W., Cao, Y., Li, L., Ding, F., Liu, B., Wang, M., Xie, R., Gao, R., Li, X., Bai, T., Zou, S., He, J., Hu, J., Xu, Y., Chai, C., Wang, S., Gao, Y., Jin, L., Zhang, Y., Luo, H., Yu, H., He, J., Li, Q., Wang, X., Gao, L., Pang, X., Liu, G., Yan, Y., Yuan, H., Shu, Y., Yang, W., Wang, Y., Wu, F., Uyeki, T. M. and Feng, Z. (2014). Epidemiology of human infections with avian influenza A(H7N9) virus in China. *N Engl J Med*, **370**, 520-532.
- Liu, C.H. (2013). History of Rabies Control in Taiwan and China. *Taiwan E B*, 29:S44-S52.
- Liu, Y., Zhang, S., Wu, X., Zhao, J., Hou, Y., Zhang, F., Velasco-Villa, A., Rupprecht, C. E. and Hu, R. (2010). Ferret badger rabies origin and its revisited importance as potential source of rabies transmission in Southeast China. *BMC Infect Dis*, **10**, 234.
- Morimoto, K., Hooper, D. C., Spitsin, S., Koprowski, H. and Dietzschold, B. (1999). Pathogenicity of different rabies virus variants inversely correlates with apoptosis and rabies virus glycoprotein expression in infected primary neuron cultures. *J Virol*, **73**, 510-518.
- Nagaraja, T., Madhusudana, S. and Desai, A. (2008). Molecular characterization of the full-length genome of a rabies virus isolate from India. *Virus Genes*, **36**, 449-459.
- Raux, H., Flamand, A. and Blondel, D. (2000). Interaction of the rabies virus P protein with the LC8 dynein light chain. *J Virol*, **74**, 10212-10216.
- Sartore, S., Bonfanti, L., Lorenzetto, M., Cecchinato, M. and Marangon, S. (2010). The effects of control measures on the economic burden associated with

- epidemics of avian influenza in Italy. *Poult Sci*, **89**, 1115-1121.
- Stallknecht, D. E. (2007). Impediments to wildlife disease surveillance, research, and diagnostics. *Curr Top Microbiol Immunol*, **315**, 445-461.
- Stein, L. T., Rech, R. R., Harrison, L. and Brown, C. C. (2010). Immunohistochemical study of rabies virus within the central nervous system of domestic and wildlife species. *Vet Pathol*, **47**, 630-633.
- Tuffereau, C., Leblois, H., Benejean, J., Coulon, P., Lafay, F. and Flamand, A. (1989). Arginine or lysine in position 333 of ERA and CVS glycoprotein is necessary for rabies virulence in adult mice. *Virology*, **172**, 206-212.
- Wandeler, A., Muller, J., Wachendorfer, G., Schale, W., Forster, U. and Steck, F. (1974a). Rabies in wild carnivores in central Europe. III. Ecology and biology of the fox in relation to control operations. *Zentralbl Veterinarmed B*, **21**, 765-773.
- Wandeler, A., Wachendorfer, G., Forster, U., Krekel, H., Muller, J. and Steck, F. (1974b). Rabies in wild carnivores in central Europe. II. Virological and serological examinations. *Zentralbl Veterinarmed B*, **21**, 757-764.
- Wandeler, A., Wachendorfer, G., Forster, U., Krekel, H., Schale, W., Muller, J. and Steck, F. (1974c). Rabies in wild carnivores in central Europe. I. Epidemiological studies. *Zentralbl Veterinarmed B*, **21**, 735-756.
- Warrell, M. J. and Warrell, D. A. (2004). Rabies and other lyssavirus diseases. *Lancet*, **363**, 959-969.
- World Health, O. (2013). WHO Expert Consultation on Rabies. Second report. *World Health Organ Tech Rep Ser*, 1-139, back cover.
- Wu, H., Chang, S. S., Tsai, H. J., Wallace, R. M., Recuenco, S. E., Doty, J. B., Vora, N. M., Chang, F. Y., Eis officer, C. D. C., Centers for Disease, C. and Prevention. (2014). Notes from the field: wildlife rabies on an island free from

canine rabies for 52 years--Taiwan, 2013. *MMWR Morb Mortal Wkly Rep*, **63**, 178.

Wunner, W. H. and Conzelmann, K. K. (2013). Rabies virus. In: *Rabies*, A. C.

Jackson, Ed, Elsevier Academic Press, pp. 17-60.

Yang, J., Koprowski, H., Dietzschold, B. and Fu, Z. F. (1999). Phosphorylation of rabies virus nucleoprotein regulates viral RNA transcription and replication by modulating leader RNA encapsidation. *J Virol*, **73**, 1661-1664.

Yousaf, M. Z., Qasim, M., Zia, S., Khan, M., Ashfaq, U. A. and Khan, S. (2012).

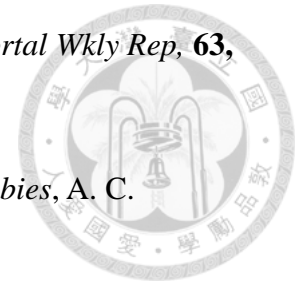
Rabies molecular virology, diagnosis, prevention and treatment. *Virol J*, **9**, 50.

Zhang, S., Tang, Q., Wu, X., Liu, Y., Zhang, F., Rupprecht, C. E. and Hu, R. (2009).

Rabies in ferret badgers, southeastern China. *Emerg Infect Dis*, **15**, 946-949.

Zhenyu, G., Zhen, W., Enfu, C., Fan, H., Junfen, L., Yixin, L., Gangqiang, D. and

Fontaine, R. E. (2007). Human rabies cluster following badger bites, People's Republic of China. *Emerg Infect Dis*, **13**, 1956-1957.



# Chapter II



## **Disease Surveillance in Rescued and Road-killed Wild-Ranging Carnivores in Taiwan**

*Reprinted from Taiwan Veterinary Journal, 2015, Authors: Hue-Ying Chiou, Kuang-Sheng Yeh, Chian-Ren Jeng, Hui-Wen Chang, Li-Jen Chang, Ying-Hui Wu, Fang-Tse Chan, Victor Fei Pang, Title of article: Disease Surveillance in Rescued and Road-killed Wild-Ranging Carnivores in Taiwan, 41(2):73-84, copyright (2015) with permission from Chinese Society of Veterinary Science and World Scientific Publishing Co. Pte. Ltd.*





## DISEASE SURVEILLANCE IN RESCUED AND ROAD-KILLED WILD-RANGING CARNIVORES IN TAIWAN

Hue-Ying Chiou\*, Kuang-Sheng Yeh\*, Chian-Ren Jeng<sup>\*,†</sup>,  
Hui-Wen Chang<sup>\*,†</sup>, Li-Jen Chang<sup>‡</sup>, Ying-Hui Wu<sup>‡</sup>,  
Fang-Tse Chan<sup>§</sup> and Victor Fei Pang<sup>\*,†,¶</sup>

<sup>\*</sup>Graduate Institute of Veterinary Medicine  
School of Veterinary Medicine  
National Taiwan University  
Taipei 10617, Taiwan, ROC

<sup>†</sup>Graduate Institute of Molecular and Comparative Pathobiology  
School of Veterinary Medicine, National Taiwan University  
Taipei 10617, Taiwan, ROC

<sup>‡</sup>Veterinary Office, Taipei Zoo, Taipei 11656, Taiwan, ROC

<sup>§</sup>Endemic Species Research Institute, Council of Agriculture  
Executive Yuan, Nantou 55244, Taiwan, ROC

Received 9 April 2015

Accepted 17 April 2015

Published 12 June 2015

### ABSTRACT

The objective of this study was to investigate the causes of death and potential diseases carried by the wild-ranging carnivores in Taiwan through a government-supported disease survey program. During the period of August 2011 to January 2015, a total of 51 carcasses from rescued but dead or road-killed carnivores were necropsied for histopathology, molecular and immunological assays, microbiology, and parasitology. The cases included 31 Taiwan ferret badgers (TWFBs) (*Melogale moschata subaurantiaca*), 12 masked palm civets (MPCs) (*Paguma larvate taiwana*), 5 small Chinese civets (SCCs) (*Viverricula indica pallida*), and 3 crab-eating mongooses (CEMs) (*Herpestes urva*). Zoonotic rabies and fatal canine distemper were diagnosed in four TWFBs and three MPCs, respectively. A high prevalence rate of lungworm infestation (23/31; 74.2%) was observed in TWFBs. In addition, a unique fatal *Staphylococcus hyicus* pneumonia and a fatal heavy systemic sarcoptic mange infestation were diagnosed in a TWFB and a suckling MPC kid, respectively. Road traffic accidents and stray dog-associated killing were the most common etiologies for the death of wild-ranging carnivores.

**Keywords:** Carnivores; Taiwan ferret badger; Masked palm civet; Small Chinese civet; Crab-eating mongoose; Rabies; Canine distemper.

<sup>¶</sup>Corresponding author: Victor Fei Pang, Graduate Institute of Molecular and Comparative Pathobiology, School of Veterinary Medicine, National Taiwan University, No. 1, Sec. 4, Roosevelt Rd., Taipei 10617, Taiwan, ROC. Tel: +886-2-33663867; Fax: +886-2-23621965; E-mail: pang@ntu.edu.tw

## INTRODUCTION

Wildlife has become widely recognized to play an important role in the epidemiology of emerging and zoonotic diseases.<sup>1–4</sup> The new and emerging wildlife diseases may pose a serious risk to animal welfare, human health, wildlife conservation, and economic productivity. Ebola virus infection is a good example, which has caused 26 outbreaks mainly in Central and West Africa since its first discovery in 1976, and the most recent outbreak in West Africa has resulted in 10,460 human deaths by the end of March 2015 (<http://apps.who.int/ebola/current-situation/ebola-situation-report-1-april-2015-0>). Current evidence has strongly implicated that bats, including fruit bats and insectivorous bats, are the reservoir hosts for Ebola viruses. It has been suggested that uptake of partially eaten fruits and pulp dropped by Ebola virus-infected fruit bats by land mammals such as gorillas and duikers forms a possible indirect transmission chain from the natural host to animal populations<sup>5</sup>; the outbreaks in human are acquired initially via close contact with these infected bats or land mammals followed by close contact among people.

Although dogs are considered the principal host of rabies, rabies virus (RABV) infection is also dispersed in many species of wild Carnivora and Chiroptera, which have become the major source of human infection in many countries in Europe and North America where dog vaccination programs are well established.<sup>6,7</sup> It was estimated that rabies caused over 60,000 human deaths in the world in 2010, primarily in Africa and Asia.<sup>8</sup> Avian influenza (AI) is an infectious viral disease of birds, which often causes no apparent signs of illness in wild water fowl such as ducks and geese. AI viruses can sometimes spread to domestic poultry and cause large-scale outbreaks of serious disease leading to severe economic impact such as H5N1, H5N8, H7N1, H7N9,<sup>9</sup> some of which have also been reported to cross the species barrier and cause disease in humans and other mammals such as H5N1, H7N9.<sup>10–12</sup>

Disease surveillance in animals is the key for early detection of the underlying or even emerging diseases.<sup>13</sup> Wildlife disease surveillance has become an integral component in the identification and control of emerging animal and zoonotic diseases potentially hazardous to human and domestic animal welfare. Both passive and active surveillance strategies have been used in wildlife disease investigation.<sup>14</sup> There are numerous situations in which it is important to determine whether a particular disease of interest is present in a free-ranging wildlife population. However, adequate disease surveillance can be labor-intensive and expensive and thus there is substantial

motivation to conduct it as efficiently as possible. Surveillance is often based on the assumption of a simple random sample, but this can almost always be improved upon if there is auxiliary information available about disease risk factors.<sup>15</sup> Owing to the fact that conducting an unbiased surveillance in free-ranging mammal populations is often more challenging, the passive opportunistic case identification is, thus, generally more often used for the detection of disease events in wild animals.<sup>16</sup>

Government-supported active and passive wildlife disease survey programs have long been carried in Taiwan, however, zoo animals were often the major target simply because the majority of these exhibited animals were imported and the varieties and population of native wild-ranging wild animals are very limited. Owing to the well-known role of wildlife on the emerging and re-emerging disease development in and between animals and humans, the target in the wildlife disease surveillance program has been readjusted and switched to the native wild-ranging wildlife since 2011. Through this program, carcasses of native wild-ranging wildlife have been routinely submitted either to the National Taiwan University (NTU) or to the National Pingtung University of Science and Technology for disease surveillance and monitoring. We report herein the findings of the causes of death and potential diseases carried by the native wild-ranging carnivores in Taiwan at NTU through the wildlife disease surveillance program during the period of August 2011 to January 2015.

## MATERIALS AND METHODS

### Animals

During the period of August 2011 to January 2015, 51 carcasses of free-ranging carnivores from wildlife first aid station, and the rescue center, animal disease control center and/or animal protection and health inspection office of different regions of Taiwan were submitted to the School of Veterinary Medicine at NTU for routine disease surveillance (Table 1). These cases included 31 Taiwan ferret badgers (TWFBs) (*Melogale moschata subaurantiaca*), 12 masked palm civets (MPCs) (*Paguma larvate taivana*), 5 small Chinese civets (SCCs) (*Viverricula indica pallida*), and 3 crab-eating mongooses (CEMs) (*Herpestes urva*).

### Sample Collection

Full necropsy was performed and representative tissue samples, including cerebrum, cerebellum, brain stem,

**Table 1. The Number of Dead Wild-Ranging Carnivores Submitted for Necropsy During the Period of August 2011 to January 2015.**

Species	Year				
	2011	2012	2013	2014	2015
TWFB	1	3	7	12	8
MPC	1	3	4	4	—
SCC	—	—	1	3	1
CEM	—	—	1	—	2

liver, spleen, lungs, heart, tongue, esophagus, gastrointestinal (GI) tract, pancreas, kidney, adrenal gland, urinary bladder, testicle, ovary, uterus, skeletal muscle, and haired skin, were collected. The tissue samples were fixed in 10% neutral buffered formalin and processed routinely for histopathological examination. Fresh tissues, especially brain, lung, and liver, were collected from each animal and stored at  $-80^{\circ}\text{C}$  for subsequent nucleic acid extraction.

### Histopathological Examination

All tissue blocks were sectioned at  $5\mu\text{m}$ , stained with hematoxylin and eosin (H&E), and examined by light microscopy.

### Microbiological Analysis

Where gross lesions suggestive of a bacterial infection were seen, tissue specimens were inoculated onto 5% sheep blood agar (CMP<sup>TM</sup>) and incubated at  $37^{\circ}\text{C}$  for overnight. Suspected colonies were further identified using a Vitek 2 Compact automated system (Biomérieux, Marcy-l'Étoile, France) to the species level.

### Immunohistochemical Staining

The IHC staining was performed using the advanced Super Sensitive<sup>TM</sup> Polymer-HRP IHC Detection System (BioGenex Lab., Fremont, CA, USA) according to the manufacturer's instructions with primary mouse anti-Rabies virus (RABV) glycoprotein IgG2a (Abcam Inc., Boston, MA, USA) and anti-Canine distemper virus (CDV) nucleoprotein IgG2b (Santa Cruz Biotechnology Inc., Dallas, Texas, USA) monoclonal antibodies. Deparaffinized slides were treated with  $100\mu\text{g}/\text{mL}$  proteinase K (AppliChem Inc, St. Louis, MO, USA) for 15 min, and then incubated in 3%  $\text{H}_2\text{O}_2$  for 10 min to quench the activity of endogenous peroxidase. Following

incubation with PowerBlock reagent (BioGenex universal blocking reagent) for 10 min and wash in Tris-buffered saline Tween-20 (TBST) buffer, the slides were incubated with primary antibody for 60 min, Super-Enhancer (BioGenex HRP kit) for 30 min, and Polymer-HRP reagent (BioGenex HRP kit) for 40 min with gentle wash in TBST buffer for 5 min after each step. Following treatment with the chromogen-DAB (BioGenex HRP kit) for 3 min, the slides were rinsed with TBST buffer, drained, and counterstained with Mayer's hematoxylin for 1 min. Positive and negative controls were run parallel in each assay.

### Fluorescent Antibody Test (FAT)

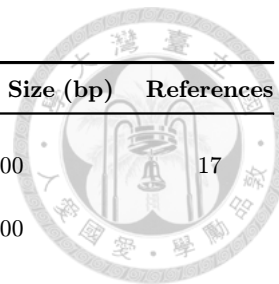
For the detection of RABV antigens, brain smears were prepared either with a frozen ground composite brain tissue suspension of cerebrum, hippocampus, thalamus, and hypothalamus left from the preparation for RNA extraction or with impression smears made from cerebrum, cerebellum, and brain stem from each necropsied animal. The smears were then air-dried at room temperature, fixed in acetone (Merck) at  $-20^{\circ}\text{C}$  for 20 min, washed 3 times with PBS, and stained with either direct (DFA) or indirect (IFA) immunofluorescence assay. For the DFA, the air-dried and acetone-fixed brain smear slides were stained with a commercially available FDI fluorescein isothiocyanate (FITC)-conjugated anti-rabies monoclonal globulin (Fujirebio Diagnostics, Inc., Malvern, PA, USA), incubated at  $37^{\circ}\text{C}$  for 30 min, and washed in PBS for 3 times. For the IFA, the air-dried and acetone-fixed brain smear slides were incubated with the primary anti-RABV glycoprotein IgG2a monoclonal antibody (Abcam) at a 1:500 dilution at room temperature for 60 min, washed in PBS for 3 times, stained with an FITC-conjugated goat anti-mouse IgG antibody (Bethyl Lab., Inc., Montgomery, TX, USA) at room temperature for 60 min, and washed in PBS for 3 times. The viral antigens targeted by the FITC-labeled antibody appeared as apple-green fluorescent finely to clumped granular aggregates under the fluorescent microscope (Optiphot II, Nikon, Tokyo, Japan).

### Reverse Transcription Polymerase Chain Reaction and Sequence Analysis

Fresh brain and lung specimens were screened for RABV and CDV by reverse transcription polymerase chain reaction (RT-PCR). Representative tissue specimen from each animal, approximately 25 mg each, was mixed

Table 2. Oligonucleotides Used in the Study.

Primer Pair	Sequence 5'-3'	Target	Amplicon Size (bp)	References
<b>Rabies virus</b>				
RV-N-F	ACGCTTAACAACAAAACCATAGAAG	N gene	1300	17
RV-N-R	CGGATTGACGAAGATCTTGCTCAT			
RV-G-F	CATCCCTCAAAAGACTTAAGGAAAG	G gene	500	
RV-G-R	CCGAGGAGATGAGGTCTTCGGGAC			
<b>Canine distemper virus</b>				
RHF	AACAATGCTCTCCTACCAAGA	H gene	1800	18
RHF4	AATGCTAGAGATGGTTTAATT			
<b><i>Angiostrongylus cantonensis</i></b>				
AngioF1	ATCATAAACCTTTTTTCGAGTATCCA	18S rRNA	1134	19
AngioR1	TCTCGAGACAGCTCAGTCCCGG			



with 1 mL of TRIzol reagent (Invitrogen, CA, USA) and homogenized. Following the addition of 0.2 mL of chloroform, the samples were centrifuged at  $12,000 \times g$  for 15 min. The upper aqueous phase was collected for total RNA extraction by using the RNeasy Mini Kit (QIAGEN Inc, Hilden, Germany) followed by cDNA synthesis by using the Transcriptor first strand cDNA synthesis kit (Roche Diagnostics, IN, USA) according to the manufacturer's instructions. Details of the RT-PCR primers<sup>17</sup> used and associated references are summarized in Table 2.<sup>17,18</sup> The amplicons were further sequenced (Tri-IBiotech Inc, Taipei, Taiwan) and compared with those viral sequences deposited in GenBank/EMBL/DDBJ using the NCBI's BLAST program (<http://www.ncbi.nlm.nih.gov/BLAST>).

### Polymerase Chain Reaction and Sequence Analysis

The total DNA was extracted from lung tissue emulsion and/or larvae obtained from lung wash using DNeasy® blood & tissue kit (QIAGEN Inc, Hilden, Germany) according to the manufacturer's instructions. Owing to the fact that *Angiostrongylus cantonensis* is a common lungworm in wild rats in Taiwan and the natural feed habitat of TWFBs for snails and earthworms, which are the common intermediate hosts of *A. cantonensis*, polymerase chain reaction (PCR) for the detection of *A. cantonensis* was performed. Details of the PCR primers used and the associated Ref. 19 are listed in Table 2. The amplicons were further sequenced (Tri-IBiotech Inc, Taipei, Taiwan) and compared with the sequences of various related parasites deposited in GenBank/EMBL/DDBJ using the NCBI's BLAST program (<http://www.ncbi.nlm.nih.gov/BLAST>).

### Phylogenetic Analysis

Multiple sequence alignments were constructed by using Clustal W<sup>20</sup> and MEGA6.06 software programs ([www.megasoftware.net](http://www.megasoftware.net)). The phylogenetic tree was generated using the maximum-likelihood method with 1000 bootstrap replicates. Scale bar indicates nucleotide substitutions per site.

### Parasitological Examination

Parasites were preserved in 70% ethanol or 10% formalin and examined by dissecting microscopy.

## RESULTS

### General Condition

Many of the carcasses received had suffered variable degrees of traumatic injuries such as punctured wounds, diaphragmatic hernia, inguinal hernia and/or bone fractures along with external and internal hemorrhages as well as tears and/or ruptures of internal organs. Death related to road traffic accident or bites from other animals were diagnosed in 77.4% of TWFBs (24/31), 75% of MPCs (9/12), 60% of SCCs (3/5), and 100% of CEMs (3/3) (Table 3). Owing to no large carnivores present in Taiwan, stray dogs are highly speculated to be responsible for the killing.

### Viral Diseases

The most significant viral diseases detected in the study were rabies in four TWFBs and canine distemper in three MPCs. Aside from emaciation and rough hair coat,

**Table 3. The Incidence of Various Categories of Disease Conditions Detected in the Necropsied Wild-Ranging Carnivores.**

Disease Condition	Animal Species			
	TWFB <i>n</i> = 31	MPC <i>n</i> = 12	SCC <i>n</i> = 5	CEM <i>n</i> = 3
Trauma	24 <sup>a</sup>	9	3	3
Virus	4	3	0	0
Bacteria	1	0	0	0
Fungus	0	1	1	0
Parasitism	25	5	3	2
Lung				
Lungworms	23	2	0	0
Liver				
Nematode larvae	9	0	0	0
Tongue				
Trichinelloidea (Capillariidae)	4	0	0	0
<i>Sarcocystis</i>	1	0	0	0
Esophagus				
Unidentified nematodes	4	0	0	0
GI tract				
Unidentified nematodes	16	2	3	1
Trichostrongyloidea	2	0	3	0
Cestodes	3	0	0	1
Ascaridida	1	0	2	0
Trematodes	0	2	0	0
Pancreas				
Trematodes	1	1	0	0
Urinary bladder				
Bladder worm ( <i>Pearsonema</i> spp. formerly <i>Capillaria</i> )	0	0	0	1
Skin				
Trichinelloidea	1	0	1	0
Demodex mites	1	0	0	0
Sarcoptic mange	0	1	0	0
Unknown <sup>b</sup>	2	1	1	0

<sup>a</sup>The number of animal with the specific disease condition.

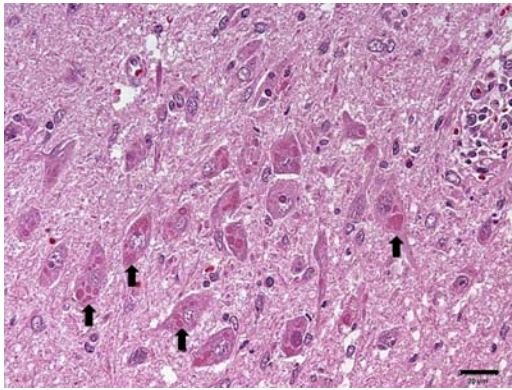
<sup>b</sup>No significant gross and/or microscopic lesions.

Note: *n* = Total number of animal examined.

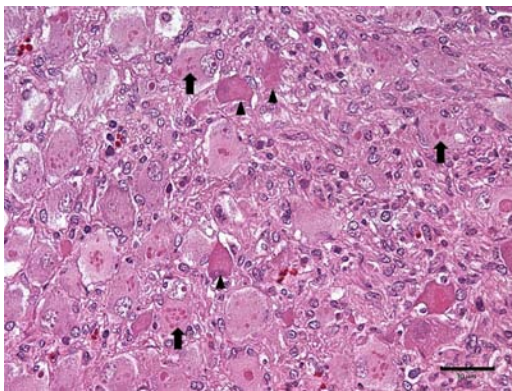
no apparent gross lesions were seen in the four rabid TWFBs. Nonsuppurative meningoencephalomyelitis and ganglionitis with formation of typical intracytoplasmic Negri bodies were the characteristic histopathological findings [Figs. 1(A) and 1(B)]. The lesions were widely distributed in the brain with brain stem affected the most. Additionally, variable spongiform degeneration, primarily in the perikaryon of neurons and neuropil, was observed in the cerebral cortex, thalamus, and brain stem. In the non-nervous tissue, representative lesions included adrenal necrosis and lymphocytic interstitial sialoadenitis. The FAT and IHC staining [Fig. 1(C)] demonstrated a widely distributed pattern of RABV antigens in the neurons and nerve processes. The results

of RT-PCR and subsequent sequence analysis of the amplicons further confirmed that the virus belonged to the classic RABV.<sup>21</sup>

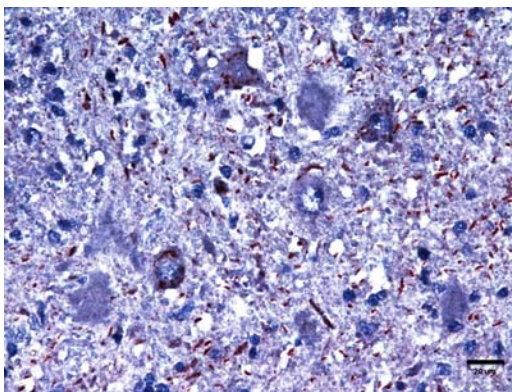
Two rescued adult MPCs displaying neurologic signs of severe ataxia and seizures prior to death were submitted. No apparent gross lesions were found. Microscopically, both had nonsuppurative meningoencephalomyelitis [Fig. 2(A)] with gliosis, areas of necrosis, accumulation of gitter cells and hypertrophied (gemistocytic) astrocytes, and occasional syncytial cell formation. No distinct intranuclear or intracytoplasmic inclusion bodies were identified in the brain tissue. Both animals had no pneumonia but mild bronchiolitis. CDV antigens were detected in the hypertrophied astrocytes



(A)

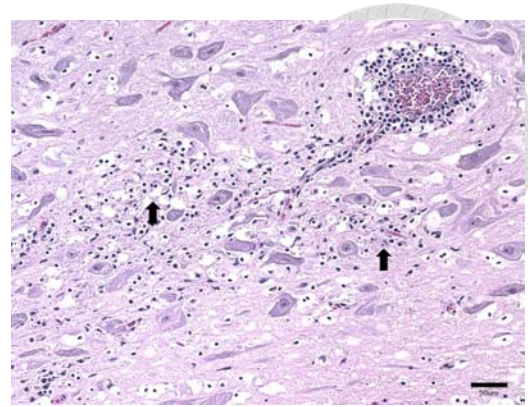


(B)

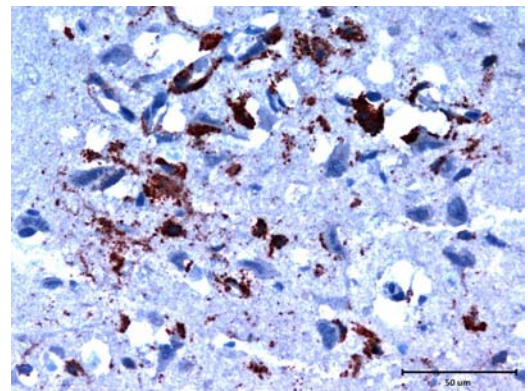


(C)

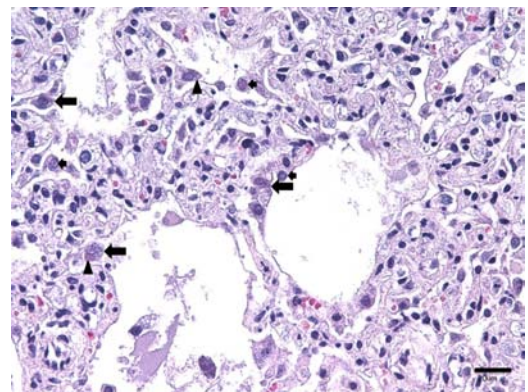
**Fig. 1** Rabies, TWFB (*Melogale moschata subaurantiaca*). (A) Cerebrum. Nonsuppurative encephalitis, characterized by lymphoplasmacytic perivascular cuffing (right up corner) with formation of varying numbers of intracytoplasmic eosinophilic Negri bodies in the neurons (arrows). H&E stain. (B) Perirenal ganglion. Ganglionitis, characterized by the infiltration of lymphocytes, plasma cells, and macrophages as well as degeneration and necrosis of ganglion cells (arrowheads) with formation of intracytoplasmic eosinophilic Negri bodies (arrows). H&E stain. (C) Brain stem. Strong rabies virus antigen-positive signals widely distributed in the neurons and nerve processes. Immunohistochemical (IHC) staining, polymer-HRP method, AEC substrate, Mayer's hematoxylin counterstain.



(A)



(B)



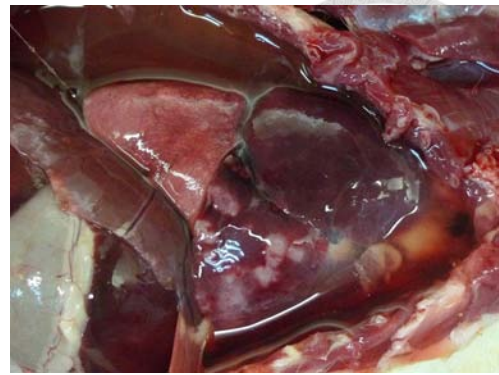
(C)

**Fig. 2** CDV infection, MPC (*Paguma larvate taiwana*). (A) Cerebrum. Nonsuppurative encephalitis, characterized by the presence of lymphoplasmacytic cuffing, areas of necrosis (arrows), and gliosis. H&E stain. (B) Cerebrum. Strong CDV antigen-positive signals widely distributed in the neurons and astrocytes. IHC staining, polymer-HRP method, DAB substrate, Mayer's hematoxylin counterstain. (C) Lung. Interstitial pneumonia, characterized by the infiltration of lymphocytes, plasma cells and macrophages and proliferation of type II pneumocytes with formation of syncytial cells (long arrows) and eosinophilic, intranuclear (short arrows) and intracytoplasmic (arrowheads) inclusion bodies in the alveolar septa. H&E stain.

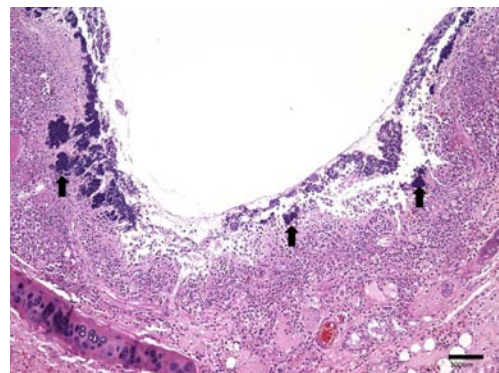
and neurons [Fig. 2(B)]. The results of RT-PCR and subsequent sequence analysis of the amplicons further confirmed CDV infection (data not shown). In another female MPC kid, weighing approximately 400 gm, the lung lobes were bilaterally pale pink and rubbery to firm when palpated. The trachea was filled with a moderate amount of serosanguineous fluid and some fibrin strands. A small amount of similar exudate and some fibrin strands oozed from the small airways and lung parenchyma. Microscopically, diffuse bronchointerstitial pneumonia along with proliferation of bronchiolar epithelial cells and alveolar type II pneumocytes and syncytial cell formation was revealed [Fig. 2(C)]. Intranuclear and intracytoplasmic eosinophilic inclusion bodies were found in the epithelium of the airway and alveoli. Syncytial cells with 3–5 nuclei were randomly distributed and some of them also contained intracytoplasmic and/or intranuclear inclusions [Fig. 2(C)]. CDV infection was further confirmed by IHC staining, RT-PCR, and sequence analysis of the amplicons (data not shown).

### Bacterial and Fungal Diseases

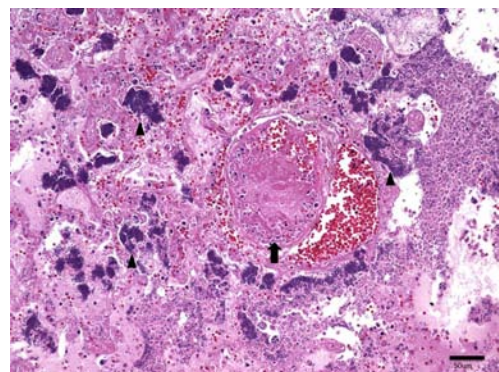
The only bacterial disease identified in the study was a fatal staphylococcal pneumonia found in a TWFB. The lesion involved the entire apical and cardiac lobes bilaterally. The affected lobes were diffusely dark red to mottled red white with some fibrin loosely attached to the antero-ventral portion and adjacent thoracic wall. There was a large amount of translucent, serosanguinous pleural effusion [Fig. 3(A)]. The hilar lymph nodes were enlarged. Microscopically, the lung lesion was characterized as a bilateral fibrinosuppurative necrotizing bronchopneumonia. There were areas of marked mucosal epithelial necrosis and transmural suppurative inflammation in the bronchi [Fig. 3(B)]. Necrosis along with variable edema, fibrin deposition, hemorrhage, and accumulation of degenerate neutrophils and macrophages was apparent in the lung parenchyma [Fig. 3(C)]. Large numbers of bacterial colonies were present on the surface of the necrotic bronchial mucosa and widely distributed in the lung parenchyma [Figs. 3(B) and 3(C)]. The lobular septa were markedly dilated by edema, fibrin deposition, and infiltration of inflammatory cells. Areas of thrombosis were also noted [Fig. 3(C)]. Bacterial culture using the lung tissue and pleural effusion successfully isolated a pure nonhemolytic bacterium forming white colonies on the blood agar. The bacterium was further identified as *Staphylococcus hyicus* via the Vitek 2 Compact automated system.



(A)



(B)



(C)

**Fig. 3** *S. hyicus* pneumonia, TWFB (*Melogale moschata subaurantiaca*). (A) Opened thoracic cavity. The apical and cardiac lung lobes are non-collapsed, firm, and dark red to mottled red white with deposition of some fibrin in the antero-ventral portion; the pleural cavity is filled with a large amount of translucent, serosanguinous effusion. (B) Bronchus. Necrotizing bronchitis, characterized by extensive mucosal necrosis and transmural inflammation along with formation of large numbers of bacterial colonies (arrows). H&E stain. (C) Lung. Necrotizing pneumonia, characterized by the presence of extensive necrosis and infiltration of neutrophils and macrophages with edema, fibrin deposition, congestion, hemorrhage, and formation of thrombus (arrows) and large numbers of bacterial colonies (arrowheads). H&E stain.

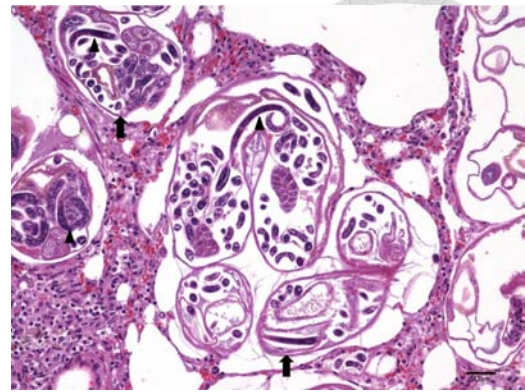
The only fungal disease detected was the *Candida*-induced glossitis in a SCC and a suckling MPC kid, which had suffered severe lethal sarcoptic mange infestation.

### Parasitism (Table 3)

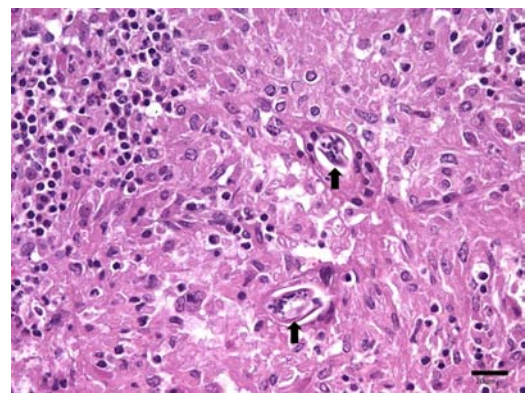
Parasitism was the most common disease condition seen in the wild-ranging carnivores in the present study, in which lungworm had the highest prevalence rate, especially in TWFBs and MPCs.

**Lungs** Lungworm infestation was recorded in 74.2% of TWFBs (23/31) and 16.7% of MPCs (2/12), but no case was seen in SCCs and CEMs. Grossly, the lungs with lungworm infestation displayed areas of consolidation and variable congestion. Multiple pale yellow to white spots, ranging from 0.1 to 0.2 cm in diameter, were randomly distributed on the surface and in the parenchyma of the lungs. Microscopic examination revealed areas of variable subacute to chronic verminous pneumonia. Multiple aggregates of varying numbers of sections of a nematode, including adults and larvae, were randomly distributed in the lung parenchyma [Fig. 4(A)]. The adult worms and larvae were present primarily in the alveolar spaces, bronchioles, and/or bronchi. The cross sections of the adult worms were approximately 200–300  $\mu\text{m}$  in diameter and characterized by having a thin cuticle, a pseudocoelom lined by coelomyarian-polymyarian musculature, an intestinal tract lined by a few multi-nucleated cells, ovaries, and uterus filled with oocytes, embryos, and developing larvae [Fig. 4(A)]. The larvae were 10–20  $\mu\text{m}$  in width, deeply basophilic, and occasionally coiled. Around the parasites, there was variable granulomatous inflammation, characterized by the infiltration of epithelioid macrophages, lymphocytes, plasma cells mixed with some eosinophils, neutrophils, and multinucleated giant cells [Fig. 4(B)]. By using the pair of primers *AngioF1/AngioR1*, PCR amplicons with the expected size of 1134 bp were obtained from the DNA extracted from lung tissue emulsion and/or larvae. However, the results of further sequencing and phylogenetic analysis at the 18S rRNA gene suggested that the lungworm found in TWFBs is more closely related to *Parafilaroides decorus*, a lungworm of sea mammals, rather than to *A. cantonesis* (Fig. 5).

**Alimentary system** In the alimentary system, parasitism was a quite common incidental finding in all wild-ranging carnivores and could be seen in various parts of the system. The incidental alimentary parasite infestation found in TWFBs included parasite migration



(A)



(B)

**Fig. 4** Lungworm infestation, TWFB (*Melogale moschata subaurantiaca*). (A) Lung. Verminous pneumonia, characterized by the presence of multiple cross sections of a nematode in the alveolar spaces and infiltration of mixed macrophages, lymphocytes, plasma cells, and neutrophils in the alveolar septa; the adult nematode (arrows) having a thin cuticle, a pseudocoelom lined by coelomyarian-polymyarian musculature, an intestinal tract lined by a few multi-nucleated cells, ovaries, and uterus filled with larvae (arrowheads). H&E stain. (B) Lung. Verminous pneumonia, characterized by the accumulation of large numbers of epithelioid macrophages mixed with some lymphocytes, plasma cells, eosinophils, and neutrophils around a few larvae (arrows) in the lung parenchyma. H&E stain.

in hepatic parenchyma (9/31), characterized by the presence of scattered necrotic migration tract surrounded by varying numbers of eosinophils and mononuclear inflammatory cells; Trichinelloidea (Capillariadae) in the lingual mucosal epithelium (4/31), characterized by having a thick cuticle in the adult worm and striated shell and bipolar plugs in the eggs; *Sarcocystis* in the muscle of tongue (1/31); unidentified nematodes in the esophageal mucosa (4/31); unidentified nematodes in the lower GI tract (16/31); Trichostrongyloidea (2/31), cestodes (3/



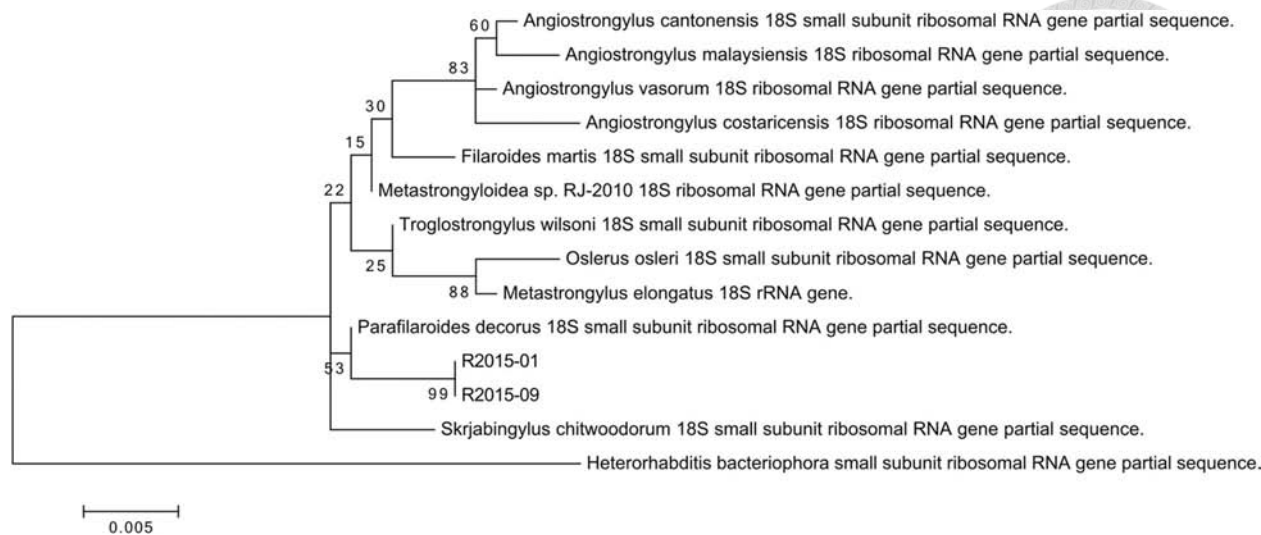


**Fig. 5** Phylogenetic analysis of the lungworm detected in TWFB (*Melogale moschata subaurantiaca*) and nematodes of the order Strongylida using 18S rRNA. Multiple sequence alignments were constructed by using Clustal W and MEGA6.06 software programs. The phylogenetic tree was generated using the maximum-likelihood method with 1000 bootstrap replicates. Scale bar indicates nucleotide substitutions per site.

31) and Ascaridida (1/31) in the small intestine; and trematodes in the pancreatic duct (1/31). In MPCs, there were unidentified nematodes (2/12) and trematodes (2/12) in the GI tract, and trematodes (1/12) in the pancreatic duct. In SCCs, unidentified nematodes (3/5), Trichostrongyloidea (3/5), and Ascaridida (2/5) were detected in the small intestine. In CEMs, unidentified nematodes (1/3) and cestodes (1/3) were found in the small intestine.

**Skin** Heavy sarcoptic mange infestation-associated death was diagnosed in a suckling MPC kid. Grossly, the skin lesion was characterized by formation of large areas of thick crusts with no alopecia. Microscopically, the affected regions showed severe epidermal hyperplasia, hyperkeratosis, and a large number of mites and eggs distributed in the upper epidermis along with mixed inflammatory cell infiltration in the epidermis and upper dermis. Other incidental cutaneous parasitic infestation included Trichinelloidea (suspected *Anatrichosoma* and Capillariidae) in a SCC (1/5) and a TWFB (1/31) co-infected with *Demodex*.

**Urinary tract** Bladder worm infestation was diagnosed in a CEM (1/3), in which there were a moderate number of adult *Pearsonema* sp. (formerly *Capillaria*) with eggs in the mucosal epithelium along with mild inflammation. The eggs had a typical oval shape and a thick capsule with striated shell and bipolar plugs.

**Skeletal muscle** Infestation with *Sarcocystis* sp. was found in 1 TWFB (1/31). Microscopically, there were many protozoal cysts, ranging from 30 to 150  $\mu$ m in the

myofibers of the tongue. The cysts had a thin hyalinized wall and contained numerous crescent bradyzoites. Minimal muscular degeneration and fibrosis with infiltration of a few mixed inflammatory cells were also noted.

## DISCUSSION

Rabies is one of the most important and possibly the oldest zoonotic diseases. Owing to the well-established canine vaccination programs, wildlife has become an important source of RABV infection in many developed countries. Through the government-supported disease surveillance program of dead wild-ranging native wild carnivores, rabies was diagnosed in TWFBs in mid-June of 2013. Since the first discovery of rabid TWFBs in 2013, rabies has been diagnosed in additional 452 TWFBs, 4 MPCs, 1 shrew, and 1 puppy bitten by rabid-TWFB by March 26, 2015. ([https://www.baphiq.gov.tw/news\\_list.php?menu=1924&typeid=1948](https://www.baphiq.gov.tw/news_list.php?menu=1924&typeid=1948)). Prior to the most recent outbreak, Taiwan had been considered as a rabies-free region for more than 50 years. Phylogeographic analyses indicated that the TWFB-associated RABV is a distinct lineage among the Asian isolates. This particular lineage might have been diverged from its closest lineages, China I and Philippines, more than 150 years.<sup>21</sup> The discovery of this re-emerging important zoonotic disease further emphasizes the essentiality of a systemic disease surveillance in wild-ranging wildlife.

CDV is a morbillivirus, which is known to cause systemic diseases in canids, mustelids (ferrets, mink), raccoons, collared peccaries, seals, and felids.<sup>3,22</sup> It has emerged as a potentially devastating pathogen in certain wild felid populations, including lions, tigers, lynx, and bobcat.<sup>23,24</sup> Although CDV has only one serotype, it has multiple strains with different virulence and neurotropism. In Taiwan, serum antibodies to CDV had been detected in a captive leopard cats<sup>25</sup>; and CDV infection had been diagnosed in 2 wild TWFBs by histopathology and RT-PCR.<sup>26</sup> However, no CDV sequences of TWFBs were submitted to the GenBank database. In the present study, CDV infection was detected only in MPCs, in which distinct eosinophilic intranuclear and intracytoplasmic inclusion bodies could be easily detected in the epithelium of airway and syncytial cells, but not in the brain tissue. CDV infection can be easily differentiated from rabid TWFBs and MPCs, in which intracytoplasmic Negri bodies could be easily found in neurons. In Taiwan, it is believed that CDV-infected dogs and/or wild carnivores are the most likely source of infection for the susceptible wild-ranging carnivores.<sup>25</sup>

*S. hyicus* is a Gram-positive coccus known to cause a fatal generalized exudative epidermitis in newborn piglets.<sup>27,28</sup> It has also been isolated from animals with septic polyarthritis and from bovine mastitis.<sup>29,30</sup> Two cases of human infection, including a donkey bite-induced wound infection<sup>31</sup> and a bacteremia in a farmer,<sup>32</sup> have been reported. To our knowledge, this is the first case of *S. hyicus*-associated pneumonia. The source of the infection and whether it requires any predisposing factor for the pneumonia development are not known.

Parasitism is a common finding in free-living wildlife, including zoo animals. Although parasitism-associated severe illness may be occasionally encountered in wildlife, most of the natural cases display limited or more often no clinical effects as an incidental finding. In the present study, parasitism was also the most common finding; however, many of the parasites cannot be identified simply based on their morphological characteristics seen in tissue sections. Lungworms are nematode of the order Strongylida that infest the lungs of vertebrates. The most common lungworms belong to the superfamily either Trichostrongyloidea or Metastrongyloidea, but not all the species in these superfamilies are lungworms. Lungworms infest a wide range of mammals and have a direct or indirect and complex life cycle. For those lungworms with indirect life cycle, snail, slug, or earthworm plays the role of intermediate host for those susceptible terrestrial mammals.<sup>33,34</sup> Owing to the conserved nature of ribosomal RNA

(rRNA) and its potential use for providing informative characters for comparative analysis with other nematode taxa, the nuclear DNA locus has been used for phylogenetic analysis in nematode, including Metastrongyloidea.<sup>33</sup> Based on the facts of host site specificity, parasite morphology, and snail and earthworm being the preferred food for TWFBs in the field, *A. cantonesis* was initially considered as a potential candidate for the worms found in the lungs of TWFBs. PCR amplicons with the expected size of 1134 bp were obtained by using the reported primers designed based on the 18S rRNA gene of *A. cantonesis*<sup>19</sup>; surprisingly, further sequencing and phylogenetic analysis of the 18S rRNA gene revealed that the lungworm seen in TWFBs was genetically more closely related to *P. decorus*, a lungworm of sea mammals, instead of *A. cantonesis*. In badger species, several different lung nematodes have been reported in European badgers (*Melesmeles*), including *A. falciiformis*, *A. vasorum*, *A. pridhami*, *Crenosoma* sp., and *Capillaria aerphil*.<sup>35</sup> For most Metastrongyloidea species, gastropods such as slugs and snails act as the intermediate hosts. However, nongastropod intermediate hosts also exist, such as fishes and earthworms in the life cycle of *P. decorus* in pinnipeds and *Metastrongylus* spp. in suids, respectively.<sup>33</sup> For *A. cantonesis*, the larvae in the permissive host such as rats will complete the pulmonary migration from the pulmonary artery to the terminal bronchioles and pharynx. Whereas in nonpermissive hosts such as mice, guinea pigs, rabbits, rhesus monkeys, and humans, the larvae generally fail to complete the pulmonary migration and remain in the central nervous system until death.<sup>34</sup> TWFBs are speculated to be a permissive host for the lungworm based on its complete life cycle. To our knowledge, this is also the first report of lungworm infestation in TWFBs; however, whether this parasite is truly a new species closely related to *P. decorus* requires further elucidation.

*Pearsonema plica* and *P. feliscati*, known as bladder worms, are nematode parasites that inhabit in the urinary bladder and rarely in the ureters and renal pelvis of various domestic and wild carnivores. This parasite has a worldwide distribution and is frequently seen in dogs and foxes. Its life cycle is indirect and involves earthworm as an intermediate host.<sup>36</sup> The species of the bladder worm found in CEMs could not be determined simply based on their morphological characteristics histologically. If the bladder worm that we found belongs to one of the two species of *Pearsonema* mentioned above, this parasite should be found in TWFBs more easily instead of in CEMs because earthworm is the known intermediate host. Whether the bladder worm found in the study is a new species or there are other

intermediate hosts aside from earthworm requires further elucidation.

Sarcoptic mange is a worldwide, highly contagious, parasitic skin disease of mammals. The etiologic agent is the burrowing mite *Sarcoptes* spp., which also causes scabies in humans. Many wild animal species, including red fox (*Vulpes vulpes*), develop extensive skin lesions and eventually die.<sup>37</sup> In Taiwan, there were only two cases of wild Formosan serows (*Capricornis swinhoei*) infested with *Sarcoptes scabiei* and *Chorioptic texanus* reported in 2007.<sup>38</sup>

In the present study, lingual capillariasis due to Trichinelloidea (Capillariidae) infestation was diagnosed in four TWFBs. Trichinelloidea infestation was also observed in the skin of one TWFB and one SCV. To our knowledge, the nematode *Capillaria xenopodis* (*Pseudocapillarioides xenopi*) which causes cutaneous and/or epidermal capillariasis has only been reported in South African clawed frogs (*Xenopus laevis*).<sup>39,40</sup> An unusual zoonotic trichuroid nematode, *Anatrichosoma* sp.,<sup>41</sup> has been identified to cause ulcerative pododermatitis in cats.<sup>41,42</sup> This parasite has also been identified occasionally in human mouth lesions.<sup>43</sup> However, no information of cutaneous and/or lingual capillariasis (Trichinelloidea) is available in wild carnivores.

The findings of the present study have clearly demonstrated that there are many unknown diseases cryptically circulating in the wildlife sharing the same habitat with us, and some of which may even have serious impacts on our and other animal's health, wildlife conservation, and economy. These findings also reinforce the importance of an effective wildlife disease surveillance. The information accumulated from years of systemic survey may allow us to predict future emergence of known and unknown pathogens.<sup>4</sup>

## Acknowledgments

The study was supported in part by Grants 101AS-10.1.2-BQ-B1(1), 102AS-10.1.1-BQ-B1(1), 102AS-10.1.1-BQ-B1(3), 103AS-10.1.1-BQ-B1(1), 104AS-10.1.2-BQ-B1(1), and MOST 103-3114-Y-518-001 from the Bureau of Animal and Plant Health Inspection and Quarantine, Council of Agriculture, Executive Yuan, Taiwan.

## REFERENCES

1. Daszak P, Cunningham AA, Hyatt AD, Emerging infectious diseases of wildlife — threats to biodiversity and human health, *Science* **287**:443–449, 2000.

2. Woodford MH, Veterinary aspects of ecological monitoring: The natural history of emerging infectious diseases of humans, domestic animals and wildlife, *Trop Anim Health Prod* **41**:1023–1033, 2009.
3. Daszak P, Cunningham AA, Hyatt AD, Anthropogenic environmental change and the emergence of infectious diseases in wildlife, *Acta Trop* **78**:103–116, 2001.
4. Daszak P, Tabor GM, Kilpatrick AM *et al.*, Conservation medicine and a new agenda for emerging diseases, *Ann NY Acad Sci* **1026**:1–11, 2004.
5. Leroy EM, Rouquet P, Formenty P *et al.*, Multiple Ebola virus transmission events and rapid decline of central African wildlife, *Science* **303**:387–390, 2004.
6. Barbosa TF, Medeiros DB, Travassos da Rosa ES *et al.*, Molecular epidemiology of rabies virus isolated from different sources during a bat-transmitted human outbreak occurring in Augusto Correa municipality, Brazilian Amazon, *Virology* **370**:228–236, 2008.
7. Wandeler A, Virus infections of non-domestic carnivores: Rabies virus. in *Virus Infections of Carnivores*, Elsevier Science Publishers, 1987.
8. World Health O. WHO Expert Consultation on Rabies, Second Report, World Health Organ Tech Rep Ser 1–139, back cover, 2013.
9. Sartore S, Bonfanti L, Lorenzetto M *et al.*, The effects of control measures on the economic burden associated with epidemics of avian influenza in Italy, *Poult Sci* **89**:1115–1121, 2010.
10. Leong HK, Goh CS, Chew ST *et al.*, Prevention and control of avian influenza in Singapore, *Ann Acad Med Singapore* **37**:504–509, 2008.
11. Li Q, Zhou L, Zhou M *et al.*, Epidemiology of human infections with avian influenza A(H7N9) virus in China, *N Engl J Med* **370**:520–532, 2014.
12. Cowling BJ, Jin L, Lau EH *et al.*, Comparative epidemiology of human infections with avian influenza A H7N9 and H5N1 viruses in China: A population-based study of laboratory-confirmed cases, *Lancet* **382**:129–137, 2013.
13. Cox-Witton K, Reiss A, Woods R *et al.*, Emerging infectious diseases in free-ranging wildlife-Australian zoo based wildlife hospitals contribute to national surveillance, *PLoS One* **9**:e95127, 2014.
14. Stallknecht DE, Impediments to wildlife disease surveillance, research, and diagnostics, *Curr Top Microbiol Immunol* **315**:445–461, 2007.
15. Heisey DM, Jennelle CS, Russell RE *et al.*, Using auxiliary information to improve wildlife disease surveillance when infected animals are not detected: A Bayesian approach, *PLoS One* **9**:e89843, 2014.
16. Duncan C, Backus L, Lynn T *et al.*, Passive, opportunistic wildlife disease surveillance in the Rocky Mountain Region, USA, *Transbound Emerg Dis* **55**:308–314, 2008.
17. Liu Y, Zhang S, Wu X *et al.*, Ferret badger rabies origin and its revisited importance as potential source of rabies transmission in Southeast China, *BMC Infect Dis* **10**:234, 2010.
18. Mochizuki M, Hashimoto M, Hagiwara S *et al.*, Genotypes of canine distemper virus determined by analysis of the hemagglutinin genes of recent isolates from dogs in Japan, *J Clin Microbiol* **37**:2936–2942, 1999.

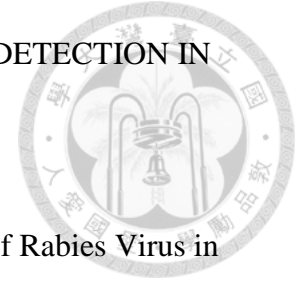
19. Qvarnstrom Y, Sullivan JJ, Bishop HS *et al.*, PCR-based detection of *Angiostrongylus cantonensis* in tissue and mucus secretions from molluscan hosts, *Appl Environ Microbiol* **73**:1415–1419, 2007.
20. Thompson JD, Higgins DG, Gibson TJ, Clustal W, Improving the sensitivity of progressive multiple sequence alignment through sequence weighting, position-specific gap penalties and weight matrix choice, *Nucleic Acids Res* **22**:4673–4680, 1994.
21. Chiou HY, Hsieh CH, Jeng CR *et al.*, Molecular characterization of cryptically circulating rabies virus from ferret badgers, Taiwan, *Emerg Infect Dis* **20**:790–798, 2014.
22. Martella V, Elia G, Buonavoglia C, Canine distemper virus, *Vet Clin North Am Small Anim Pract* **38**:787–797, vii–viii, 2008.
23. Beineke A, Puff C, Seehusen F *et al.*, Pathogenesis and immunopathology of systemic and nervous canine distemper, *Vet Immunol Immunopathol* **127**:1–18, 2009.
24. Terio KA, Craft ME, Canine distemper virus (CDV) in another big cat: Should CDV be renamed carnivore distemper virus? *MBio* **4**:e00702–00713, 2013.
25. Ikeda Y, Nakamura K, Miyazawa T *et al.*, Seroprevalence of canine distemper virus in cats, *Clin Diagn Lab Immunol* **8**:641–644, 2001.
26. Chen CC, Pei KJ, Liao MH *et al.*, Canine distemper virus in wild ferret-badgers of Taiwan, *J Wildl Dis* **44**:440–445, 2008.
27. Schulz W, Exudative epidermitis of the piglet (piglet eczema)—etiology and pathogenesis with special reference to *Staphylococcus hyicus*. I. Literature review, *Monatsh Veterinarmed* **25**:428–435, 1970.
28. Amsberg G, Animal experimental studies on the pathogenesis of localized and generalized swine exudative eczema and polyarthritis due to *Staphylococcus hyicus*, *Dtsch Tierarztl Wochenschr* **85**:433–438, 1978.
29. Phillips WE, Jr., King RE, Kloos WE, Isolation of *Staphylococcus hyicus* subsp *hyicus* from a pig with septic polyarthritis, *Am J Vet Res* **41**:274–276, 1980.
30. Roberson JR, Fox LK, Hancock DD *et al.*, Prevalence of coagulase-positive staphylococci, other than *Staphylococcus aureus*, in bovine mastitis, *Am J Vet Res* **57**:54–58, 1996.
31. Osterlund A, Nordlund E, Wound infection caused by *Staphylococcus hyicus* subspecies *hyicus* after a donkey bite, *Scand J Infect Dis* **29**:95, 1997.
32. Casanova C, Iselin L, von Steiger N *et al.*, *Staphylococcus hyicus* bacteremia in a farmer, *J Clin Microbiol* **49**:4377–4378, 2011.
33. Carreno RA, Nadler SA, Phylogenetic analysis of the Metastrongyloidea (Nematoda: Strongylida) inferred from ribosomal RNA gene sequences, *J Parasitol* **89**:965–973, 2003.
34. OuYang L, Wei J, Wu Z *et al.*, Differences of larval development and pathological changes in permissive and nonpermissive rodent hosts for *Angiostrongylus cantonensis* infection, *Parasitol Res* **111**:1547–1557, 2012.
35. Davidson RK, Handeland K, Gjerde B, The first report of *Aelurostrongylus falciformis* in Norwegian badgers (*Meles meles*), *Acta Vet Scand* **48**:6, 2006.
36. Alic A, Hodzic A, Kadric M *et al.*, *Pearsonema plica* (*Capillaria plica*) infection and associated urinary bladder pathology in red foxes (*Vulpes vulpes*) from Bosnia and Herzegovina, *Parasitol Res* **114**: 1933–1938, 2015.
37. Nimmervoll H, Hoby S, Robert N *et al.*, Pathology of sarcoptic mange in red foxes (*Vulpes vulpes*): Macroscopic and histologic characterization of three disease stages, *J Wildl Dis* **49**:91–102, 2013.
38. Chen CC, Pei KJ, Lai YC *et al.*, Participatory epidemiology to assess sarcoptic mange in serow of Taiwan, *J Wildl Dis* **48**:869–875, 2012.
39. Feldman SH, Ramirez MP, Molecular phylogeny of *Pseudocapillaroides xenopi* (Moravec et Cosgrove 1982) and development of a quantitative PCR assay for its detection in aquarium sediment, *J Am Assoc Lab Anim Sci* **53**:668–674, 2014.
40. Iglauer F, Willmann F, Hilken G *et al.*, Anthelmintic treatment to eradicate cutaneous capillariasis in a colony of South African clawed frogs (*Xenopus laevis*), *Lab Anim Sci* **47**:477–482, 1997.
41. Ramiro-Ibanez F, Winston J, O'Donnell E *et al.*, Ulcerative pododermatitis in a cat associated with *Anatrichosoma* sp, *J Vet Diagn Invest* **14**:80–83, 2002.
42. Noden BH, Du Plessis EC, Morkel C *et al.*, *Anatrichosoma* sp. in the footpads of a cat: Diagnosis and pathology of Namibian case, *Vet Parasitol* **191**:386–389, 2013.
43. Nunez FA, Trichuris, *Capillaria* or *Anatrichosoma*? [corrected], *Parasitol Int* **59**:303, 2010.

# Chapter III



## **Pathological Characterization and Molecular Detection of Rabies Virus in the Rabid Ferret Badgers of a Recent Outbreak in Taiwan**

*Authors: Hue-Ying Chiou, Chian-Ren Jeng, Hurng-Yi Wang, Satoshi Inoue, Fang-Tse Chan, Jiunn-Wang Liao, Ming-Tang Chiou, Victor Fei Pang, Title of article: Pathological Characterization and Molecular Detection of Rabies Virus in the Rabid Ferret Badgers of a Recent Outbreak in Taiwan, Journal of Wildlife Diseases, 2015, accepted for publication*



1 **Running head:** CHIOU ET AL. –PATHOLOGY AND VIRAL DETECTION IN

2 RABID TWFBs

3 **Full title:** Pathological Characterization and Molecular Detection of Rabies Virus in

4 the Rabid Ferret Badgers of a Recent Outbreak in Taiwan

5 **Authors:** Hue-Ying Chiou<sup>1</sup>, Chian-Ren Jeng<sup>1,2</sup>, Hurng-Yi Wang<sup>3</sup>, Satoshi Inoue<sup>4</sup>,

6 Fang-Tse Chan<sup>5</sup>, Jiunn-Wang Liao<sup>6</sup>, Ming-Tang Chiou<sup>7</sup>, Victor Fei Pang<sup>1,2</sup>

7 <sup>1</sup> Graduate Institute of Veterinary Medicine, School of Veterinary Medicine, National

8 Taiwan University, Taipei 10617, Taiwan, ROC

9 <sup>2</sup> Graduate Institute of Molecular and Comparative Pathobiology, School of

10 Veterinary Medicine, National Taiwan University, Taipei 10617, Taiwan, ROC

11 <sup>3</sup> Graduate Institute of Clinical Medicine, College of Medicine, National Taiwan

12 University, Taipei 10048, Taiwan, ROC

13 <sup>4</sup> Laboratory of Transmission Control of Zoonosis, Department of Veterinary Science,

14 National Institute of Infectious Diseases, Tokyo 162-8640, Japan

15 <sup>5</sup> Endemic Species Research Institute, Council of Agriculture, Executive Yuan,

16 Nantou 55244, Taiwan, ROC

17 <sup>6</sup> Graduate Institute of Veterinary Pathobiology, College of Veterinary Medicine,

18 National Chung Hsing University, Taichung 40227, Taiwan, ROC

19 <sup>7</sup> Department of Veterinary Medicine, College of Veterinary Medicine, National

20 Pingtung University of Science and Technology, Pingtung 91201, Taiwan, ROC

21

22 **Corresponding Author:**

23 Victor Fei Pang, Graduate Institute of Molecular and Comparative Pathobiology,

24 School of Veterinary Medicine, National Taiwan University, No.1, Sec. 4, Roosevelt

25 Rd., Taipei 10617, Taiwan, ROC

26 TEL: +886-2-33663867

27 FAX: +886-2-23621965

28 E-mail: pang@ntu.edu.tw

29

30

31 **TEXT – 3980 words**

32





33 **Abstract**

34       Until the rabid cases of Taiwan ferret badger (TWFB) (*Melogale moschata*  
35 *subaurantiaca*) were diagnosed in mid-June of 2013, Taiwan had been considered as a  
36 rabies-free region for more than 50 years. Although rabies had also been reported in  
37 ferret badgers in China, the pathological changes and distribution of viral antigens of  
38 ferret badger-associated rabies have not yet been described. Here, a comprehensive  
39 pathological study and molecular detection of rabies virus (RABV) were performed in  
40 three necropsied rabid TWFBs. In addition, retrospective evaluation of archival  
41 paraffin-embedded tissue blocks of six other TWFBs, obtained from different  
42 diagnostic laboratories, necropsied during 2004 and 2012 was also performed. As  
43 seen in other RABV-infected animal species, the characteristic pathological changes  
44 in TWFBs were nonsuppurative meningoencephalomyelitis, ganglionitis, and  
45 formation of typical intracytoplasmic Negri bodies with brain stem affected the most.  
46 Additionally, variable spongiform degeneration, primarily in the perikaryon of  
47 neurons and neuropil, was observed in the cerebral cortex, thalamus, and brain stem.  
48 In the non-nervous tissue, representative lesions included adrenal necrosis and  
49 lymphocytic interstitial sialoadenitis. By immunohistochemical (IHC) staining as well  
50 as fluorescent antibody test (FAT), viral antigens were detected in the perikaryon of  
51 the neurons and axonal and/or dendritic processes throughout the nervous tissue and



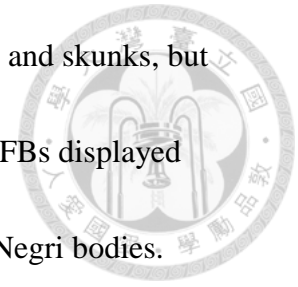
52 in the macrophages scattered in various tissues. Similar to raccoons and skunks, but  
53 unlike dogs, cats, cattle, and horses, the nervous tissue of rabid TWFBs displayed  
54 widely dispersed lesions, RABV antigens and/or large numbers of Negri bodies.  
55 Retrospective study could trace the earliest rabid TWFB case back to 2004 by  
56 histopathology and IHC staining. This is the first report regarding the characteristic  
57 pathological changes and viral antigen distribution in TWFBs naturally infected by  
58 the strain of FB-associated RABV.

59

60 **Keywords:** Taiwan ferret badger, *Melogale moschata subaurantiaca*, Rabies,

61 Pathology, Immunohistochemistry

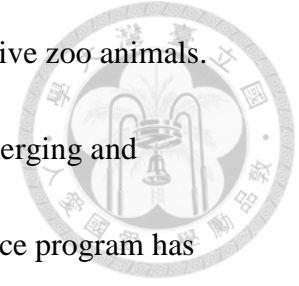
62





## 63 **Introduction**

64 Rabies, possibly the oldest zoonotic disease, is caused by the rabies virus  
65 (RABV), belonging to the *Lyssavirus* of Rhabdoviridae. It is a worldwide disease and  
66 only a small number of countries and regions are free from this disease. The RABV  
67 infects nearly all warm-blooded animals (Jackson and Fu 2013). According to World  
68 Health Organization (WHO), there were over 60,000 rabies-associated human deaths  
69 worldwide in 2010, primarily in Africa and Asia (WHO 2013). Dogs are considered  
70 as the principal host of the disease in developing countries. Wildlife has become the  
71 most important source of RABV infection in many developed countries due to well  
72 established canine vaccination programs (Wandeler 1987; Blanton et al. 2007). The  
73 disease is generally regarded as having a single-species reservoir with spillover to other  
74 dead-end hosts (Smith and Wilkinson 2002; Krebs et al. 2003). Bats, raccoons, skunks,  
75 and foxes are regarded as the main reservoir and vector of rabies (Jackson 2008).  
76 Mustelids, including *Melogale*, *Meles*, and *Mellivora* of the weasel family Mustelidae,  
77 are also susceptible to rabies (Smith 2002). Chinese ferret badgers (CNFBs)  
78 (*Melogale moschata moschata*) have been considered as a primary rabies host and  
79 source of human rabies in southeast China (Zhang et al. 2009; Liu et al. 2010).  
80 Active/passive wildlife disease surveillance has long been carried out in Taiwan with  
81 government support; however, due to the limited species and populations of native



82 wild-ranging wild animals, the targets were mainly focused on captive zoo animals.  
83 Because of the increased importance of wild-ranging wildlife in emerging and  
84 re-emerging diseases of animals and humans, the disease surveillance program has  
85 readjusted and started to include native wild-ranging wildlife since 2011. Through this  
86 program, carcasses of native wild-ranging wildlife have been submitted routinely to  
87 the selected laboratories for necropsy and further examination since 2012. Until the  
88 first three rabid Taiwan FBs (TWFBs) (*M. moschata subaurantiaca*) were diagnosed in  
89 mid-June of 2013 through this program (Chiou et al. 2014), Taiwan had been  
90 considered as a rabies-free region for more than 50 years with the last autochthonous  
91 human and animal rabies cases recorded in 1959 and 1961, respectively.

92 In natural or experimental RABV infection, non-suppurative  
93 meningoencephalomyelitis, ganglionitis, and sialoadenitis are the characteristic  
94 histopathological findings (Maxie and Youssef 2007). However, the lesion severity  
95 and distribution and the amount and distribution of viral antigens are variable,  
96 depending on the host, viral strain, and clinical course (Hicks et al. 2009; Stein et al.  
97 2010). Although FB-associated rabies had been reported in China (Zhang et al. 2009;  
98 Liu et al. 2010), the associated pathological changes and viral antigen distribution have  
99 not yet been described. The information is essential for establishing more accurate  
100 sampling and diagnosis modalities for FB-associated rabies, especially when composite



101 sampling is not feasible. The objective of the present study was to characterize the  
102 pathological changes and the pattern of viral antigen distribution regarding the recent  
103 rabies outbreak in TWFBs.

104

## 105 **Materials and Methods**

### 106 **Animals**

107       During May 2012 and January 2013, three female adult TWFBs were rescued  
108 from central Taiwan and submitted to the wildlife first aid station for treatment.  
109 Clinically, TWFB No.1 showed signs of emaciation, coma, paddling, loss of pain  
110 response, and reduced body temperature with a 2 cm skin wound on the chin; TWFB  
111 No.2 was extremely weak and unable to move; and TWFB No.3 displayed signs of  
112 weakness, labored breathing, increased breath sound, hypersalivation, and exuding of  
113 foamy fluid from the mouth and nose. Initial supportive treatment was provided, but  
114 they died within 1-3 days and were then submitted to National Taiwan University for  
115 routine disease surveillance.

116

### 117 **Sample collection**

118       Full necropsy was performed in TWFB No.1-3, the entire brain and  
119 representative tissue samples from other major organs were collected. The 1<sup>st</sup> (C1)

120 and 2<sup>nd</sup> (C2) segments of cervical spinal cord and submandibular salivary gland were  
121 also collected from TWFB No.3. All samples were fixed in 10% neutral buffered  
122 formalin. Representative sections of various parts of the brain, C1/C2 spinal cord, and  
123 other tissues were processed for routine embedding in paraffin wax.

124 Retrospectively, various formalin-fixed and paraffin-embedded tissue blocks,  
125 containing cerebrum and/or cerebellum, from six other TWFBs, including 1  
126 necropsied in 2004 (TWFB No.4), 2 in 2006, 2 in 2011, and 1 in 2012, kindly  
127 provided by other diagnostic laboratories were also included in the study. Within the  
128 six TWFBs, the TWFB No.4 (female) and one obtained in 2011 (TWFB No.5) (male)  
129 were extremely weak when they were found, but died in the next day on arrival the  
130 rescue station; other four TWFBs were road-kills. All six carcasses had been frozen  
131 for certain periods of time before sent for necropsy and displayed variable  
132 postmortem autolysis. Apart from paraffin blocks, no other frozen tissues were  
133 available.

134

### 135 **Histopathological examination**

136 All tissue blocks were sectioned at 5  $\mu$ m, stained with hematoxylin and eosin  
137 (HE), and examined by light microscopy. Based on the frequency and severity, the  
138 lesions of nervous and non-nervous system were further graded as mild, moderate or

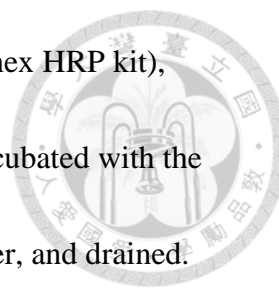
139 severe.

140

141 **Immunohistochemical (IHC) staining**

142 The IHC staining was performed using the advanced Super Sensitive™  
143 Polymer-HRP IHC Detection System (BioGenex Lab., Fremont, CA, USA) according  
144 to the manufacturer's instructions with a mouse anti-RABV glycoprotein IgG2a  
145 monoclonal antibody (Abcam Inc., Boston, MA, USA) or a rabbit anti-attenuated  
146 challenge virus strand (aCVSr) nucleoprotein polyclonal antibody kindly provided by  
147 Laboratory of Transmission Control of Zoonosis, Department of Veterinary Science,  
148 National Institute of Infectious Diseases, Japan. Serial tissue sections at 5 µm were  
149 laid on coated slides, deparaffinized, rehydrated in ethanol successively from 100% to  
150 70%, and washed in deionized water (DW). After treatment with 100 µg/ml  
151 proteinase K (AppliChem Inc, St. Louis, MO, USA), the tissue slides were washed in  
152 Tris-buffered saline Tween-20 (TBST) buffer and incubated in 3% H<sub>2</sub>O<sub>2</sub> to quench the  
153 endogenous peroxidase. After rinsing with DW and washed in TBST buffer, the tissue  
154 slides were incubated with the PowerBlock reagent (BioGenex universal blocking  
155 reagent). Following rinsed with DW and washed in TBST buffer, the tissue slides were  
156 incubated with the anti-RABV glycoprotein IgG2a monoclonal antibody at 1:500  
157 dilution or with the anti-aCVSr nucleoprotein polyclonal antibody at 1:5000 dilution,



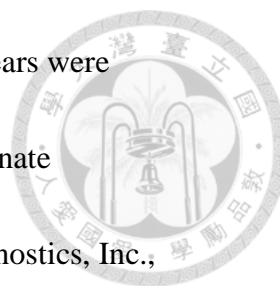


158 washed in TBST buffer, incubated with the SuperEnhancer (BioGenex HRP kit),  
159 washed in TBST buffer, and drained. The tissue slides were then incubated with the  
160 Polymer-HRP reagent (BioGenex HRP kit), rinsed with TBST buffer, and drained.  
161 Following treatment with chromogen-AEC (BioGenex HRP kit), the slides were  
162 rinsed with TBST buffer, counterstained with Mayer's hematoxylin, rinsed with DW,  
163 and then covered with coverslip using aqueous mounting media. Positive and negative  
164 controls were run parallel in each assay. The positive control was an IHC  
165 staining-positive brain tissue block from a rabid bovine case kindly provided by Dr.  
166 Chuen B. Hong at Kentucky University. Negative controls included corresponding  
167 tissue sections from RABV-negative TWFBs and substituting the monoclonal  
168 antibody with phosphate buffered saline (PBS). Samples were considered positive for  
169 rabies only when distinct red-brown finely to clumped granular cytoplasmic deposits  
170 were revealed in the samples and positive control but not in the negative controls.

171

## 172 **Fluorescent antibody test (FAT)**

173 For FAT, brain smears prepared with a frozen ground composite brain tissue  
174 suspension of cerebrum, hippocampus, thalamus, and hypothalamus left from a  
175 preparation for RNA extraction from each of TWFB No.1-3 were air-dried and fixed  
176 in acetone (Merck). Following 3 PBS washes and air-dry, direct (DFA) or indirect



177 (IFA) immunofluorescence assay was performed. For DFA, the smears were  
178 incubated with a commercially available FDI fluorescein isothiocyanate  
179 (FITC)-conjugated anti-rabies monoclonal globulin (Fujirebio Diagnostics, Inc.,  
180 Malvern, PA, USA) with 3 PBS washes. For IFA, the smears were incubated with the  
181 primary anti-RABV glycoprotein IgG2a monoclonal antibody (Abcam) at 1:500  
182 dilution with 3 PBS washes, and then stained with an FITC-conjugated goat  
183 anti-mouse IgG antibody (Bethyl Lab., Inc., Montgomery, TX, USA) with 3 PBS  
184 washes. The stained smears, with either DFA or IFA, were then counterstained with  
185 Hoechst stain at 1:200 dilution (Sigma-Aldrich Co., St. Louis, MO, USA) followed by  
186 immediate PBS wash. The positive-viral antigens appeared as apple-green fluorescent  
187 finely to clumped granular aggregates under the fluorescent microscope (Optiphot II,  
188 Nikon, Tokyo, Japan).

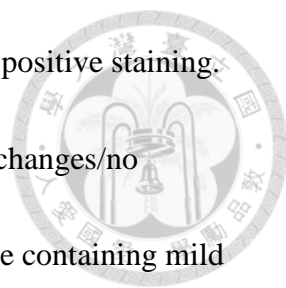
189

#### 190 **Assessment of the histopathological changes and the results of**

#### 191 **immunohistochemical and immunofluorescent stainings**

192 The histopathological changes and the results of IHC and immunofluorescent  
193 stainings were scored in a semiquantitative fashion according to the severity and  
194 distribution of the lesion as well as the intensity and frequency of the positive signals  
195 of a specific staining. The score was determined on the basis of the percentage of the  
196 entire section of a particular tissue with lesion involvement and the percentage of





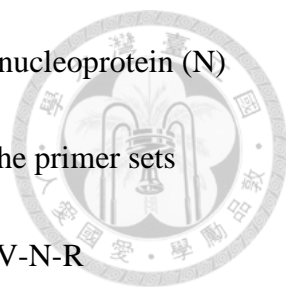
197 neurons in the entire section of a particular tissue or smear showing positive staining.  
198 The scoring system consisted of four categories, -: no pathological changes/no  
199 positive staining ; +: < 25% of the entire section of a particular tissue containing mild  
200 to moderate pathological changes/< 25% of the neurons in the entire section of a  
201 particular tissue or in the entire smear containing weak to moderate positive staining;  
202 ++: 25-50% of the entire section of a particular tissue containing mild to severe  
203 pathological changes/25-50% of the neurons in the entire section of a particular tissue  
204 or in the entire smear containing weak to strong positive staining; +++: > 50% of the  
205 entire section of a particular tissue containing severe pathological changes/> 50% of  
206 the neurons in the entire section of a particular tissue or in the entire smear containing  
207 strong positive staining.

208

## 209 **Reverse transcription polymerase chain reaction (RT-PCR) and sequence**

### 210 **analysis**

211 For fresh brain, 25 mg tissue were mixed with 1 ml of TRIzol reagent  
212 (Invitrogen, CA, USA) and homogenized. Following adding 0.2 ml of chloroform and  
213 centrifuged at 12,000 xg for 15 min, the upper aqueous phase was collected for total  
214 RNA extraction by using RNeasy Mini Kit (Qiagen, CA, USA) followed by cDNA  
215 synthesis with the Transcriptor first strand cDNA synthesis kit (Roche Diagnostics,



216 IN, USA) according to the manufacturer's instructions. The RABV nucleoprotein (N)  
217 and glycoprotein (G) genes were then amplified by RT-PCR using the primer sets  
218 RV-N-F (1-25): 5'-ACGCTTAACAACAAAACCATAGAAG-3'/RV-N-R  
219 (1515-1538): 5'-CGGATTGACGAAGATCTTGCTCAT-3' and RV-G-F  
220 (3291-3315): 5'-CATCCCTCAAAAGACTTAAGGAAAG-3'/RV-G-R (4918-4941):  
221 5'-CCGAGGAGATGAGGTCTTCGGGAC-3', respectively, as described (Liu et al.,  
222 2010); the amplicon sizes were 1300 and 500 bp, respectively. For paraffin-embedded  
223 brain tissue, 10 pieces of 10 µm sections from each of the six archival cases and  
224 TWFB No.1-3 were deparaffinized with xylene. Following centrifugation, the cell  
225 pellets were collected for RNA extraction by using the RNeasy FFPE kit (Qiagen) and  
226 subsequent cDNA synthesis according to the manufacturer's instructions. The RABV  
227 N gene was then amplified by RT-PCR using 2 primer sets P4(509): 5'  
228 -GAGAAGGAACT(C/T)CA(G/T)GAGTA-3'/P4(110BT): 5'  
229 -(G/T)TTCACATGTTCGAGTAT-3' and S4(CN12): 5'  
230 -AATCTCACCGCGAGAGAGG-3'/S4(CN13): 5'  
231 -GTGGCATTAAAGAGACCTGAC-3' as described (Wacharapluesadee et al. 2006);  
232 the amplicon sizes were 150 and 236 bp, respectively. The amplicons obtained were  
233 further sequenced (Tri-IBiotech, Inc, Taipei, Taiwan) and compared with those viral  
234 sequences deposited in GenBank/EMBL/DDBJ

235 (<http://www.ncbi.nlm.nih.gov/BLAST>).

236

## 237 **Results**

### 238 **Pathological changes**

#### 239 **Gross findings**

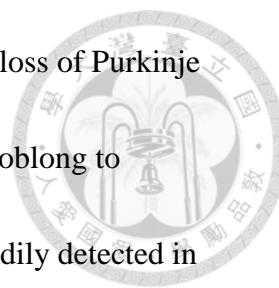
240       Aside from poor nutritional condition (TWFB No.1), moderate lung edema  
241 (TWFB No.3), and congested leptomeninges (TWFB No.1-3), no other significant  
242 changes were observed.

243

#### 244 **Histopathological findings**

245       In the nervous tissue, nonsuppurative meningoencephalomyelitis and/or  
246 ganglionitis with formation of Negri bodies were seen in TWFB No.1-3, and archival  
247 TWFB No.4 and 5 (Table 1). The lesions consisted of multifocal, mild to severe  
248 infiltration of lymphocytes and plasma cells mixed with some macrophages,  
249 eosinophils and/or neutrophils in the leptomeninges and/or Virchow-Robin spaces of  
250 the gray matter (Fig. 1A) and part of the white matter throughout the brain and C1/C2  
251 spinal cord. Except for cerebellum, variable gliosis was present throughout the  
252 neuropil (Fig. 1A). Many neurons are undergoing degeneration and necrosis,  
253 characterized by variable cytoplasmic hyper-eosinophilia, atrophy and/or





254 vacuolization, karyorrhexis, and/or loss of cell integrity. Segmental loss of Purkinje  
255 cells was noted in the cerebellum. Varying numbers of round, oval, oblong to  
256 irregular, discrete to amorphous, eosinophilic Negri bodies were readily detected in  
257 the cytoplasm of the neuronal bodies and nervous processes throughout the brain (Fig.  
258 1B), C1/C2 spinal cord, and ganglia (Table 1 and 2) (Fig. 1C).

259 Spongiform degeneration characterized by focal to multifocal variable neuronal  
260 perikaryon and/or neuropil vacuolization was noted in the cerebral cortex, thalamus,  
261 brainstem, and junction of the granular and Purkinje cell layers of cerebellum of  
262 TWFB No.1-3 (Fig. 1D). The vacuoles were round, oval to polygonal and variable in  
263 sizes; they were empty or contained some amorphous membranous to granular  
264 structure and/or proteinaceous substance. In TWFB No.4 and 5, postmortem autolysis  
265 precluded a satisfactory evaluation of the spongiform degeneration.

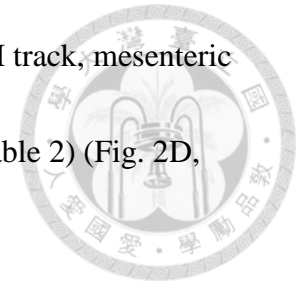
266 Mild to severe ganglionitis, characterized by lymphocytic infiltration mixed with  
267 other inflammatory cells, degeneration and necrosis of ganglion cells similar to those  
268 seen in the neurons, and formation of Negri bodies, was observed in the peri-adrenal,  
269 peri-renal, and myenteric plexus ganglia (Fig. 1C). Areas of necrosis accompanied  
270 with infiltration of mixed inflammatory cells were seen in the adrenal cortex (Fig. 1E,  
271 1F) and/or medulla of TWFB No.1-3. In addition, the submandibular salivary gland of  
272 TWFB No. 3 had scattered mild lymphocyte infiltration in the interstitium.

273

274 **RABV antigen detection by immunohistochemical staining**



275 Apparent but variable IHC-positive signals for RABV antigens were revealed in  
276 TWFB No.1-3 (Fig. 2A) and TWFB No.4 and 5, in which the earliest positive case,  
277 TWFB No.4, occurred in 2004 (Fig. 2B). There were no apparent differences in the  
278 distribution, intensity, and frequency of the positive signals by using the mouse  
279 anti-RABV glycoprotein IgG2a monoclonal antibody or the rabbit anti-aCVS<sub>r</sub>  
280 nucleoprotein polyclonal antibody (data not shown). The positive signals were  
281 observed almost exclusively in the gray matter of cerebrum and cerebellum, and in the  
282 hippocampus, thalamus, hypothalamus, brainstem, and gray matter of the C1/C2  
283 spinal cord (Table 1) (Fig. 2A, 2B). The positive signals were characterized as  
284 sparsely to widely distributed, finely to clumped granules throughout the perikaryon  
285 of the neurons and the axonal and/or dendritic processes. Similar positive signals  
286 could also be detected in the ganglion cells of peri-adrenal, peri-renal (Fig. 2C),  
287 sublingual, and myenteric plexus ganglia, skin, trachea, bronchi, heart, and pancreas;  
288 nerve bundles of the submucosa and tunica muscularis of GI tract; acinar epithelial  
289 cells and ganglion cells of the submandibular salivary gland; remaining parenchymal  
290 cells and infiltrating macrophages of the adrenal necrotic regions (Fig. 1F inset); as  
291 well as macrophages (lysozyme positive, toluidine blue negative) randomly scattered



292 in the mucosa, submucosa, and muscular layer of the tongue and GI track, mesenteric  
293 adipose tissue, dermis, urinary bladder, heart, and Kupffer cells (Table 2) (Fig. 2D,  
294 2E).

295

### 296 **RABV antigen detection by fluorescent antibody test**

297 By DFA or IFA, apparent immunofluorescent positive signals were readily  
298 observed in the brain smears of TWFB No.1-3. Strongly positive, finely to clumped  
299 granular to global signals were seen in the neuronal perikaryon, nervous processes,  
300 and amorphous tissue debris (Table 1) (Fig. 2F).

301

### 302 **RABV nucleic acid detection by RT-PCR and sequence analysis**

303 By using fresh brain tissue, the results of RT-PCR (Fig. 3) and subsequent  
304 sequence analysis of the N and G genes confirmed that TWFB No.1-3 were  
305 RABV-infected. By using paraffin-embedded brain tissues, the RT-PCR also  
306 demonstrated specific amplicons of N gene with the anticipated sizes of 150 and 236  
307 bp in TWFB No.1-3, but failed to demonstrate any detectable amplicons in the six  
308 archival cases which were run parallel (data not shown). The strain of RABV of  
309 TWFBs (RABV-TWFB) belongs to *lyssavirus* genotype 1 and the nucleotide identity  
310 of the N gene within the 3 isolates of TWFB No.1-3 was 97-99%. The N gene of the 3

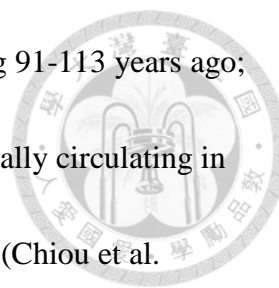


311 RABV-TWFB isolates showed an 89-90% identity to the CNFB isolates (F02, F04,  
312 JX08-45, JX08-48, JX09-18), 91% to the dog-related RABV within the China I  
313 lineage (HN10, GD-SH-01, CTN-1, CTN-181), 88% to the Southeast Asia dog isolate  
314 (QS-05), 88% to the dog-related RABV isolates within the China II lineage (JX09-17,  
315 SH06), 86-87% to the cosmopolitan isolates (serotype 1, FluryLEP, DRV-NG11,  
316 9147FRA, SAD B19), 87% to the golden palm civet and human India isolates  
317 (H-08-1320, H-1413-09), and 84% to the North American bat-related RABV  
318 (SHBRV-18).

319

## 320 **Discussion**

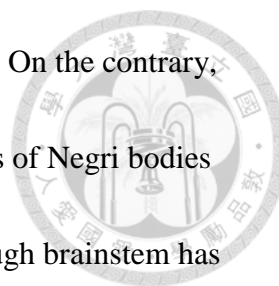
321 Aside from China, Taiwan is the second region in the world where FB-associated  
322 rabies has been diagnosed. The TWFB-associated rabies was diagnosed based on 1)  
323 characteristic pathological findings of non-suppurative meningoencephalomyelitis,  
324 ganglionitis, and Negri bodies; 2) positive IHC staining and DFA/IFA test for RABV  
325 antigens; and 3) positive viral nucleic acid detection by RT-PCR followed by genomic  
326 sequencing (GenBank accession numbers KF620487-KF620489) (Chiou et al. 2014)  
327 in TWFB No.1-3 collected during 2012 and 2013. The most recent phylogeographic  
328 study has shown that the RABV-TWFB is a distinct lineage within the Asian group  
329 and has been differentiated from the RABV of CNFBs 158-210 years before present



330 with the most recent common ancestor of RABV-TWFB originating 91-113 years ago;  
331 and the data suggest that the RABV-TWFB could have been cryptically circulating in  
332 the environment without being recognized for a long period of time (Chiou et al.  
333 2014). The result of retrospective study, which could trace the occurrence of  
334 TWFB-associated rabies back to more than 10 years ago, further supports this  
335 speculation. However, the postmortem autolysis and limited paraffin-blocks of  
336 archival brain tissues preclude satisfactory morphological and molecular evaluation.  
337 Following the diagnosis of rabies in TWFB No.1-3, rabies has been diagnosed by  
338 FAT in additional 459 TWFBs, 5 gem-faced civets (*Paguma larvata*), 1 shrew, and 1  
339 FB-bitten puppy by May 7, 2015 (data not shown).

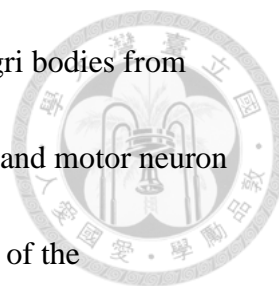
340 In rabid TWFBs, lesions and RABV antigens were widely distributed in the  
341 brainstem, cerebrum, cerebellum, anterior cervical spinal cord, peri-adrenal, peri-renal,  
342 and myenteric plexus ganglia, and adrenal gland. Similar extensive lesion and/or  
343 RABV antigen distribution in the central nervous system (CNS) has also been seen in  
344 naturally acquired rabid raccoons and skunks (Stein et al. 2010; Hamir 2011).  
345 However, hippocampus, brainstem/cerebellum, and cervical spinal cord/adjacent  
346 brainstem were the best site for RABV antigen detection in dogs/cats, cattle, and  
347 horses, respectively (Stein et al. 2010). In carnivores and herbivores/humans,  
348 hippocampus and Purkinje cells of cerebellum are the common sites for finding Negri





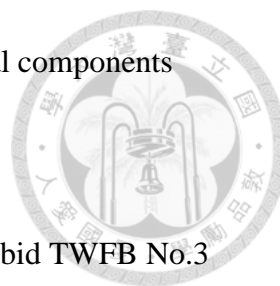
349 bodies, respectively (Jackson et al. 2001; Maxie and Yousset 2007). On the contrary,  
350 TWFBs, similar to raccoons, have widely distributed, large numbers of Negri bodies  
351 readily observed in both central and peripheral neural tissues, although brainstem has  
352 a better detection rate.

353       The formation of Negri bodies in the neural tissue of a rabid animal seems  
354 related to the type of viral isolate to which the animal is exposed. A previous study  
355 showed that raccoons infected with the raccoon isolate developed numerous neuronal  
356 Negri bodies in the CNS and ganglion cells of non-CNS tissues; however, dog or bat  
357 isolate resulted in the formation of either no or only occasional Negri bodies in  
358 raccoons (Hamir 2011). Suspicious natural canine isolate-induced rabies cases in  
359 CNFBs have been reported in China (Zhang et al. 2009). If the RABV  
360 strain-dependent phenomenon observed in raccoons also occurs in FBs, the presence  
361 of large numbers of Negri body in the neural tissue of the rabid TWFBs along with  
362 the results of nucleotide identity of the N gene between RABV-TWFB isolates and  
363 other known RABV isolates may further support that the RABV-TWFB is a distinct  
364 lineage and has been circulating in TWFB population for some times, instead of a  
365 recent spill-over from a canine or bat source. However, this assumption requires  
366 further clarification.



367 In some animal species, care must be taken to differentiate Negri bodies from  
368 nonspecific inclusions such as Hirano, Pick, Lewy, Lafora, Bunina, and motor neuron  
369 disease inclusion bodies that have been found in the pyramidal cells of the  
370 hippocampus or the lateral geniculate nucleus neurons in cats, skunks, dogs, and  
371 horses and in the larger neurons of the medulla and spinal cord of old sheep and cattle  
372 (Maxie and Youssef 2007). Owing to the fact that TWFBs are susceptible to canine  
373 distemper virus (CDV) infection (Chen et al. 2008), intracytoplasmic CDV inclusion  
374 bodies should also be considered as a possible differentiation. However, aside from  
375 non-suppurative meningoencephalitis and neuronal intracytoplasmic inclusions as  
376 seen in rabid TWFBs, CDV-infected TWFBs may also have neuronal and/or glial  
377 intranuclear inclusions (Chen et al. 2008). Based on the results of pathological  
378 findings and RABV antigen detection, brainstem seems an ideal place for sampling  
379 and diagnosing FB-associated RABV infection, although cerebral cortex,  
380 hippocampus, thalamus or hypothalamus is also suitable.

381 The spongiform change seen in the brain of rabid TWFBs is similar to that  
382 reported in RABV-infected skunks and foxes (Charlton 1984; Charlton et al. 1987)  
383 and a heifer (Foley and Zachary 1995). The pathogenesis of such change in the rabid  
384 animals is unclear. Electron-microscopic findings suggested the lesion development  
385 starting gradationally from small to large membrane-bound vacuoles in the neuronal



386 processes, primarily dendrites, with no need of incorporation of viral components

387 (Charlton et al. 1987).

388 The changes seen in the submandibular salivary gland of the rabid TWFB No.3

389 are similar to those seen in the parotid salivary gland of those experimentally

390 RABV-infected skunks and foxes, characterized as an interstitial sialoadenitis

391 (Balachandran and Charlton 1994). They also share a similar scattered distribution

392 pattern of RABV antigens in the ganglia, nerve bundles, and acinar epithelial cells

393 (Balachandran and Charlton 1994). The positive result of the RT-PCR of saliva swab

394 obtained from the rabid TWFB No.3 further demonstrated that RABV nucleic acid

395 was also produced and released (unpublished data).

396 To our knowledge, adrenal necrosis has not been described as a rabies-associated

397 histopathological change in rabid animals so far, although Negri bodies have been

398 found in the ganglion cells of the adrenal medulla (Hamir et al. 1992). Scattered to

399 significant amounts of IHC staining-positive signals for RABV antigens were seen in

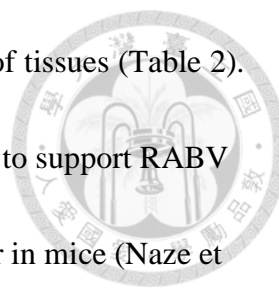
400 the remaining parenchymal cells and some macrophages located in the necrotic areas

401 of both cortex and medulla, but not in the neuron and/or nerve fibers within the

402 parenchyma. Although RABV antigens were detected in the remaining adrenal

403 parenchymal cells in the necrotic regions, whether the necrosis is directly

404 RABV-induced requires further elucidation. Aside from the adrenal gland, sporadic

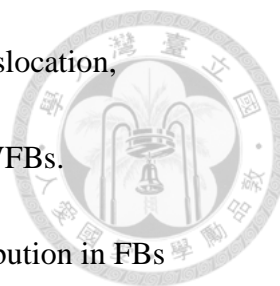


405 IHC staining-positive macrophages could also be seen in a variety of tissues (Table 2).  
406 A recent study has shown that although macrophages are less likely to support RABV  
407 production, they can act as a source of infectious virus upon transfer in mice (Naze et  
408 al. 2013). This may explain why IHC-positive RABV antigens could be detected in  
409 the macrophages widely distributed in various tissues in the present study.

410 The currently accumulated data show that the FB-associated RABV infection in  
411 Taiwan still occurs mainly in TWFBs, although sporadic spill-over to other animal  
412 species occurs. The gradual increase in the population of TWFBs in the past 10 years  
413 has been considered possibly playing certain role on the recent outbreak; however,  
414 whether there is (are) other co-factor(s) or other cause(s) is not known and requires  
415 further investigation. The origin of the TWFB-associated RABV is an interesting but  
416 remaining answered question. The earliest written record of rabies in Taiwan was in  
417 the early nineteen century when Taiwan was under Japanese colonization.

418 Human-mediated animal translocation and animal self-movement are considered to  
419 play the major role on the dispersal of RABV (Fèvre et al. 2006; Bourhy et al. 2008).

420 The dog has been suggested to serve as the main vector for inter-species RABV  
421 transmission, through which viral lineages are generated and then spread to other taxa  
422 (Bourhy et al. 2008). Taiwan is an island and, aside from being ruled by Chinese, it  
423 has also been colonized by Spanish, Dutch, and Japanese for various time periods.



424 Thus, it is reasonable to speculate that human-mediated animal translocation,  
425 especially dogs, was one of the most likely sources of RABV in TWFBs.

426 This first reported pathological changes and viral antigen distribution in FBs  
427 naturally infected with the strain of RABV-TWFB may provide some bases for future  
428 studies such as cross-species disease spreading and vaccine development. The  
429 diagnosis of rabies in TWFBs has clearly demonstrated that some known or unknown  
430 diseases may cryptically circulate in the wild-ranging wildlife sharing the same  
431 habitat with us. These underlying diseases may have serious impacts on our and other  
432 animal's health, wildlife conservation, and/or economy. This incident also reminds us  
433 once again the essentiality of systematic wildlife disease surveillance.

434

#### 435 **Acknowledgements**

436 We thank Jen-Tzu Yang, Ying-Hui Wu, and staffs of the Taiwan Endemic Species  
437 Research Institute, Council of Agriculture, for the collection and submission of  
438 carcasses of the free-range wildlife. Special thanks to Dr. Tsung-Chou Chang from  
439 National Pingtung University of Science and Technology for his kind help in the  
440 study and in memory of his recent passing away. The study was supported in part by  
441 grants 102AS-10.1.1-BQ-B1(3), 103AS-10.1.1-BQ-B1(1), 104AS-10.1.2-BQ-B3(1),  
442 MOST 103-3114-Y-518-001, and MOST 104-3114-Y-518-002 from the Bureau of



443 Animal and Plant Health Inspection and Quarantine, Council of Agriculture,

444 Executive Yuan, Taiwan.

445

446 **Literature Cited**

447 Balachandran A, Charlton K. 1994. Experimental rabies infection of non-nervous

448 tissues in skunks (*Mephitis mephitis*) and foxes (*Vulpes vulpes*). *Vet Pathol*

449 31:93-102.

450 Blanton JD, Hanlon CA, Rupprecht CE. 2007. Rabies surveillance in the United

451 States during 2006. *J Am Vet Med Assoc* 231:540-556.

452 Bourhy H, Reynes JM, Dunham EJ, Dacheux L, Larrous F, Huong VT, Xu G, Yan J,

453 Miranda ME, Holmes EC, 2008. The origin and phylogeography of dog rabies virus. *J*

454 *Gen Virol* 89:2673-2681.

455 Charlton KM. 1984. Rabies: spongiform lesions in the brain. *Acta Neuropathologica*.

456 63, 198-202.

457 Charlton KM, Casey GA, Webster WA, Bundza A. 1987. Experimental rabies in

458 skunks and foxes. Pathogenesis of the spongiform lesions. *Lab Invest* 57:634-645.

459 Chen CC, Pei KJ, Liao MH, Mortenson JA. 2008. Canine distemper virus in wild

460 ferret-badgers of Taiwan. *J Wildl Dis* 44:440-445.

461 Chiou HY, Hsieh CH, Jeng CR, Chan FT, Wang HY, Pang VF. 2014. Molecular

462 characterization of cryptically circulating rabies virus from ferret badgers, Taiwan.

463 *Emerg Infect Dis* 20:790-798.

464 Fèvre EM, Bronsvoort BM, Hamilton KA, Cleaveland S. 2006. Animal movements

465 and the spread of infectious diseases. *Trends Microbiol* 14:125-131.

466 Foley GL, Zachary JF. 1995. Rabies-induced spongiform change and encephalitis in a

467 heifer. *Vet Pathol* 32:309-311.

468 Hamir AN. 2011. Pathology of neurologic disorders of raccoons (*Procyon lotor*). *J*  
469 *Vet Diagn Invest* 23:873-884.

470 Hamir AN, Moser G, Rupprecht CE. 1992. Morphologic and immunoperoxidase  
471 study of neurologic lesions in naturally acquired rabies of raccoons. *J Vet Diagn*  
472 *Invest* 4:369-373.

473 Hamir AN, Niezgoda M, Rupprecht CE. 2011. Recovery from and clearance of rabies  
474 virus in a domestic ferret. *J Am Assoc Lab Anim Sci* 50:248-251.

475 Hicks DJ, Nunez A, Healy DM, Brookes SM, Johnson N, Fooks AR. 2009.  
476 Comparative pathological study of the murine brain after experimental infection with  
477 classical rabies virus and European bat lyssaviruses. *J Comp Pathol* 140:113-126.

478 Jackson AC, Fu ZF. 2013. Pathogenesis. In: Rabies, Jackson AC editor. London:  
479 Elsevier Academic Press, pp.299-349.

480 Jackson AC. 2008. Rabies. *Neurol Clin* 26:717-726, ix.

481 Jackson AC, Ye H, Ridaura-Sanz C, Lopez-Corella E. 2001. Quantitative study of the  
482 infection in brain neurons in human rabies. *J Med Virol* 65:614-618.

483 Krebs JW, Wheeling JT, Childs JE. 2003. Rabies surveillance in the United States  
484 during 2002. *J Am Vet Med Assoc* 223:1736-1748.

485 Liu Y, Zhang SF, Wu XF, Zhao JH, Hou YL, Zhang F, Velasco-Villa A, Rupprecht  
486 CE, Hu RL. 2010. Ferret badger rabies origin and its revisited importance as potential  
487 source of rabies transmission in Southeast China. *BMC Infect Dis* 10:234.

488 Maxie MG, Youssef S. 2007. Nervous system. In: *Jubb, Kennedy, and Palmer's*  
489 *Pathology of Domestic Animals. Volume 1*, Edited by Maxie MG. Elsevier,  
490 Philadelphia, PA, pp.286-458.

491 Naze F, Suin V, Lamoral S, Francart A, Brochier B, Roels S, Mast J, Kalai M, Van



492 Gucht S. 2013. Infectivity of rabies virus-exposed macrophages. *Microbes Infect*  
493 15:115-125.

494 Smith GC. 2002. The role of the Badger (*Meles meles*) in rabies epizootiology and the  
495 implications for Great Britain. *Mammal Rev* 32:12-25.

496 Smith GC, Wilkinson D. 2002. Modelling disease spread in a novel host: rabies in the  
497 European badger *Meles meles*. *J Appl Ecol* 39:865-874.

498 Stein LT, Rech RR, Harrison L, Brown CC. 2010. Immunohistochemical study of  
499 rabies virus within the central nervous system of domestic and wildlife species. *Vet*  
500 *Pathol* 47:630-636.

501 Wacharapluesadee S, Ruangvejvorachai P, Hemachudha T. 2006. A simple method  
502 for detection of rabies viral sequences in 16-year old archival brain specimens with  
503 one-week fixation in formalin. *J Virol Methods* 134:267-271.

504 Wandeler A. 1987. Virus infections of non-domestic carnivores: rabies virus. In:  
505 Appel M.J. (ed), *Virus Infections of Carnivores*. Amsterdam: Elsevier Science  
506 Publishers, pp. 449-461.

507 WHO. 2013. WHO Expert Consultation on Rabies: second report. Geneva: The  
508 Organization. WHO Technical Report Series, No. 982, pp. 1-139.

509 Zhang SF, Tang Q, Wu XF, Liu Y, Zhang F, Rupprecht CE, Hu RL. 2009. Rabies in  
510 Ferret Badgers, Southeastern China. *Emerg Infect Dis* 15:946-949.

511





**Table 1. Histopathological findings and rabies virus antigen expression in the nervous tissue of rabid Taiwan ferret badgers (TWFBs)**

Tissue	TWFB No. 1*					TWFB No. 2*					TWFB No. 3*					TWFB No. 4*					TWFB No. 5*					
	IF	ND	NB	IHCS	FAT	IF	ND	NB	IHCS	FAT	IF	ND	NB	IHCS	FAT	IF	ND	NB	IHCS	FAT	IF	ND	NB	IHCS	FAT	
<b>Cerebrum</b>																										
Cortex	+++	++	++	++		++	+++	+++	+++		++	+++	+++	+++		++	++	++	++		++	+++	++	++		
Medulla	++	-	-	+		++	-	-	+		++	-	-	+		++	-	-	+		++	-	-	-	NA	
Leptomeninges	+++	-	-	-	+++	+	-	-	-	+++	++	-	-	-	+++	+	-	-	-	NA	++	-	-	-	-	
<b>Hippocampus</b>	+++	++	++	+++		++	+++	+++	+++		++	+++	+++	+++		++	+++	++	++							
<b>Thalamus</b>	+++	++	++	+++		++	+++	+++	+++		++	+++	+++	+++		+	++	++	++							
<b>Hypothalamus</b>	+++	++	++	+++		++	+++	+++	+++		++	+++	+++	+++		+	++	++	++							
<b>Cerebellum</b>																										
Cortex																										
Molecular layer	-	-	+\$	+++§		-	++§	+\$	+++§		-	+\$	+\$	+++§		-	-	+\$	+++§						NA	
Purkinje cell layer	-	++	++	++		-	+++	+++	++		-	++	+++	+++		-	+++	++	++							
Granular layer	-	-	-	-	NA	-	-	-	+	NA	-	-	-	+	NA	-	-	-	+	NA					NA	
Medulla	-	-	-	+		-	-	-	+		-	-	-	+		-	-	-	+						NA	
Leptomeninges	++	-	-	-		+	-	-	-		++	-	-	-		+	-	-	-						NA	
<b>Brain stem</b>																										
Midbrain	+++	++	+++	+++		++	+++	+++	+++		++	+++	+++	+++					NA						NA	
Pons	+++	++	+++	+++	NA	++	+++	+++	+++	NA	++	+++	+++	+++	NA				NA							NA
Medulla oblongata	++	++	+++	+++		++	+++	+++	+++		++	+++	+++	+++					NA							NA
<b>C1/C2 spinal cord</b>			NA					NA			++	++	++	++	NA				NA							NA
<b>Peri-adrenal ganglion</b>	++	++	++	+++	NA	+++	+++	+++	+++	NA	+	++	++	++	NA				NA							NA
<b>Peri-renal ganglion</b>	+	+	-	++ <sup>‡</sup>	NA	-	-	-	-	NA				NA					NA							NA

IF: Inflammation; ND: Neuronal degeneration; NB: Negri body; IHCS: Immunohistochemical staining; FAT: Fluorescent antibody test; NA: Not available

\*The scoring system used for the assessment of the histopathological changes and the results of immunohistochemical and immunofluorescent staining is divided into four categories as "-", "+", "++", and "+++". Details of the scoring system are described in Materials and Methods.

§Dendrites of Purkinje cells; <sup>‡</sup>Macrophages; <sup>†</sup>Ganglion cells

**Table 2. Histopathological findings and rabies virus antigen expression in the non-nervous tissue of rabid Taiwan ferret badgers (TWFBs)**

Tissue	TWFB No. 1*				TWFB No. 2*				TWFB No. 3*				TWFB No. 4*				TWFB No. 5*			
	IF	ND	NB	IHCS	IF	ND	NB	IHCS	IF	ND	NB	IHCS	IF	ND	NB	IHCS	IF	ND	NB	IHCS
<b>Submandibular</b>																				
<b>salivary gland</b>			NA				NA		+	-	-	+ <sup>§, †</sup>			NA					
<b>Tongue</b>	+	-	-	+ <sup>¥, †</sup>	+	-	-	+ <sup>¥</sup>	+	-	-	+ <sup>¥, †</sup>	+	-	-	+ <sup>¥</sup>				
<b>Esophagus</b>	-	-	-	+ <sup>¥</sup>	+	-	-	+ <sup>¥</sup>	+	-	-	+ <sup>¥</sup>	+	-	-	+ <sup>¥, †</sup>				
<b>Stomach</b>	+ <sup>†</sup>	+	+ <sup>†</sup>	+ <sup>¥, †</sup>	+ <sup>†</sup>	+	+ <sup>†</sup>	+ <sup>¥, †</sup>	+ <sup>†</sup>	+	+ <sup>†</sup>	+ <sup>¥, †</sup>	+	-	-	+ <sup>†</sup>	+	-	-	+ <sup>†</sup>
<b>Intestine</b>	-	-	-	+ <sup>¥, †</sup>	-	-	-	+ <sup>¥, †</sup>	+	-	-	+ <sup>¥, †</sup>	+	-	-	+ <sup>†</sup>	+	-	-	+ <sup>†</sup>
<b>Pancreas</b>	-	-	-	± <sup>¥</sup>	-	-	-	-	-	-	-	-	-	-	-	-	-	-	-	-
<b>Liver</b>	+	-	-	+ <sup>¥</sup>	+	-	-	-	-	-	-	-	+	-	-	-	-	-	-	-
<b>Trachea</b>	+	-	-	+ <sup>¥</sup>	+	-	-	-	-	-	-	-	+	-	-	+ <sup>¥, †</sup>			NA	
<b>Lungs</b>	+	-	-	+ <sup>¥, †</sup>	+	-	-	+ <sup>¥</sup>	+	-	-	+ <sup>¥</sup>	-	-	-	+ <sup>†</sup>	-	-	-	-
<b>Heart</b>	-	-	-	+ <sup>¥, †</sup>	-	-	-	-	-	-	-	-	-	-	-	-	-	-	-	-
<b>Spleen</b>	-	-	-	+ <sup>¥</sup>	-	-	-	+ <sup>¥</sup>	-	-	-	-	-	-	-	-	-	-	-	-
<b>Adrenal gland</b>	++	-	-	+++ <sup>¥</sup>	+++ <sup>†</sup>	-	-	+++ <sup>¥</sup>	++	-	-	-			NA				NA	
<b>Kidney</b>	+	-	-	+ <sup>¥</sup>	-	-	-	-	-	-	-	-	-	-	-	-	-	-	-	-
<b>Urinary bladder</b>	+	-	-	+ <sup>¥, †</sup>	+	-	-	-	-	-	-	+ <sup>¥</sup>	+	-	-	+ <sup>¥, †</sup>	+	-	-	+ <sup>¥, †</sup>
<b>Uterus</b>	+	-	-	+ <sup>¥</sup>	-	-	-	-	-	-	-	-			NA					
<b>Ovary</b>	-	-	-	-	-	-	-	-	-	-	-	-			NA					
<b>Testis</b>																				NA
<b>Skeletal muscle</b>	-	-	-	-	-	-	-	-	-	-	-	+ <sup>¥</sup>			NA					NA
<b>Haired skin</b>	+++ <sup>#</sup>	-	-	-	+	-	-	+ <sup>¥, †</sup>			NA		+	-	-	-				NA

IF: Inflammation; ND: Neuronal degeneration; NB: Negri body; IHCS: Immunohistochemical staining; NA: Not available

\*The scoring system used for the assessment of the histopathological changes and the results of immunohistochemical and immunofluorescent staining is divided into four categories as "-", "+", "++", and "+++". Details of the scoring system are described in Materials and Methods.

<sup>§</sup>Acinar epithelial cells; <sup>†</sup>Myenteric plexus ganglia or other peripheral ganglia; <sup>¥</sup>Macrophages or Kupffer cells; <sup>‡</sup>Smooth muscle cells; <sup>#</sup>Focal ulcerative dermatitis of chin

## Figure Captions

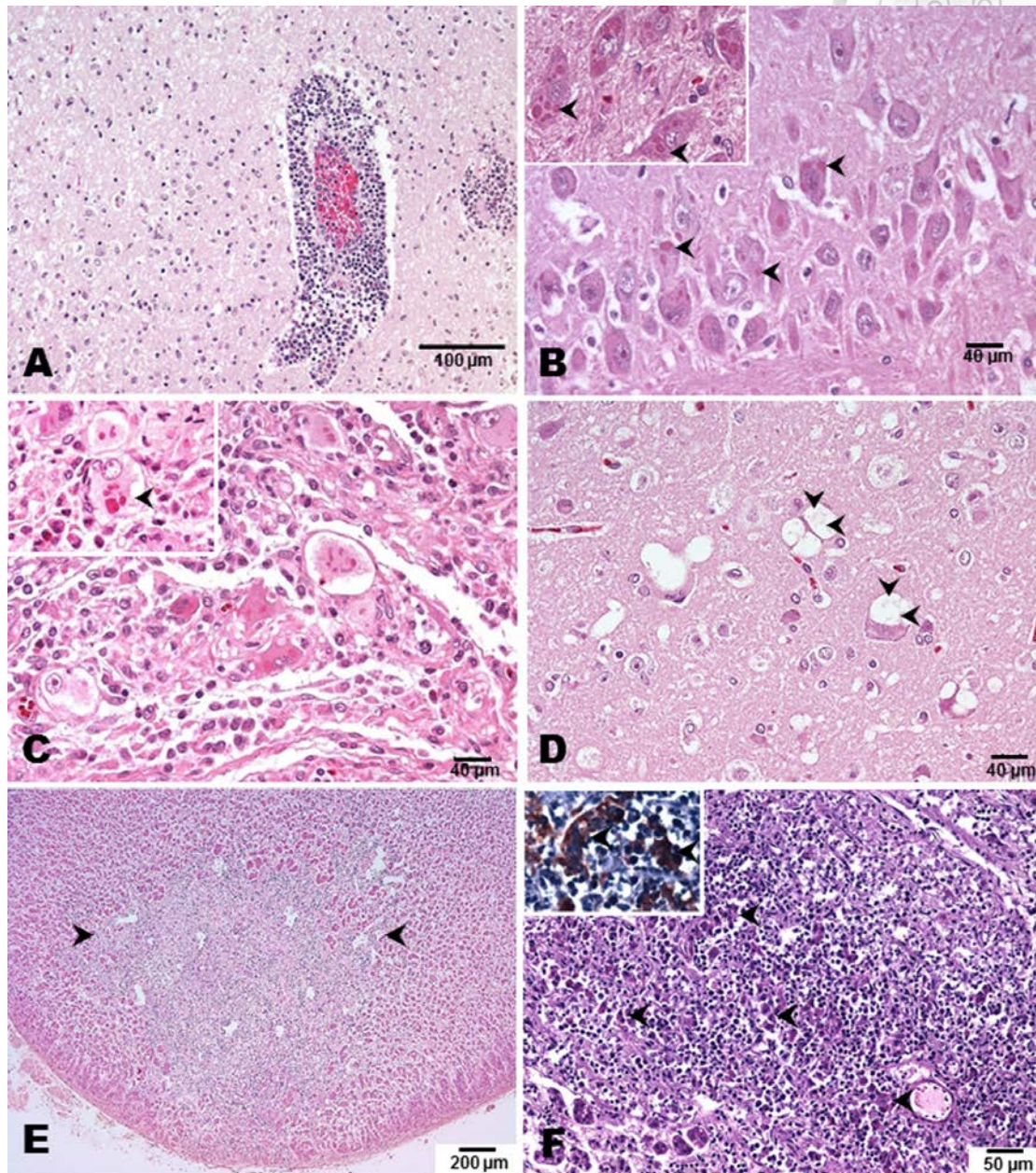


**Figure 1.** Histopathological changes and viral antigen detection in the nervous and non-nervous tissues of rabid Taiwan ferret badger (TWFB) (*Melogale moschata subaurantiaca*). (A) Cerebrum; TWFB No.1. Nonsuppurative encephalitis. Note the prominent perivascular cuffing of lymphocytes, plasma cells, and macrophages as well as gliosis in the cerebral cortex. Hematoxylin and eosin (H & E) stain. (B)

Hippocampus; TWFB No.3. Neuronal degeneration and formation of Negri bodies.

Note the angular-shaped neurons and formation of Negri bodies (arrowheads). Inset:

Brain stem; TWFB No.2. Negri bodies. Note multiple variably sized and shaped

Negri bodies formed in individual neuron. H & E stain. (C) Peri-adrenal ganglion;

TWFB No.2. Ganglionitis. Note the diffuse infiltration of mixed inflammatory cells along with degeneration and necrosis of ganglion cells. Inset: Higher magnification.

Note the prominent neuronal degeneration and necrosis with formation of Negri

bodies (arrowhead). H & E stain. (D) Thalamus; TWFB No.2. Spongiform

degeneration. Note the formation of single to multiple, round, oval to polygonal

vacuoles in the neuronal perikaryon (arrowheads). H & E stain. (E) Adrenal gland;

TWFB No.1. Adreno-cortical necrosis. Note the locally extensive necrosis in the

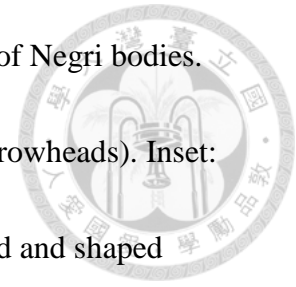
cortex (arrowheads). H & E stain. (F) Adrenal gland; TWFB No.1. Adreno-cortical

necrosis. Note the locally extensive necrosis accompanied with infiltration of mixed

inflammatory cells and the remaining parenchymal cells (arrowheads). H & E stain.

Inset: Adrenal cortex; TWFB No. 1. Note strong RABV-positive signals in the

cytoplasm of remaining parenchymal cells (arrowheads). Immunohistochemical stain.



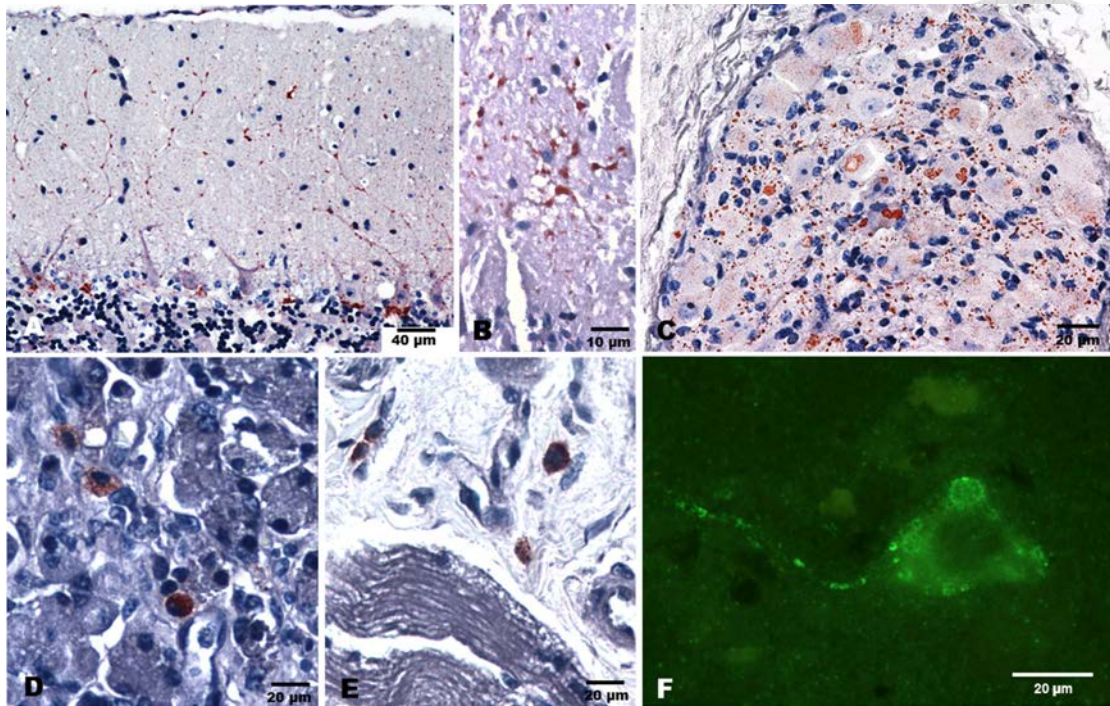


**Figure 2.** Viral antigen detection in the nervous and non-nervous tissues of rabid

Taiwan ferret badgers (TWFBs) (*Melogale moschata subaurantiaca*). (A) Cerebellum;

TWFB No.3. RABV-positive signals detected mainly in the perikaryon of the

Purkinje cells and their dendrites extending into the molecular layer in a linear and granular pattern with scattered weak-positive signals in the stellate cells.

Immunohistochemical (IHC) stain. (B) Cerebellum. TWFB No.4. Strong

RABV-positive signals readily seen in the archival case collected in 2004. IHC stain.

(C) Periadrenal ganglion; TWFB No.1. Note the RABV-positive signals widely

distributed in the ganglion cells and perineuronal spaces. IHC stain. (D) Stomach.

TWFB No.2. Note the RABV-positive macrophages (size up to 10-15  $\mu\text{m}$  in diameter)

scattered in the lamina propria of mucosa. IHC stain. (E) Myocardium. TWFB No.1.

Note the RABV-positive macrophages scattered in the interstitium. IHC stain. (F)

Brain emulsion smear; TWFB No.3. Note the granular to global RABV-positive fluorescent signals present in the perikaryon and dendrite of a neuron. Direct immunofluorescence assay.

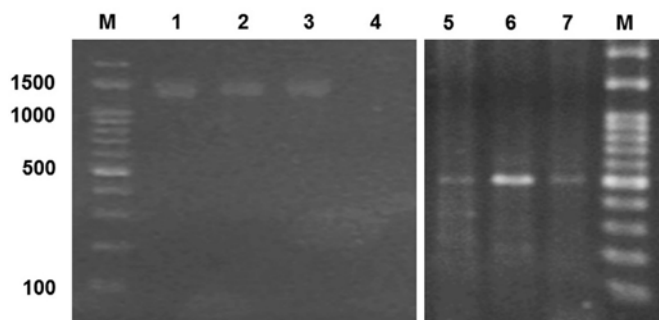


**Figure 3.** The result of agarose gel electrophoresis of the amplicons of RT-PCR for the N and G genes of rabies virus of the brain specimens of Taiwan ferret badgers (TWFBs). Note the expected 1300 bp and 500 bp amplicons for the N and G genes, respectively, amplified from all of the 3 necropsied TWFBs. M: marker; lanes 1 to 3: N gene detection for TWFB No.1, No.2, and No.3, respectively; lane 4: Negative control; lanes 5 to 7: G gene detection for TWFB No.1, No.2, and No.3, respectively.

# Chapter IV



## **Molecular Characterization of Cryptically Circulating Rabies Virus from Ferret Badgers, Taiwan**

*Reprinted from Emerging Infectious Diseases, 2014, Authors: Hue-Ying Chiou, Chia-Hung Hsieh, Chian-Ren Jeng, Fang-Tse Chan, Hurng-Yi Wang, Victor Fei Pang, Title of article: Molecular Characterization of Cryptically Circulating Rabies Virus from Ferret Badgers, Taiwan, 20:790-798*

# Molecular Characterization of Cryptically Circulating Rabies Virus from Ferret Badgers, Taiwan

Hue-Ying Chiou, Chia-Hung Hsieh, Chian-Ren Jeng, Fang-Tse Chan, Hurng-Yi Wang,<sup>1</sup> and Victor Fei Pang<sup>1</sup>

After the last reported cases of rabies in a human in 1959 and a nonhuman animal in 1961, Taiwan was considered free from rabies. However, during 2012–2013, an outbreak occurred among ferret badgers in Taiwan. To examine the origin of this virus strain, we sequenced 3 complete genomes and acquired multiple rabies virus (RABV) nucleoprotein and glycoprotein sequences. Phylogeographic analyses demonstrated that the RABV affecting the Taiwan ferret badgers (RABV-TWFB) is a distinct lineage within the group of lineages from Asia and that it has been differentiated from its closest lineages, China I (including isolates from Chinese ferret badgers) and the Philippines, 158–210 years ago. The most recent common ancestor of RABV-TWFB originated 91–113 years ago. Our findings indicate that RABV could be cryptically circulating in the environment. An understanding of the underlying mechanism might shed light on the complex interaction between RABV and its host.

Rabies is possibly one of the oldest zoonotic diseases. It is caused by the rabies virus (RABV), a neurotropic virus in the family *Rhabdoviridae*, genus *Lyssavirus*. Except for a small number of countries and regions, particularly islands, RABV is found worldwide. The virus infects nearly all warm-blooded animals and causes severe neurologic signs, which almost invariably lead to death (1). It was estimated that worldwide in 2010, the disease caused >60,000 human deaths, primarily in Africa and Asia (2). Although dogs are considered the principal host of RABV in developing countries, the virus is also dispersed among many species of wild carnivora and chiroptera, especially

in those countries of Europe and North America that have well-established vaccination programs (3). Mustelids, including various species of the genera *Melogale*, *Meles*, and *Mellivora* of the weasel family Mustelidae, can carry RABV (4–6). In southeastern China, Chinese ferret badgers (CNFB; *Melogale moschata moschata*) have been associated with human rabies for many years and are considered to be a primary host in this region (7–9).

After what were considered to be the last reported cases of rabies in a human and a nonhuman animal in 1959 and 1961, respectively, Taiwan was rabies free for >50 years until the 2012–2013 outbreak of ferret badger-associated rabies. During May 2012–January 2013, through a government-supported program of routine disease surveillance of free-range dead wild animals that had been killed by vehicles or were receiving treatment for injuries and/or illness at the wildlife first aid station, 3 dead Taiwan ferret badgers (TWFB; *M. moschata subaurantiaca*) were submitted to the School of Veterinary Medicine, National Taiwan University, for further examination.

Pathologic examination revealed nonsuppurative meningoencephalomyelitis with formation of eosinophilic intracytoplasmic inclusion bodies in all 3 animals; reverse transcription PCR and immunohistochemical staining excluded the possibility of infection with the canine distemper virus. However, the results of fluorescence antibody testing, immunohistochemical staining, and reverse transcription PCR, followed by sequencing for RABV, were positive (H.-Y. Chiou, unpub. data). After the rabies diagnoses for the initial 3 ferret badgers were confirmed, by the end of August of 2013, rabies had been diagnosed by fluorescence antibody testing for an additional 105 dead or ill and euthanized ferret badgers and 1 shrew.

Author affiliations: National Taiwan University, Taipei, Taiwan, Republic of China (H.-Y. Chiou, C.-H. Hsieh, C.-R. Jeng, H.-Y. Wang, V.F. Pang); and Council of Agriculture, Executive Yuan, Nantou County, Taiwan, Republic of China (F.-T. Chan)

DOI: <http://dx.doi.org/10.3201/eid2005.131389>

<sup>1</sup>Joint senior authors who contributed equally to this article.



Our objective in this study was to clarify whether the current outbreak of the TWFB-associated rabies is an emerging, a reemerging, or a cryptically circulating disease. We investigated the possible origin of this outbreak and its relations with CNFB-associated rabies in mainland China via genomic organization and characterization and analysis of genetic diversity and phylogeographic origin of RABV-TWFB. In addition, we propose a mechanism that might be contributing to the limited host range of RABV-TWFB.

## Materials and Methods

### Animals and Specimen Collection

During May 2012–January 2013, three ill TWFB were collected from different regions of central Taiwan (Figure 1). One was in the Xitou nature education area at Lugu Township, Nantou County (R2012–26); one was in Gukeng Township, Yunlin County (R2012–88); and one was in Yuchih Township, Nantou County (R2013–01). These 3 TWFB, respectively, showed the following clinical

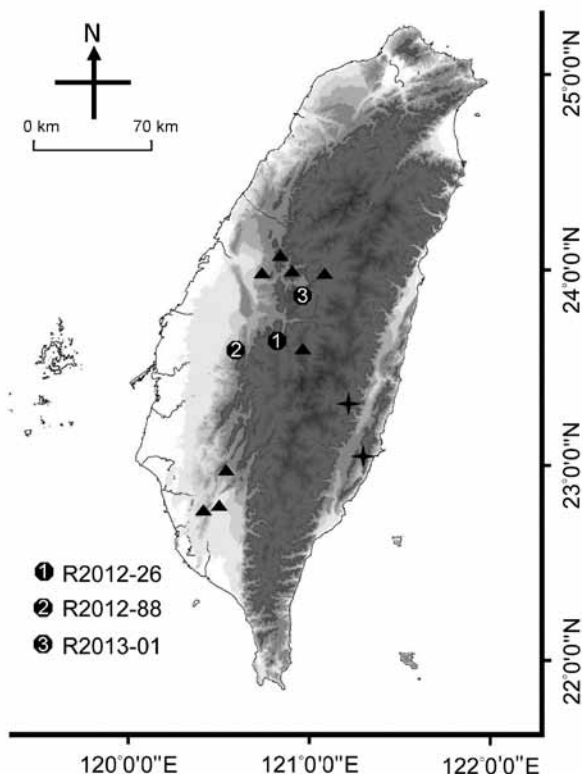


Figure 1. Collection sites of rabies-positive Taiwan ferret badgers (TWFB), Taiwan. Solid circles marked with 1–3 represent the collection sites of the first 3 rabies-positive animals. Triangles represent the collection sites of other rabies virus (RABV) sequences included in this study. Crosses represent the most diverged lineages of rabies virus from Taiwan ferret badgers (TWFB, TW1614, and TW1955), shown in Figure 5, panel B, Appendix ([wwwnc.cdc.gov/EID/article/20/5/13-1389-F5.htm](http://wwwnc.cdc.gov/EID/article/20/5/13-1389-F5.htm)), and the easternmost cross represents the isolate from a shrew, TW1955.

signs: emaciation, coma, paddling, loss of pain response, reduced body temperature, and a 2-cm skin wound on the chin; extreme weakness and inability to move; and signs of weakness and respiratory signs, including labored breathing and increased breath sounds with hypersalivation and exudation of foamy fluid from the mouth and nose. Initial supportive treatment was provided at the wildlife first aid station, but the ferret badgers died within 1–3 days, and their carcasses were submitted to the School of Veterinary Medicine, National Taiwan University, for routine disease surveillance. Full necropsy was performed, during which half of the left cerebral hemisphere was collected from each animal and stored at  $-80^{\circ}\text{C}$  for subsequent nucleic acid extraction. Representative tissue samples were taken from all major organs and fixed in 10% neutral buffered formalin for histopathologic examination.

### Sample Preparation and Genome Sequencing

Approximately 25 mg of brain specimen from each animal was homogenized, and 1 mL of TRIzol reagent (Invitrogen, Carlsbad, CA, USA) was added. Total RNA was extracted by using an RNeasy Mini Kit (QIAGEN, Valencia, CA, USA), and cDNA was synthesized by using a Transcriptor First Strand cDNA Synthesis Kit (Roche Diagnostics, Indianapolis, IN, USA) according to the manufacturer's instructions. To amplify the whole genome, we used 19 pairs of primers (Table 1), including the forward primer for the 5' end and the reverse primer for the 3' end designed to be complementary to the respective ends of the genome, as described (10).

### Sequence Analyses and Phylogenetic Reconstruction

Sequences were assembled by using the Seqman program (Lasergene 8, Madison, WI, USA) (GenBank accession nos. KF620487–KF620489) and then aligned by using the ClustalW program (11). The genetic distance was estimated by using the Kimura 2-parameter substitution model implemented in MEGA version 5.0 (12). The nucleotide diversity within populations was calculated by using DnaSP version 5.0 (13). To test for the deviation of neutral expectation, we conducted the Tajima D (14) and the Fu and Li D\* (15) tests implemented in DnaSP. Significance was assessed by  $10^4$  coalescent simulations (13).

To investigate the phylogenetic position of RABV-TWFB isolates, we included 24 complete RABV genomes representing the 3 major phylogenetic groups (16). For global phylogeny of RABV, we analyzed 218 full-length (1,335-nt) sequences of the nucleoprotein (N) gene, including 11 sequences from Taiwan. We also analyzed 125 full-length (1,575-nt) sequences of the glycoprotein (G) gene, including 13 sequences from Taiwan (17). For each gene, phylogenetic trees were inferred by using maximum-likelihood and Bayesian inference methods.

Table 1. Primers used for the amplification and sequencing of rabies virus genome\*

Primer	Sequence, 5'→3'	Amplicon size, nt	Position, nt
3'F	GTACCTAGACGCTTAAACAAC	499	1–499
3'R	AAGACCGACTAAGGACGCAT		
NF	ATGTAACACCTCTACAATGG	1,533	55–1587
NR	CAGTCTCYTCNGCCATCT		
PF	GAACCAAYCCCAAAYATGAG	1,001	1500–2500
PR	TTCATTTTRTYAGTGGTGTTCG		
MF	AAAAACRGGCAACACCACT	641	2479–3119
MR	TCCTCYAGAGGTAWACAAGTG		
G1F	TGGTGTATAACATGRAYTC	1,097	3000–4096
G1R	ACCCATGTYCCRTCATAAG		
G2F	TGGATTTGTGGATKAAAGAGGC	1,542	3995–5536
G2R	GAGTTNAGRTTGARTCAGAG		
L1F	TGGRGAGGTYTATGATGACCC	726	5430–6155
L1R	CAGCATNAGTGTRTAGTTTCTGTC		
L2F	GGTCGATTATGATAAKGCATTTGG	704	5885–6588
L2R	TTGACAGACCCTTTGATAATC		
L3F	GGATCAATTCGACAACATACATG	550	6473–7024
L3R	AAGTCTTCATCHGGCARTCCTCC		
L4F	AGACTAGCTTCHTGGYTGTCAG	708	6882–7589
L4R	TACTTTGGTTCTTGTTCCCTG		
L5F	AGTGTGGATTGAAGAGAGTGTT	662	7337–7998
L5R	GAAAGACTGCCTGCACTGACAT		
L6F	AATAGTCAACCTCGCCAATAATG	767	7897–8645
L6R	GGATCTCTGAGTTGTAGAAGGATTC		
L7F	CCGAGTCAATCATTGGATTGATAC	621	8517–9137
L7R	GAATACCCTCCTTCGCTGTATCTG		
L8F	GAGAAGGTCACCAATGTTGATG	1,045	8958–10002
L8R	AGATCCAYARCCAGTCATTCTC		
L9F	ACATAATGCTCAGAGAACCGT	503	9820–10322
L9R	CCATTCTGAACATCCTACCTT		
L10F	TGTTCCAGAATGGGTCTGCTCT	509	10302–10811
L10R	TGCATCGCAAATAATGAGGT		
L11F	ATTATTTGCGATGCAGAAGT	524	10797–11320
L11R	ATGATAGCCACTTTAGACAGAGT		
L12F	GTTACAGAGGGGAACTCTGTCT	386	11285–11670
L12R	TCTTCACTATCTTGTAATCAACCT		
5'F	TGGATCAGTTGATTTACAAGATAGT	293	11640–11932
5'R	ACGCTTAAACAAATAAACAAAAAT		

\*Primers were from Lei et al. (10).

The maximum-likelihood analysis was conducted by using PhyML 3.0 online (18); the starting tree was derived from the neighbor-joining method, and the nearest neighbor interchange topology search option was used. The nucleotide substitution model for phylogenetic reconstruction was determined by using the Akaike information criterion implemented in jModeltest 0.1.1 (19). The method of Bayesian inference was performed by using MrBayes version 3.1.2 (20). Analyses were initiated with random starting trees, and Metropolis-coupled Markov chain Monte Carlo (MCMC) analyses were run for  $1 \times 10^6$  generations and sampled every 100 generations. The steady state of the log-likelihood was reached at  $\approx 20,000$  generations. Subsequently, the first 201 trees were excluded and the remaining 9,800 trees were retained to compute a 50% majority-rule consensus tree.

### Divergence Dating

The divergence time between different viral lineages and the time to the most recent common ancestor (TMRCA)

of virus isolates were estimated by using an established Bayesian MCMC approach implemented in BEAST version 1.7 (21). The analysis was performed by using the general time-reversible model of nucleotide substitution assuming an uncorrelated lognormal molecular clock (22). We linked substitution rates for the first and second codon positions and allowed independent rates in the third codon position. The molecular clocks were  $2.3 \times 10^{-4}$  (range  $1.1\text{--}3.6 \times 10^{-4}$ ) and  $3.9 \times 10^{-4}$  ( $1.2\text{--}6.5 \times 10^{-4}$ ) substitutions/site/year for N and G genes, respectively (17). A slightly faster clock,  $4.3 \times 10^{-4}$  ( $3.1\text{--}5.6 \times 10^{-4}$ ) substitutions/site/year for N gene (23), was also used in a separate analysis.

Because a previous study revealed that the population dynamics of RABV supported a model of constant population size through time (17), we restricted our analysis to this demographic model. For each analysis, we performed 2 independent runs with  $2 \times 10^7$  MCMC steps, of which the first 10% were discarded as burn-in. To confirm that both were sampling the same distribution, we compared and then combined the results. Log files were checked by

using Tracer (<http://beast.bio.ed.ac.uk/Tracer>), and the effective sample size for each parameter was >300, which is adequate according to the authors of BEAST software.

**Results**

**Genomic Organization and Characterization of RABV-TWFB**

Similar to previous analyses (16,17), our phylogenetic analysis that used whole RABV genomes revealed 3 major groups with high bootstrap support (Figure 2). Although the 3 RABV-TWFB isolates are clustered within the Asia group, composed of 3 distinct lineages, (China I [including CNFB], China II [16], and Southeast Asia), they do not appear close to any of the 3 lineages. More noteworthy, the 3 isolates of RABV-TWFB are not close to those of RABV-CNFB, indicating that they may have originated independently.

The genome of RABV-TWFB is 11,923 nt long and encodes 5 proteins. The nucleotide lengths of different genomic regions are within the range of variations in different Asia lineages (Table 2), except the matrix protein (M)-G intergenic region, which is 1 nt longer than in the rest of the lineages from Asia (212 vs. 211). Within the group of Asia

lineages, the most conserved protein is M, followed by N, the virion-associated RNA polymerase (L), and G; the least conserved is phosphoprotein (P) (Table 3). Among the RABV groups, however, N becomes the most conserved followed by L, M, G, and P. The RABV-TWFB is closest to China I lineage in the N, P, and L gene regions, but it is closest to RABV-CNFB in the M and G gene regions.

The genetic variations across the whole genome among different lineages can be viewed in a sliding window analysis (Figure 3). Within N, there seems to be a conserved central domain previously identified in RABV at residues 182–328 (24), which is also conserved in RABV-TWFB. The P, the last quarter of G and G–L intergenic regions, and the last part of L are more variable among different lineages of RABV than is the rest of the genome. The conserved M is functional in viral assembly and budding (25); is involved in the regulation of transcription and replication of viral RNA (26); and has been reported to induce apoptosis (27), suggesting its role in host-cell interplay. The involvement of M in multiple interactions explains its conservation among lineages. G is responsible for cell attachment and fusion and is the main viral protein responsible for the induction of neutralization antibodies and cell-mediated immune responses. The region between aa 189 and aa 214,

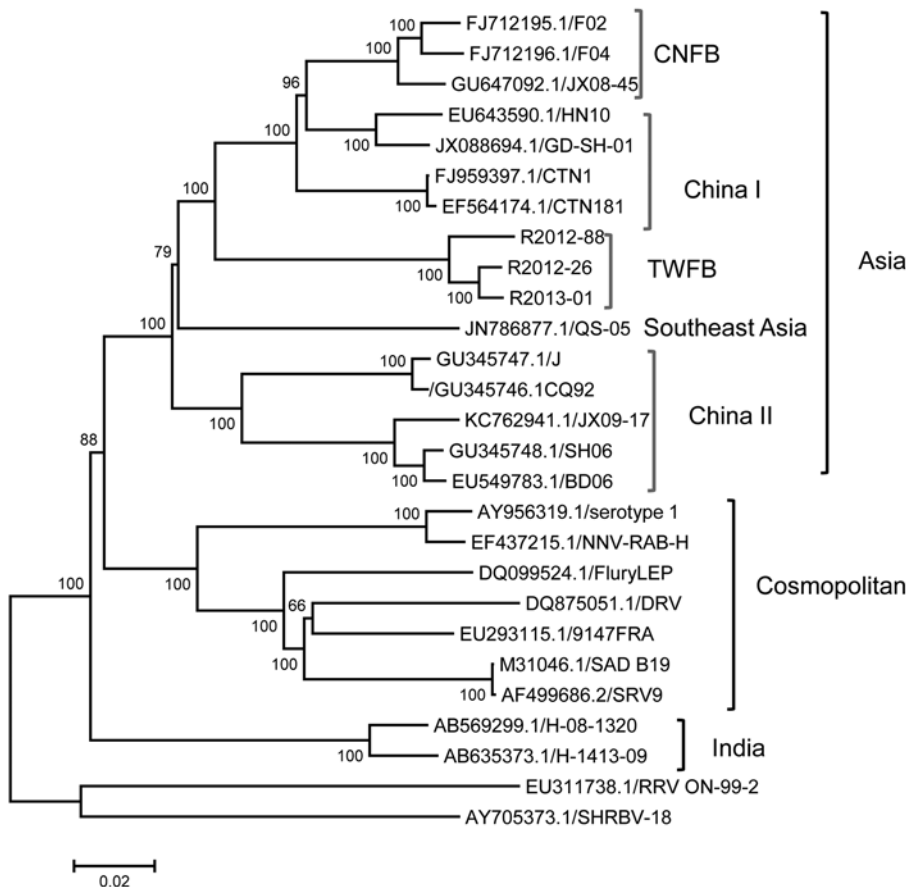


Figure 2. Phylogenetic relationships of 27 rabies virus (RABV) genomes constructed by maximum-likelihood method. Numbers close to the nodes were from 1,000 bootstrap replications. The tree was rooted with RABV from bats and raccoons. Three major groups, Asia, Cosmopolitan, and India, are strongly supported, as indicated (17). There are 4 major lineages within the group from Asia, including previously recognized China I, China II (16), Southeast Asia, and RABV from Taiwan ferret badgers (TWFB). RABVs derived from Chinese ferret badgers (CNFB) are clustered with China I, indicating that RABVs of TWFB and CNFB are of independent origin. Scale bar indicates nucleotide substitutions per site.

Table 2. Genomic organization and nucleotide lengths of terminal and intergenic regions and viral genes of rabies virus from Taiwan and other lineages from Asia\*

Isolate	3'-UTR	Gene, nucleotide length										5'-UTR	Genome size
		N	N-P	P	P-M	M	M-G	G	G-L	L			
TWFB	70	1,353	91	894	86	609	212	1,575	519	6,384	130	11,923	
CNFB	70	1,353	91	894	86	609	211	1,575	519	6,384	130-131	11,922-11,923	
China I†	70	1,353	90-91	894	87-88	609	211	1,575	519	6,384	130	11,923	
China II†	70	1,353	91	894	87	609	211	1,575	518-519	6,384	131	11,923-11,924	

\*UTR, untranslated region; TWFB, Taiwan ferret badgers; CNFB, Chinese ferret badgers.

†The definitions of China I and II are based on He et al. (16). China I does not include CNFB.

proposed to be needed for G binding to the nicotinic acetylcholine receptor (28), is relatively conserved in the dataset. Nevertheless, 3 substitutions (N194Y, R196K, and G203E) are found exclusively in RABV-TWFB G. In L, Poch et al. (29) recognized 6 conserved blocks, including B1 (233-424), B2 (504-608), B3 (609-832), B4 (890-1061), B5 (1091-1326), and B6 (1674-1749) (29). In addition, 2 regions, L1 (1418-1515) and L2 (1884-1961), are also conserved across lyssaviruses (30). In RABV-TWFB, the B4 and L1 regions in L are variable, and the rest of the blocks are conserved (Figure 3).

#### Genetic Diversity and Phylogeographic Origin of RABV-TWFB

The data shown in Figure 2 indicate that RABV-TWFB is a distinct lineage within the Asia group of viruses. To further explore the detailed origin of RABV-TWFB, we included the representative N and G sequences of RABV from human and various animal species for analysis (17,31). Because maximum-likelihood and Bayesian inference methods yielded similar topologies, we report only the results derived from the former. Both N and G gene trees support the conclusion that RABV-TWFB is a distinct lineage within the Asia group, clustered with the China I lineage, including RABV-CNFB, and sequences from the Philippines (Figure 4, Appendix, [wwwnc.cdc.gov/EID/article/20/5/13-1389-F4.htm](http://wwwnc.cdc.gov/EID/article/20/5/13-1389-F4.htm)).

Divergence time was estimated by using a Bayesian coalescent approach. In this analysis, we included only sequences of the Asia group. On the basis of the molecular clock of  $4.3 \times 10^{-4}$ /site/year for N gene (23), the substitution rate at the third codon position is  $1.1 \times 10^{-3}$ /site/year, and

RABV-TWFB was separated from China I and the Philippines isolates 158 years ago with 95% highest posterior density (HPD) ranging from 110 to 225 years (Figure 5, panel A, Appendix, [wwwnc.cdc.gov/EID/article/20/5/13-1389-F5.htm](http://wwwnc.cdc.gov/EID/article/20/5/13-1389-F5.htm)). The divergence between China I and the Philippines isolates occurred 132 (95% HPD, 90-192) years ago, which is similar to previous estimations (23,32). The TMRCA of isolates from Taiwan was 91 years (95% HPD, 57-137). A similar timescale, with overlapping 95% HPD, was derived by using the molecular clock of  $2.3 \times 10^{-4}$ /site/year for N gene (17) (Figure 5, panel A, hatched numbers, Appendix). The mean substitution rate for G gene sequences was  $3.5 \times 10^{-4}$ /site/year ( $7.8 \times 10^{-4}$  for the third codon position), and the divergence of RABV-TWFB, China I, and the Philippines isolates was initiated 210 (107-553) years ago, and the TMRCA of isolates from Taiwan was 113 (53-296) years (Figure 5, panel B, Appendix). It is notable that the TMRCA of RABV-TWFB was more ancient than that of several distinct lineages in Figure 5, Appendix. For example, the TMRCA was 62-116 years for the Southeast Asia lineage and 54-102 years for RABV of the Philippines. The origin of RABV-CNFB was relatively recent; TMRCA was 13-25 years.

The nucleotide diversities of RABV-TWFB are 3.14% for the N and 4.21% for the G genes (Table 4), which are almost 5 times higher than those of RABV-CNFB, which are 0.67% for the N and 0.87% for G genes. For comparison purposes, the 65 N and 232 G gene sequences of RABV isolates from the Philippines were also included for analysis (33). The nucleotide diversities are 2.00% for the N gene and 2.57% for the G gene. The results of both the Tajima D and the Fu and Li D\* tests are not significant for

Table 3. Genetic distances between Taiwan isolates and other rabies virus lineages or groups in different genomic regions\*

Rabies virus group†	Gene						Genome
	N	P	M	G	L		
Asia							
CNFB	0.115	0.172	0.105	0.129	0.130	0.134	
China I‡	0.104	0.157	0.107	0.133	0.123	0.127	
China II	0.130	0.186	0.132	0.172	0.142	0.152	
Southeast Asia	0.140	0.189	0.125	0.169	0.147	0.155	
Cosmopolitan	0.161	0.216	0.173	0.209	0.177	0.192	
India	0.152	0.229	0.183	0.211	0.175	0.191	
Outgroup	0.200	0.284	0.212	0.237	0.209	0.232	

\*CNFB, Chinese ferret badgers; outgroup, rabies virus derived from bat and raccoon.

†Groups of rabies virus are based on the work of Bourhy et al. (17).

‡In this analysis, China I does not include CNFB.

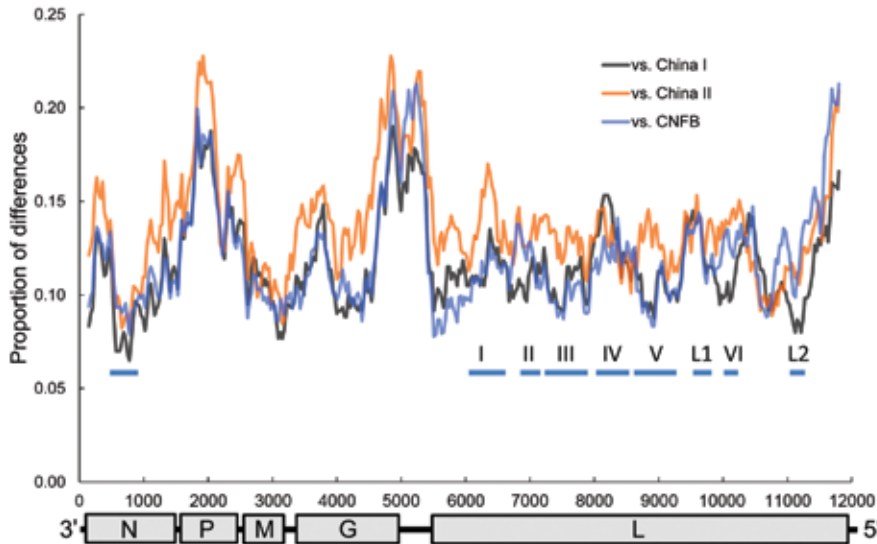


Figure 3. Sliding window analysis of rabies virus (RABV) genetic variations between Taiwan ferret badgers and China I, China II, and Chinese ferret badgers (CNFB). The genomic organization of RABV is shown at the bottom with nucleotide positions on the x-axis. The thick horizontal lines indicate conserved regions across lyssaviruses. N, nucleoprotein; P, phosphoprotein; M, matrix protein; G, glycoprotein; L, virion-associated RNA polymerase.

RABV-TWFB, indicating that the viral population is under neutral equilibrium, which in turn suggests that RABV was not recently introduced to TWFB. In contrast, the results of the Tajima D and the Fu and Li D\* tests are significantly negative for the sequences of RABV-CNFB and sequences from the Philippines isolates, which are caused by an excessive of low-frequency mutation or by differentiation among populations.

## Discussion

### The Ancient Origin of RABV-TWFB

We sequenced and characterized a RABV strain, RABV-TWFB, recently isolated from ferret badgers in Taiwan. Our data showed that RABV-TWFB is clustered with sequences from the Philippines, China I, and RABV-CNFB. This relationship is strongly supported on the basis of multiple sequences of the N and G genes and of the complete genome (Figures 2 and 4, Appendix). Of ferret badger isolates, RABV-TWFB and RABV-CNFB come from phylogenetically distinct lineages, indicating that multiple RABV colonization events in this species probably occurred. A major question addressed in this study is whether RABV was recently introduced into the population of TWFB or perpetuated in TWFB without revealing its presence pathogenically after it was first introduced in the ancient past. Our divergence dating showed that the RABV has been circulating in TWFB for  $\approx 100$  years.

Our divergence and TMRCA estimations have a few potential sources of error. First, the RABV isolates from Taiwan might have originated from several introduction events, including the probability that multiple viral lineages occurred in the recent past and that the inflated TMRCA resulted from the combination of different, highly

differentiated virus strains. Nevertheless, all isolates from Taiwan formed a monophyletic lineage distinct from other virus isolates. Unless several undetected virus strains were circulating around Taiwan, which is highly unlikely, the phylogenetic analyses support the existence of only 1 origin of RABV-TWFB.

Second, the ancient estimates could have resulted from the application of an inadequate molecular clock. However, the nucleotide substitution (mutation) rates of  $2.3\text{--}4.3 \times 10^{-4}$  and  $3.9 \times 10^{-4}$ /site/year, for the N and G genes, respectively, used in the study reported here are in agreement with findings of other studies of lyssavirus evolution (17,23,32,34,35). In a study of RABV in bats, Streicker et al. (34) found that the nucleotide substitution rates in the third codon position, which are predominately silent (synonymous) substitutions, among viral lineages in different bat species spanned  $8.3 \times 10^{-5}$ – $2.1 \times 10^{-3}$ /site/year. Our estimations of mutations of  $1.1 \times 10^{-3}$  and  $7.8 \times 10^{-4}$ /site/year for the third codon position of the N and G genes, respectively, are actually close to the upper boundary of their estimations. Therefore, our results should be conservative.

Third, RABV-TWFB exhibits high nucleotide diversity in the N and G genes. Notably, 232 G gene sequences collected from a large area of the Philippines showed nucleotide diversity that was two thirds that of RABV-TWFB. Taken together, all current genetic evidence supports the hypothesis of the ancient origin of RABV-TWFB. In addition, RABV-TWFB has been maintained in a large population for a long time.

Last, our recent retrospective study that used the archived formalin-fixed and paraffin-embedded brain tissues of ferret badgers, kindly provided by various institutes, demonstrated that the current earliest TWFB-associated

Table 4. Nucleotide diversity of rabies virus from TWFB, CNFB, and the Philippines\*

Virus, gene	Length, nt	Sample size, no.	$\Pi$ , %	Tajima D	Fu and Li D*
TWFB					
N	1,335	11	3.14	-0.886	0.735
G	1,575	12	4.21	-0.264	0.740
CNFB					
N	1,350	12	0.67	-1.294†	-1.918†
G	1,575	14	0.87	-1.168†	-1.336†
Philippines					
N	1,124	65	2.00	-1.380†	-1.759†
G	1,575	232	2.57	-1.676†	-3.80‡

\*TWFB, Taiwan ferret badgers; CNFB, Chinese ferret badgers.

† $p < 0.05$ .

‡ $p < 0.01$ .

RABV infection could be traced back to 2004 (H.-Y. Chiou, unpub. data), representing the oldest specimens that we have so far. That finding is consistent with the notion of a long history of RABV-TWFB in Taiwan.

### Mutations in the G Gene of RABV-TWFB

The ancient history of RABV-TWFB raises 2 issues. First, because for the past 50 years Taiwan was believed to have been free from rabies, learning that the virus must have been cryptically circulating in the environment for such a long time is surprising. Because previous rabies surveillance was mainly focused on dogs and bats ([www.baphiq.gov.tw](http://www.baphiq.gov.tw)), cases in remote areas might have gone unnoticed. However, Taiwan is an island with a high population density; 23 million persons live in an area of 36,188 km<sup>2</sup>, and for rabies cases to have gone unnoticed for >50 years would be very unusual. Second, according to a recent survey about wildlife, the ferret badger population has been increasing in the past 5 years (L.-K. Lin, pers. comm.). Therefore, despite the ancient history of the ferret badger's association with RABV, the fact that its population is seemingly unaffected by infection with RABV is perplexing.

Except for 1 isolate from a shrew, all RABV isolates in the recent rabies outbreak in Taiwan have come from ferret badgers. The close relationship between the shrew RABV and ferret badger RABV collected from the same area suggests that the former probably resulted from spillover from the latter (Figure 5, panel B, Appendix). According to the most recent rabies surveillance data, the ferret badger is probably the only source of RABV in the current outbreak in Taiwan. Speculation that this RABV strain has adapted to and has been circulating in TWFB for a long time is reasonable. Its ability to transmit across species (e.g., ferret badger to shrew) is, thus, worthy of further investigation.

Among the multiple substitutions in RABV-TWFB genome that distinguish it from other virus strains, several substitutions in G (i.e., N194Y, R196K, and G203E) might merit additional attention. It has been demonstrated that a

single amino acid mutation, N194K, in the nonpathogenic RABV vaccine strain SAD B19 was solely responsible for its increased pathogenicity. The increased pathogenicity is caused by increased virus spread in vivo and faster internalization of the virus into cells (36), both of which are consistent with the notion that G plays a major role in RABV pathogenesis. When the amino acid N was exchanged with amino acid S at position 194 (N194S), the pathogenic phenotype was reversed (36,37). Faster internalization of the virus into cells after N194K substitution might suggest that this region has some role in host cell binding. Evidence is strong that the muscular form of the nicotinic acetylcholine receptor, the neuronal cell adhesion molecule, and the p75 neurotrophin receptor serve as receptor sites for RABV binding and/or facilitate its entry into host cells (38,39). The 3 above-mentioned substitutions in RABV-TWFB are located in the region (aa 189 and 214) proposed to be needed for the binding of the G to the nicotinic acetylcholine receptor (28).

In our analysis of 113 G gene sequences from dog-associated RABV, no amino acid substitution was observed at the above-mentioned sites. In a total of 120 G gene sequences from bat-associated RABV (40), 8 N194T (6.7%), 2 N194S (1.7%), and 36 R196K (30.0%) amino acid substitutions were revealed with no amino acid change at G203. Taken together, the 3 aa substitutions (N194Y, R196K, and G203E) found in all 13 G gene sequences of RABV-TWFB are unique and worthy of further investigation.

### Acknowledgments

We thank the Animal Health Research Institute, Council of Agriculture, Executive Yuan (ROC) for providing 8 and 10 full-length sequences of the N and G genes, respectively, for phylogenetic analysis. Special thanks go also to the Taiwan Endemic Species Research Institute, Council of Agriculture, for collection and submission of carcasses of free-range wildlife.

This research was supported in part by grants 101AS-10.1.2-BQ-B1(1) and 102AS-10.1.1-BQ-B1(1) from the Bureau of Animal and Plant Health Inspection and Quarantine, Council of Agriculture, Executive Yuan, Taiwan (ROC) (to V.F.P.) and

NSC102-2313-B-002-062 from the Ministry of Science and Technology, Taiwan (ROC) (to H.-Y.W.).

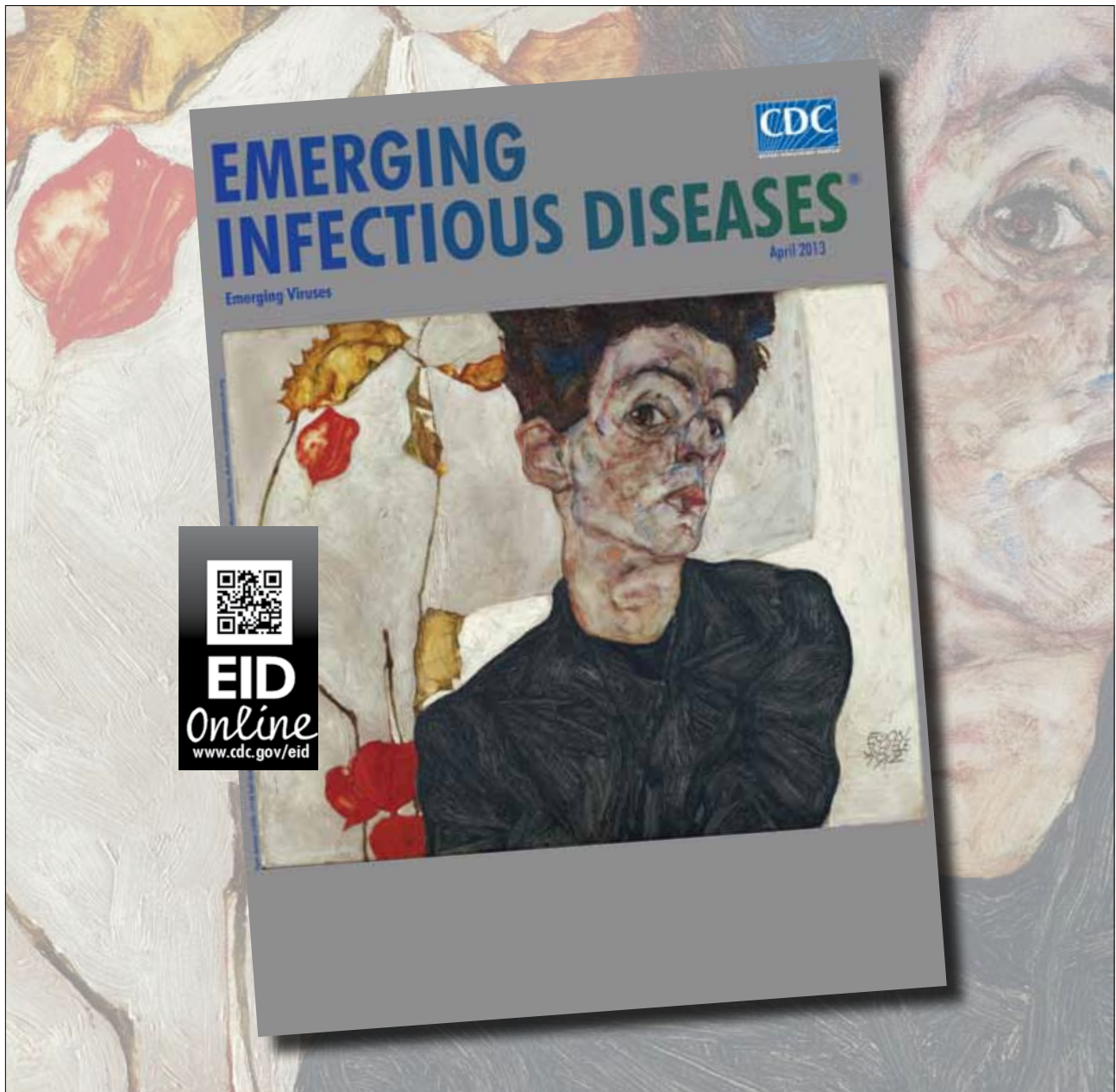
Dr Chiou is a chief pathology resident and a PhD candidate in the School of Veterinary Medicine, National Taiwan University. Her primary research interests include disease surveillance and monitoring of wildlife and zoonotic diseases.

## References

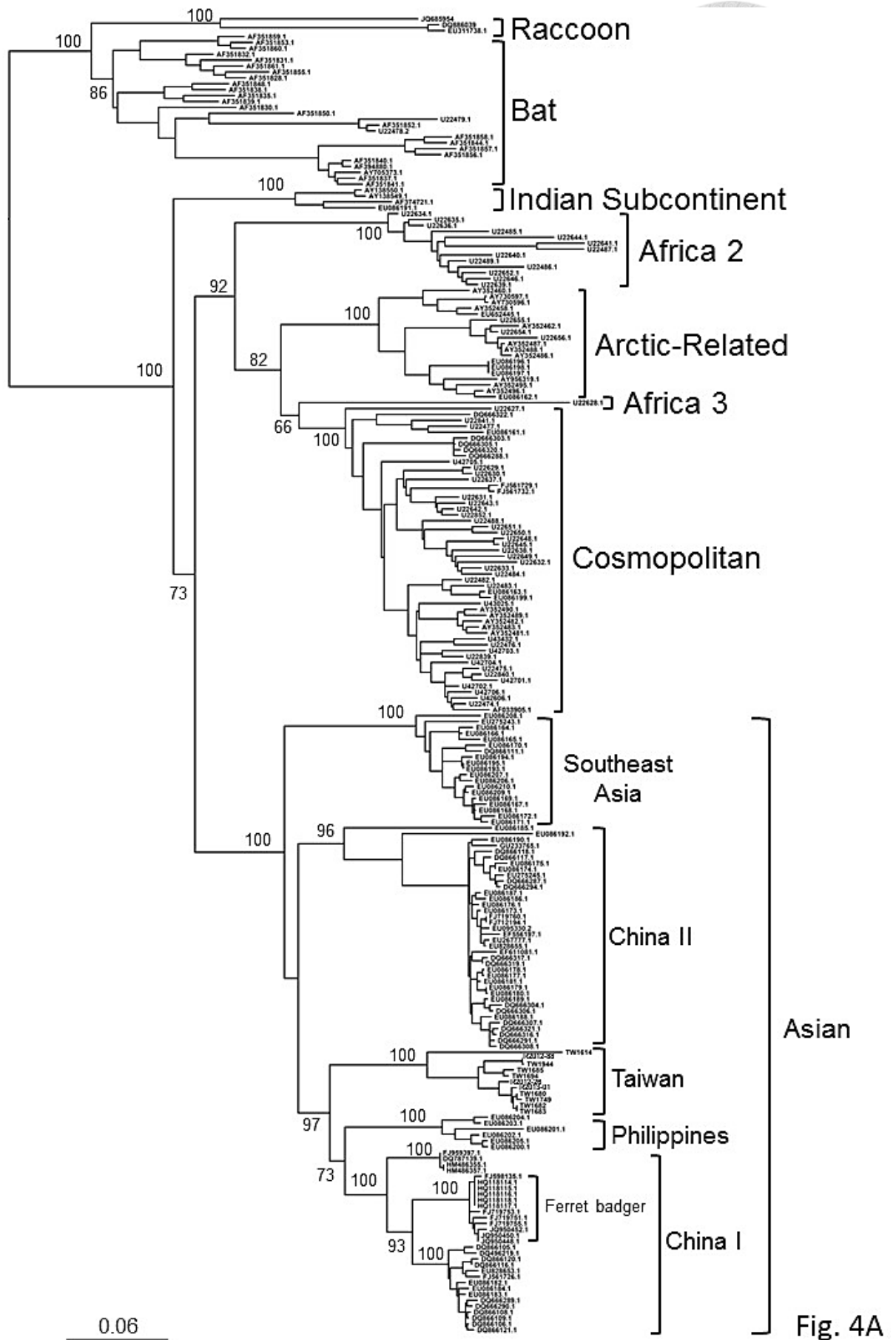
- Jackson AC. Pathogenesis. In: Jackson AC, Wunner WH, editors. Rabies. London: Elsevier Academic Press; 2007.
- World Health Organization. WHO Expert Consultation on Rabies: second report. Geneva: The Organization; 2013. p. 1–139.
- Wandeler A. Virus infections of non-domestic carnivores: rabies virus. In: Appel MJ, editor. Virus infections of carnivores. Amsterdam: Elsevier Science Publishers; 1987. p. 449–61.
- Barnard BJH. The role played by wildlife in the epizootiology of rabies in South Africa and South-West Africa. Onderstepoort J Vet Res. 1979;46:155–63.
- Smith GC, Wilkinson D. Modelling disease spread in a novel host: rabies in the European badger *Meles meles*. Journal of Applied Ecology. 2002;39:865–74. <http://dx.doi.org/10.1046/j.1365-2664.2002.00773.x>
- Wandeler A, Wachendorfer G, Forster U, Krekel H, Muller J, Steck F. Rabies in wild carnivores in central Europe. II. Virological and serological examinations. Zentralbl Veterinarmed B. 1974;21:757–64. <http://dx.doi.org/10.1111/j.1439-0450.1974.tb00479.x>
- Liu Y, Zhang SF, Wu XF, Zhao JH, Hou YL, Zhang F, et al. Ferret badger rabies origin and its revisited importance as potential source of rabies transmission in southeast China. BMC Infect Dis. 2010;10:234. <http://dx.doi.org/10.1186/1471-2334-10-234>
- Zhenyu G, Zhen W, Enfu C, Fan H, Junfen L, Yixin L, et al. Human rabies cluster following badger bites, People's Republic of China. Emerg Infect Dis. 2007;13:1956–7. <http://dx.doi.org/10.3201/eid1312.070465>
- Zhang S, Tang Q, Wu XF, Liu Y, Zhang F, Rupprecht CE, et al. Rabies in ferret badgers, southeastern China. Emerg Infect Dis. 2009;15:946–9. <http://dx.doi.org/10.3201/eid1506.081485>
- Lei YL, Wang XG, Liu FM, Chen XY, Ye BF, Mei JH, et al. Complete genome sequencing and analyses of rabies viruses isolated from wild animals (Chinese ferret-badger) in Zhejiang Province [in Chinese]. Zhonghua Liu Xing Bing Xue Za Zhi. 2009;30:824–8.
- Thompson JD, Higgins DG, Gibson TJ. CLUSTAL W: improving the sensitivity of progressive multiple sequence alignment through sequence weighting, position-specific gap penalties and weight matrix choice. Nucleic Acids Res. 1994;22:4673–80. <http://dx.doi.org/10.1093/nar/22.22.4673>
- Tamura K, Peterson D, Peterson N, Stecher G, Nei M, Kumar S. MEGA5: Molecular Evolutionary Genetics Analysis using maximum likelihood, evolutionary distance, and maximum parsimony methods. Mol Biol Evol. 2011;28:2731–9. <http://dx.doi.org/10.1093/molbev/msr121>
- Librado P, Rozas J. DnaSP v5: a software for comprehensive analysis of DNA polymorphism data. Bioinformatics. 2009;25:1451–2. <http://dx.doi.org/10.1093/bioinformatics/btp187>
- Tajima F. Statistical method for testing the neutral mutation hypothesis by DNA polymorphism. Genetics. 1989;123:585–95.
- Fu YX, Li WH. Statistical tests of neutrality of mutations. Genetics. 1993;133:693–709.
- He CQ, Meng SL, Yan HY, Ding NZ, He HB, Yan JX, et al. Isolation and identification of a novel rabies virus lineage in China with natural recombinant nucleoprotein gene. PLoS ONE. 2012;7:e49992. <http://dx.doi.org/10.1371/journal.pone.0049992>
- Bourhy H, Reynes JM, Dunham EJ, Dacheux L, Larrous F, Huong VT, et al. The origin and phylogeography of dog rabies virus. J Gen Virol. 2008;89:2673–81. <http://dx.doi.org/10.1099/vir.0.2008/003913-0>
- Guindon S, Gascuel O. A simple, fast, and accurate algorithm to estimate large phylogenies by maximum likelihood. Syst Biol. 2003;52:696–704. <http://dx.doi.org/10.1080/10635150390235520>
- Posada D. jModelTest: phylogenetic model averaging. Mol Biol Evol. 2008;25:1253–6. <http://dx.doi.org/10.1093/molbev/msn083>
- Ronquist F, Huelsenbeck JP. MrBayes 3: Bayesian phylogenetic inference under mixed models. Bioinformatics. 2003;19:1572–4. <http://dx.doi.org/10.1093/bioinformatics/btg180>
- Drummond AJ, Suchard MA, Xie D, Rambaut A. Bayesian phylogenetics with BEAUti and the BEAST 1.7. Mol Biol Evol. 2012;29:1969–73. <http://dx.doi.org/10.1093/molbev/mss075>
- Drummond AJ, Ho SY, Phillips MJ, Rambaut A. Relaxed phylogenetics and dating with confidence. PLoS Biol. 2006;4:e88. <http://dx.doi.org/10.1371/journal.pbio.0040088>
- Meng S, Sun Y, Wu X, Tang J, Xu G, Lei Y, et al. Evolutionary dynamics of rabies viruses highlights the importance of China rabies transmission in Asia. Virology. 2011;410:403–9. <http://dx.doi.org/10.1016/j.virol.2010.12.011>
- Kissi B, Tordo N, Bourhy H. Genetic polymorphism in the rabies virus nucleoprotein gene. Virology. 1995;209:526–37. <http://dx.doi.org/10.1006/viro.1995.1285>
- Mebatsion T, Weiland F, Conzelmann KK. Matrix protein of rabies virus is responsible for the assembly and budding of bullet-shaped particles and interacts with the transmembrane spike glycoprotein G. J Virol. 1999;73:242–50.
- Finke S, Mueller-Waldeck R, Conzelmann KK. Rabies virus matrix protein regulates the balance of virus transcription and replication. J Gen Virol. 2003;84:1613–21. <http://dx.doi.org/10.1099/vir.0.19128-0>
- Kassis R, Larrous F, Estaquier J, Bourhy H. Lyssavirus matrix protein induces apoptosis by a TRAIL-dependent mechanism involving caspase-8 activation. J Virol. 2004;78:6543–55. <http://dx.doi.org/10.1128/JVI.78.12.6543-6555.2004>
- Lentz TL, Wilson PT, Hawrot E, Speicher DW. Amino acid sequence similarity between rabies virus glycoprotein and snake venom curaremimetic neurotoxins. Science. 1984;226:847–8. <http://dx.doi.org/10.1126/science.6494916>
- Poch O, Blumberg BM, Bougueleret L, Tordo N. Sequence comparison of five polymerases (L-proteins) of unsegmented negative-strand RNA viruses: theoretical assignment of functional domains. J Gen Virol. 1990;71:1153–62. <http://dx.doi.org/10.1099/0022-1317-71-5-1153>
- Kuzmin IV, Wu X, Tordo N, Rupprecht CE. Complete genomes of Aravan, Khujand, Irkut and West Caucasian bat viruses, with special attention to the polymerase gene and non-coding regions. Virus Res. 2008;136:81–90. <http://dx.doi.org/10.1016/j.virusres.2008.04.021>
- Zhang S, Zhao J, Liu Y, Fooks AR, Zhang F, Hu R. Characterization of a rabies virus isolate from a ferret badger (*Melogale moschata*) with unique molecular differences in glycoprotein antigenic site III. Virus Res. 2010;149:143–51. <http://dx.doi.org/10.1016/j.virusres.2010.01.010>
- Gong W, Jiang Y, Za Y, Zeng Z, Shao M, Fan J, et al. Temporal and spatial dynamics of rabies viruses in China and Southeast Asia. Virus Res. 2010;150:111–8. <http://dx.doi.org/10.1016/j.virusres.2010.02.019>
- Saito M, Oshitani H, Orbina JR, Tohma K, de Guzman AS, Kamigaki T, et al. Genetic diversity and geographic distribution of genetically distinct rabies viruses in the Philippines. PLoS Negl Trop Dis. 2013;7:e2144. <http://dx.doi.org/10.1371/journal.pntd.0002144>
- Streicker DG, Lemey P, Velasco-Villa A, Rupprecht CE. Rates of viral evolution are linked to host geography in bat rabies. PLoS Pathog. 2012;8:e1002720. <http://dx.doi.org/10.1371/journal.ppat.1002720>

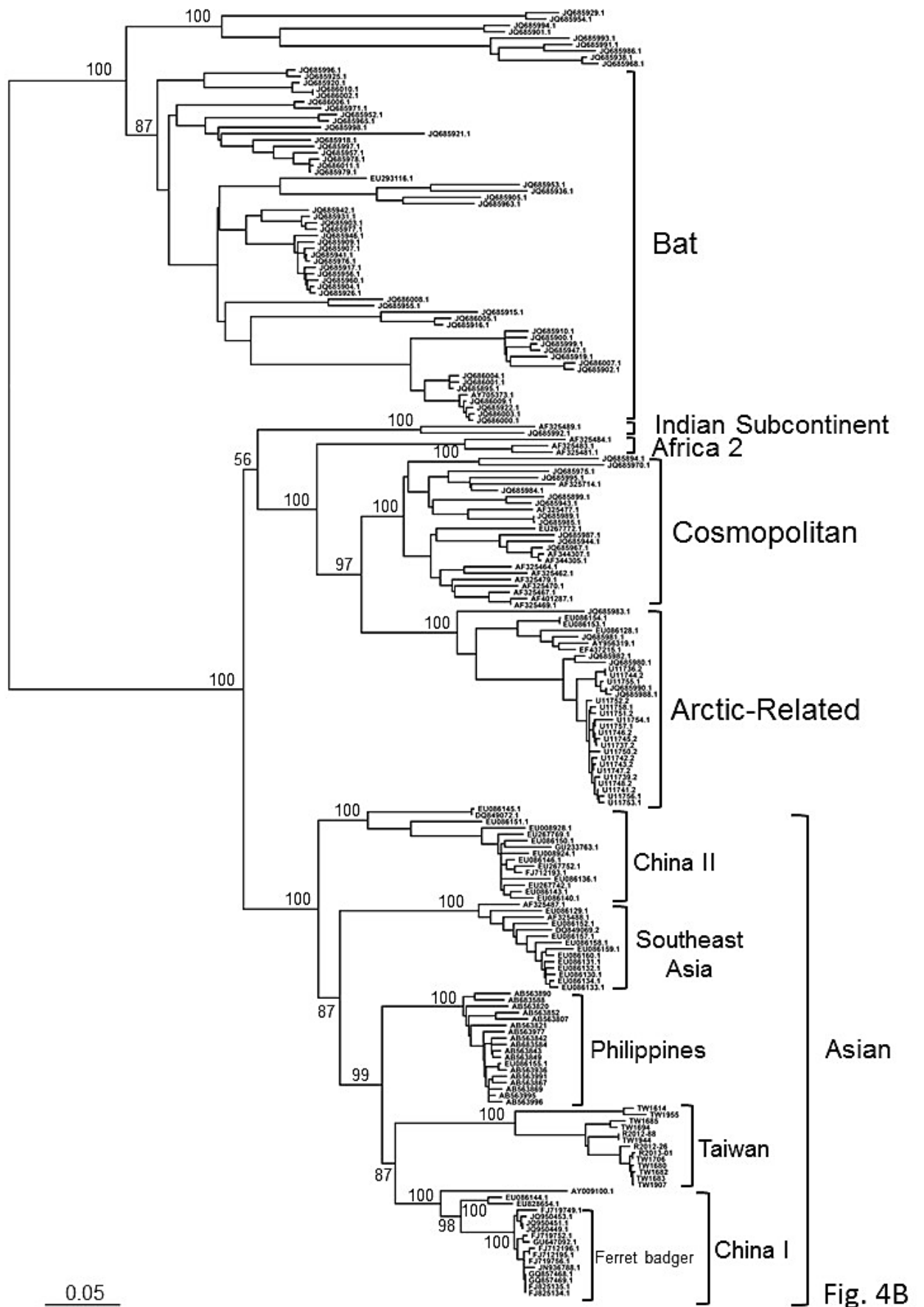
35. Biek R, Henderson JC, Waller LA, Rupprecht CE, Real LA. A high-resolution genetic signature of demographic and spatial expansion in epizootic rabies virus. *Proc Natl Acad Sci U S A*. 2007;104:7993–8. <http://dx.doi.org/10.1073/pnas.0700741104>
36. Faber M, Faber ML, Papaneri A, Bette M, Weihe E, Dietzschold B, et al. A single amino acid change in rabies virus glycoprotein increases virus spread and enhances virus pathogenicity. *J Virol*. 2005;79:14141–8. <http://dx.doi.org/10.1128/JVI.79.22.14141-14148.2005>
37. Faber M, Li J, Kean RB, Hooper DC, Alugupalli KR, Dietzschold B. Effective preexposure and postexposure prophylaxis of rabies with a highly attenuated recombinant rabies virus. *Proc Natl Acad Sci U S A*. 2009;106:11300–5. <http://dx.doi.org/10.1073/pnas.0905640106>
38. Lafon M. Rabies virus receptors. *J Neurovirol*. 2005;11:82–7. <http://dx.doi.org/10.1080/13550280590900427>
39. Tuffereau C, Schmidt K, Langevin C, Lafay F, Dechant G, Koltzenburg M. The rabies virus glycoprotein receptor p75NTR is not essential for rabies virus infection. *J Virol*. 2007;81:13622–30. <http://dx.doi.org/10.1128/JVI.02368-06>
40. Kuzmin IV, Shi M, Orciari LA, Yager PA, Velasco-Villa A, Kuzmina NA, et al. Molecular inferences suggest multiple host shifts of rabies viruses from bats to mesocarnivores in Arizona during 2001–2009. *PLoS Pathog*. 2012;8:e1002786. <http://dx.doi.org/10.1371/journal.ppat.1002786>

Address for correspondence: Victor Fei Pang, Graduate Institute of Molecular and Comparative Pathobiology, School of Veterinary Medicine, National Taiwan University, No. 1, Sec. 4, Roosevelt Rd., Taipei 10617, Taiwan, ROC; email: pang@ntu.edu.tw



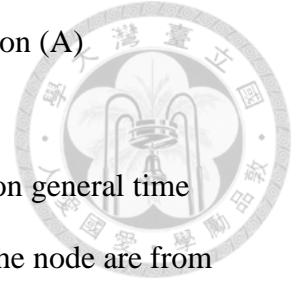






**Figure 4.** Phylogenetic relationships of major RABV groups based on (A) nucleoprotein and (B) glycoprotein gene sequences.

The trees were constructed by Maximum-likelihood method based on general time reversible (GTR) nucleotide substitution model. Numbers close to the node are from 100 bootstrap replications. The definition of major clades was based on Bourhy et al. (16) and He et al. (17).



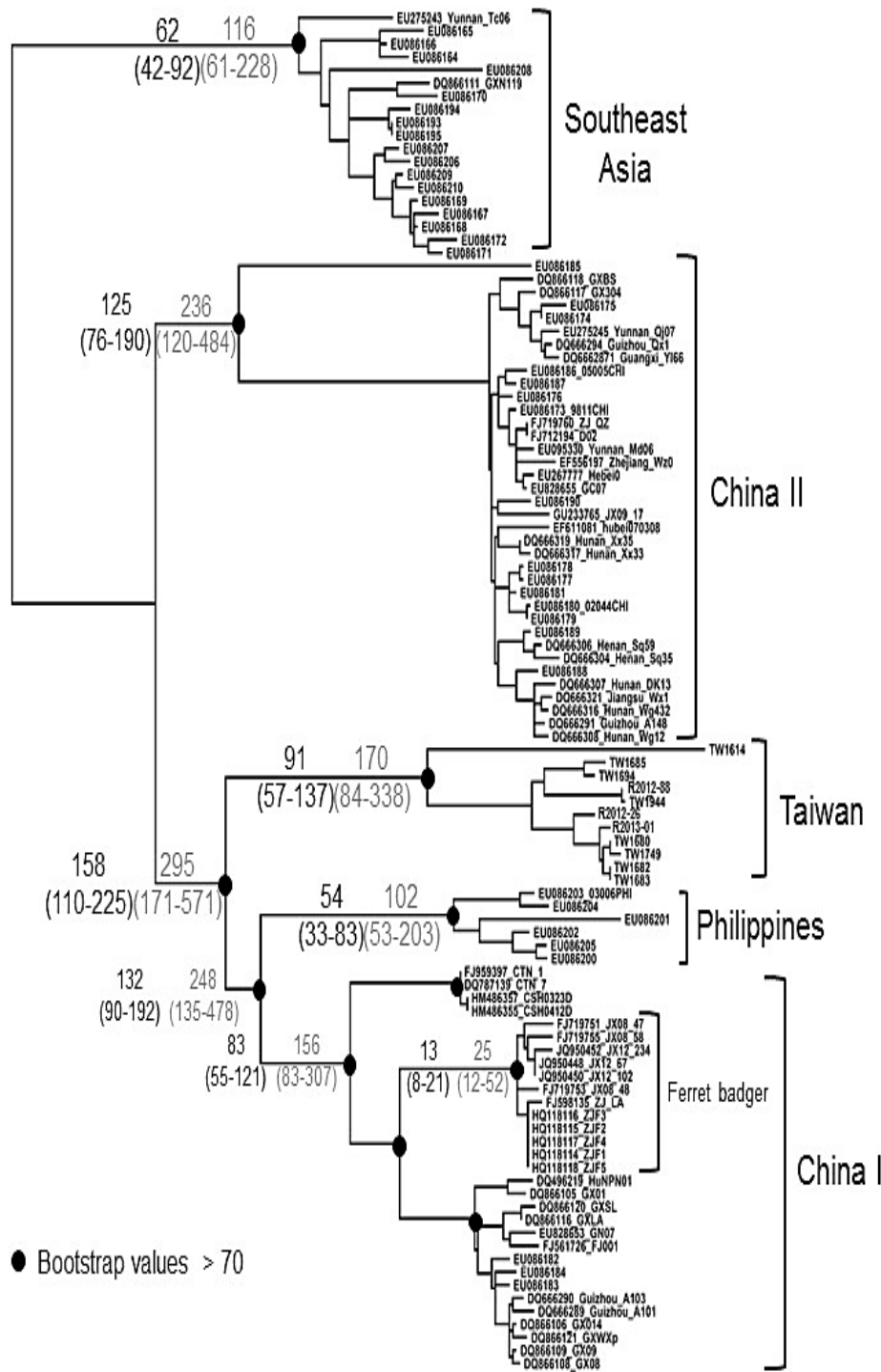


Fig. 5A

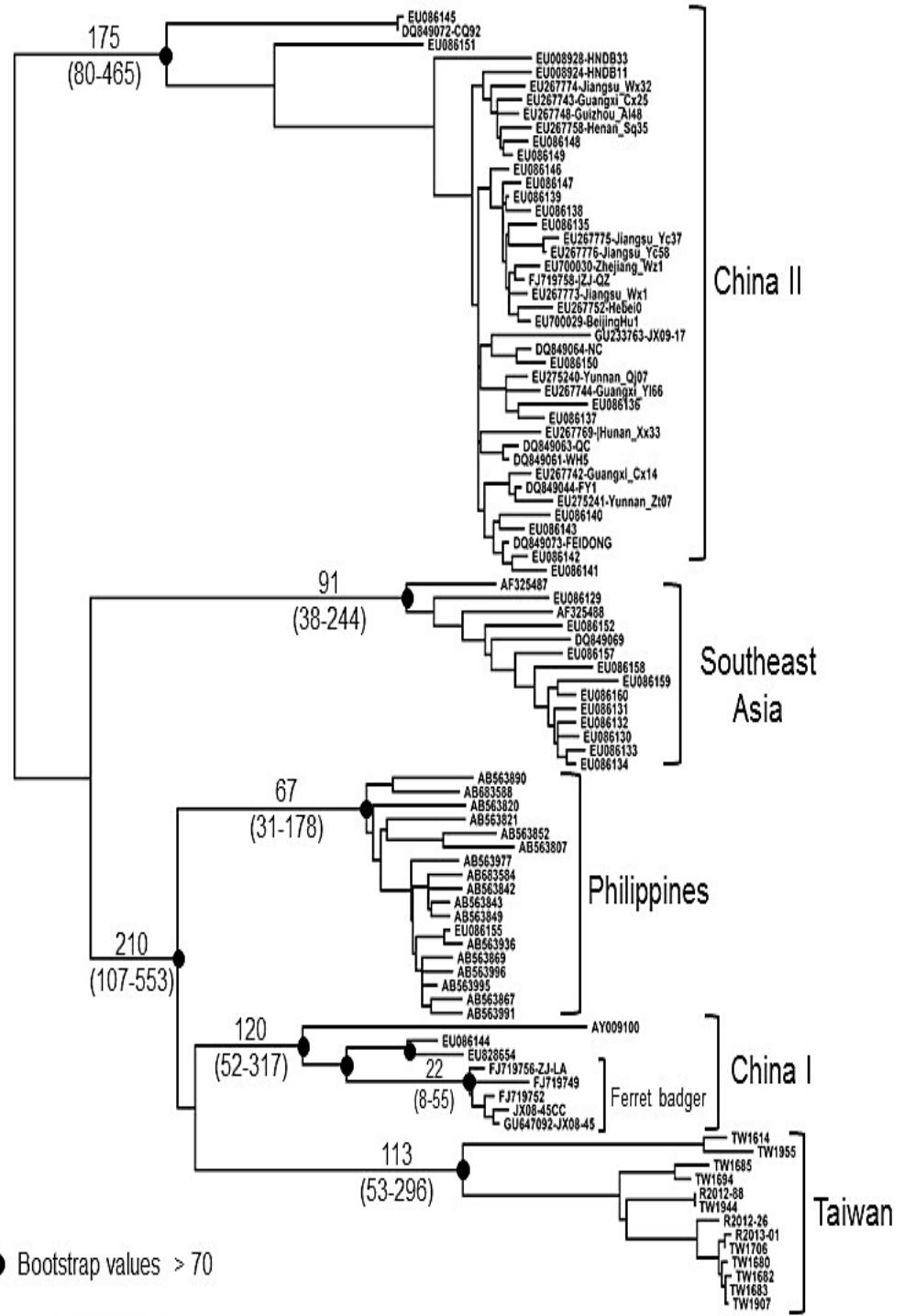


Fig. 5B ● Bootstrap values > 70

**Figure 5.** Maximum-likelihood trees of RABV based on (A) nucleoprotein and (B) glycoprotein gene sequences.

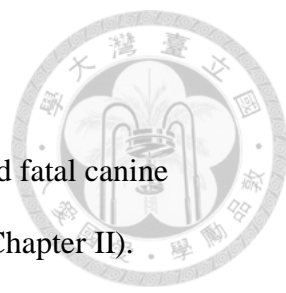
Numbers on the branches are estimated divergences (above) and their 95% highest posterior density (below). The divergence time between different viral lineages and time to the most recent common ancestor (TMRCA) of viral isolates were estimated using an established Bayesian MCMC approach implemented in BEAST vers. 1.7 (21). The substitution rate was assumed to be  $4.3 \times 10^{-4}$  (ranging  $3.1-6.6 \times 10^{-4}$ ) or  $2.3 \times 10^{-4}$  (ranging  $1.1-3.6 \times 10^{-4}$ ) /site/year (hatched numbers) for N and  $3.9 \times 10^{-4}$  ( $1.2-6.5 \times 10^{-4}$ )/site/year for G genes (17, 23). The analysis was performed using the general time reversible (GTR) model of nucleotide substitution assuming uncorrelated lognormal molecular clock (22). TW1955 is the only isolate from a shrew which is very close to TW1614 collected from its vicinity, suggesting that TW1955 was a spillover from ferret badger (See also Fig. 1).

# Chapter V



# Conclusions

## Conclusions



The present study has demonstrated that the zoonotic rabies and fatal canine distemper were diagnosed in 4 TWFBs and 3 MPCs, respectively (Chapter II). Retrospective study using archived formalin-fixed and paraffin-embedded tissues of TWFBs revealed the earliest IHC-positive rabid TWFB case in 2004 (Chapter III)(Chiou *et al.*, 2014). A high prevalence rate of lungworm infestation (23/31; 74.2%) was observed in TWFBs. Road traffic accidents and stray dog-associated killing were the most common etiologies for the death of wild-ranging carnivores (Chapter II).

The characteristic pathological changes of rabid-TWFB were nonsuppurative meningoencephalomyelitis, ganglionitis, and formation of typical intracytoplasmic Negri bodies with brain stem affected the most. Additionally, variable spongiform degeneration, primarily in the perikaryon of neurons and neuropil, was observed in the cerebral cortex, thalamus, and brain stem. In the non-nervous tissue, representative lesions included adrenal necrosis and lymphocytic interstitial sialoadenitis. By immunohistochemical (IHC) staining as well as fluorescent antibody test (FAT), positive viral antigens were detected in the perikaryon of the neurons and axonal and/or dendritic processes in the nervous tissue and in the macrophages scattered in various tissues throughout the body (Chapter III). Similar extensive lesion distribution in the central nervous system has also been seen in the naturally acquired rabid raccoons, babcats, and skunks (Hamir, 2011; Hamir *et al.*, 1992b; Stein *et al.*, 2010). It is known that hippocampus is the common site for finding Negri bodies in carnivores (Burkel *et al.*, 1970; Tobiume *et al.*, 2009) and Purkinje cells of cerebellum are the place where Negri bodies are most often observed in herbivores (Hamir *et al.*,

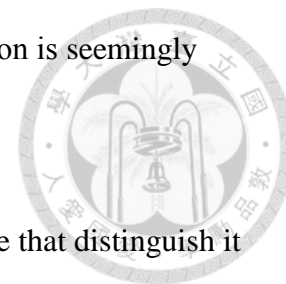


1992a) and humans (Jackson *et al.*, 2001). However, Negri bodies are widely distributed and readily found in both central and peripheral neural tissues in TWFBs. Based on the results of pathological findings and RABV antigen detection, brain stem (Chapter III) seems to be an ideal place of tissue sampling for the diagnosis of TWFB-associated RABV infection, although cerebral cortex, hippocampus, thalamus or hypothalamus is also suitable.

To examine the origin of this viral strain, we sequenced and characterized a RABV strain, RABV-TWFB, recently isolated from TWFB. Phylogeographic analyses demonstrated that the RABV of TWFB (RABV-TWFB) is a distinct lineage within the Asian group, and has been differentiated from its closest lineages, China I (including Chinese ferret badger isolates; RABV-CNFB) and Philippines, 158-210 years before present. The most recent common ancestor of RABV-TWFB was originated 91-113 years ago. Our data showed that the RABV-TWFB is clustered with sequences from Philippines, China I, and RABV-CNFB. Of ferret badger isolates, RABV-TWFB and RABV-CNFB come from phylogenetically distinct lineages, indicating that there were likely multiple RABV colonization events in this species. A major question addressed in this study is whether the RABV was recently introduced into the population of TWFB, or it perpetuated in the TWFB population without revealing its presence pathogenically after it was first introduced in the ancient past. Our divergence dating showed that the RABV has been circulating in TWFB for about a hundred years (Chapter IV).

Taiwan is an island with a high population density, with 23 million people living in an area of 36,188 Km<sup>2</sup>. Under this circumstance, it would be very unusual not to notice rabies cases for more than 50 years. Therefore, despite the ancient history of

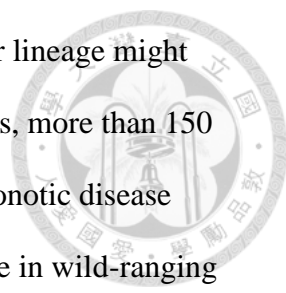
the ferret badger's association with RABV, the fact that its population is seemingly unaffected by infection with RABV is perplexing.



Among the multiple substitutions in the RABV-TWFB genome that distinguish it from other viral strains, several substitutions in the G protein, i.e. N194Y, R196K, and G203E (Chapter IV), may merit additional attention. It has been demonstrated that a single amino acid mutation, N194K, in the nonpathogenic RABV vaccine strain, SAD B19, was solely responsible for its increase in pathogenicity. The increased pathogenicity is due to increased viral spread *in vivo* and faster internalization of the virus into cells (Faber *et al.*, 2005), both of which are consistent with the notion that the G protein plays a major role in RABV pathogenesis. When N was exchanged with S at position 194 (N194S), the pathogenic phenotype was reversed (Faber *et al.*, 2005; Faber *et al.*, 2009).

In our analysis of 113 G gene sequences from dog-associated RABV, no amino acid substitution was observed at the above mentioned sites. In a total of 120 G gene sequences from bat-associated RABV (Kuzmin *et al.*, 2012), 8 N194T (6.7%), 2 N194S (1.7%), and 36 R196K (30.0%) amino acid substitutions, were revealed with no amino acid change at G203. Taken together, the 3 amino acid substitutions, N194Y, R196K, and G203E, found in all 13 G gene sequences of RABV-TWFB are unique and may be worthy of further investigation (Chapter IV).


Since the first discovery of rabid TWFBs in 2012, rabies has been diagnosed in additional 464 TWFBs, 5 MPCs, 1 shrew, and 1 puppy bitten by rabid-TWFB by May 21, 2015. ([https://www.baphiq.gov.tw/news\\_list.php?menu=1924&typeid=1948](https://www.baphiq.gov.tw/news_list.php?menu=1924&typeid=1948)). Prior to the most recent outbreak, Taiwan had been considered as a rabies-free region for more than 50 years. Phylogeographic analyses indicated that the TWFB-associated



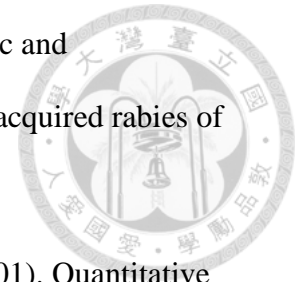
RABV is a distinct lineage among the Asian isolates. This particular lineage might have been diverged from its closest lineages, China I and Philippines, more than 150 years (Chapter IV). The discovery of this re-emerging important zoonotic disease further emphasizes the essentiality of a systemic disease surveillance in wild-ranging wildlife. The current surveillance data show that the FB-associated RABV infection in Taiwan still occurs mainly in TWFBs, the actual cause for the recent outbreak is still unknown and requires further investigation. Although CDV infection has been reported in TWFBs (Chen *et al.*, 2008), this infectious disease seems mainly to occur in MPCs in wild-ranging carnivores in Taiwan.

Veterinarians work on both domestic and wildlife diseases and have a unique comparative perspective to bring to investigating zoonoses. It is known that a high percentage of emerging infectious diseases are zoonoses, in those studies the involvement of multidisciplinary scientists is required. Conservation medicine belongs to this emerging field of multidisciplinary study. Conservation medicine field work can be enhanced by the understanding of pathology. Pathological investigations can rapidly indicate the very mild nature of lesions; however, without the involvement of pathology ignoring significant lesions and/or misinterpretation can easily occur (Daszak *et al.*, 2004). The present study has demonstrated that there are many unknown diseases cryptically circulating in the wildlife that share the same habitat with us, and some of which may even have serious impacts on our and other animal's health, wildlife conservation, and economy. The findings of the present study also re-emphasize the importance of an effective wildlife disease surveillance. Moreover, the information accumulated from years of systemic survey may allow us to predict future emergence of known and unknown pathogens (Daszak *et al.*, 2004).

## References:

- 
- Burkel, M. D., Andrews, M. F. and Meslow, E. C. (1970). Rabies detection in road-killed skunks (*Mephitis mephitis*). *J Wildl Dis*, **6**, 496-499.
- Chen, C. C., Pei, K. J., Liao, M. H. and Mortenson, J. A. (2008). Canine distemper virus in wild ferret-badgers of Taiwan. *J Wildl Dis*, **44**, 440-445.
- Chiou, H. Y., Hsieh, C. H., Jeng, C. R., Chan, F. T., Wang, H. Y. and Pang, V. F. (2014). Molecular characterization of cryptically circulating rabies virus from ferret badgers, Taiwan. *Emerg Infect Dis*, **20**, 790-798.
- Daszak, P., Tabor, G. M., Kilpatrick, A. M., Epstein, J. and Plowright, R. (2004). Conservation medicine and a new agenda for emerging diseases. *Ann N Y Acad Sci*, **1026**, 1-11.
- Faber, M., Faber, M. L., Papaneri, A., Bette, M., Weihe, E., Dietzschold, B. and Schnell, M. J. (2005). A single amino acid change in rabies virus glycoprotein increases virus spread and enhances virus pathogenicity. *J Virol*, **79**, 14141-14148.
- Faber, M., Li, J., Kean, R. B., Hooper, D. C., Alugupalli, K. R. and Dietzschold, B. (2009). Effective preexposure and postexposure prophylaxis of rabies with a highly attenuated recombinant rabies virus. *Proc Natl Acad Sci U S A*, **106**, 11300-11305.
- Hamir, A. N. (2011). Pathology of neurologic disorders of raccoons (*Procyon lotor*). *J Vet Diagn Invest*, **23**, 873-884.
- Hamir, A. N., Moser, G. and Rupprecht, C. E. (1992a). A five year (1985-1989) retrospective study of equine neurological diseases with special reference to rabies. *J Comp Pathol*, **106**, 411-421.

Hamir, A. N., Moser, G. and Rupprecht, C. E. (1992b). Morphologic and immunoperoxidase study of neurologic lesions in naturally acquired rabies of raccoons. *J Vet Diagn Invest*, **4**, 369-373.



Jackson, A. C., Ye, H., Ridaura-Sanz, C. and Lopez-Corella, E. (2001). Quantitative study of the infection in brain neurons in human rabies. *J Med Virol*, **65**, 614-618.

Kuzmin, I. V., Shi, M., Orciari, L. A., Yager, P. A., Velasco-Villa, A., Kuzmina, N. A., Streicker, D. G., Bergman, D. L. and Rupprecht, C. E. (2012). Molecular inferences suggest multiple host shifts of rabies viruses from bats to mesocarnivores in Arizona during 2001-2009. *PLoS Pathog*, **8**, e1002786.

Stein, L. T., Rech, R. R., Harrison, L. and Brown, C. C. (2010). Immunohistochemical study of rabies virus within the central nervous system of domestic and wildlife species. *Vet Pathol*, **47**, 630-633.

Tobiume, M., Sato, Y., Katano, H., Nakajima, N., Tanaka, K., Noguchi, A., Inoue, S., Hasegawa, H., Iwasa, Y., Tanaka, J., Hayashi, H., Yoshida, S., Kurane, I. and Sata, T. (2009). Rabies virus dissemination in neural tissues of autopsy cases due to rabies imported into Japan from the Philippines: immunohistochemistry. *Pathol Int*, **59**, 555-566.